ELECTRONIC CONDUCTION IN HOMOPOLAR CRYSTALS

THESIS FOR THE DEGREE OF Ph.D

UNIVERSITY OF LONDON, 1953

TABLE OF CONTENTS

	Page
PART I - GENERAL INTRODUCTION	2
PART II - ELECTRONIC CONDUCTION IN GREY TIN	5
PART III - ELECTRONIC CONDUCTION IN SILICON CARBIDE	105
PART IV - REVIEW OF ELECTRICAL PROPERTIES OF HOMOPOLAR CRYSTALS	128

APPENDIX 1.	List of Symbols Used	135
APPENDIX 2.	List of Figures	136
APPENDIX 3.	Acknowledgments	137
APPENDIX 4	Reprints of Publications	138

Figures 1 - 26.

PART I - GENERAL INTRODUCTION

The electrical properties of the typical homoplar substances diamond, silicon and germanium have been extensively studied by many workers. An extension of this series of substances leads to grey tin which is also homopolar. At the time this investigation started there was no published work on the electrical properties of grey tin. It was therefore natural to choose it as a typical homopolar substance for the present study.

Crystals with many homopolar characteristics may also be formed by compounds. Typical of these is the substance silicon carbide. As the author had previously worked on this substance it was chosen as the second substance for study. The experimental work described in this thesis is therefore concerned with these two interesting substances - grey tin and silicon carbide.

Part II deals with the preparation of grey tin and alloys and the measurement of their electrical properties. The actual preparation is not new, but the experiments in which attempts were made to produce single crystals are original - if unfortunately unsuccessful.

The work described on the electrical properties of grey tin is original; it includes measurements of the electrical conductivity and Hall co-efficient, and their variation in a magnetic field. Since the work was begun parallel measurements have been published by BUSCH, WIELAND and ZOLLER (1) and BLUM and GORYUNOVA (2) a brief note by the author was published simultaneously (3).

Part III deals with the preparation and electrical properties of silicon carbide. The method of preparation was originally described by MOERS (4) and was further developed by the author in collaboration with YEO (5). In the present work the method has been still further developed in the direction of greater reliability and incorporation of a greater range of impurity elements. The spectographic analyses of silicon carbide crystals were carried out by Miss J.M.Rooke of the Research Department of Metropolitan-Vickers Electrical Co.Ltd, Manchester.

Part III also contains a new theory of electronic conduction in silicon carbide. The quantitative experimental basis for the theory is largely provided by the work of BUSCH and his colleagues (6) (7)

In Part IV the electrical properties of the homopolar semiconductors are compared.

REFERENCES

(1) BUSCH G., SIELAND J. & ZOLLER H - Helv. Phys. Acta 24, 49 (1951)

(2) BLUM A.I & GORYUNOVA N.A - Doklady Akad.Nauk (S.S.S.R) 75, 367 (1950)

(3) KENDALL J.T. - Proc.Phys. Soc. 63B, 821 (1950)

(4) MOERS K. - Z. Anorg.Chem. 198, 243 (1931)

(5) KENDALL J.T. & YEO D. - Proc. Internat. Cong. Pure. & Appl.Chem. 11, 167 (1947)

(6) BUSCH G. - Helv. Phys. Acta 19, 167 (1946)

(7) BUSCH G.& LABHART H. - Helv.Phys.Acta 19, 463 (1946)

PART II - ELECTRONIC CONDUCTION IN GREY TIN

CONTENTS

		PAGE
1.	INTRODUCTION	6
	1.1. Energy Levels in Grey Tin	7
2.	PREPARATION OF SAMPLES	8
	2.1. Review of Previous Work	8
	2.2. Preparation of Pure Grey Tin and Alloys	10
	2.3. Attempted Preparation of Single Crystals	12
	2.4. Preparation of Pressed-Powder Specimens	16
3.	EXPERIMENTAL PROCEDURE	19
	3.1. Conductivity	20
	3.2. Hall Effect	22
4.	EXPERIMENTAL RESULTS	23
	4.1. Variation of R and σ with H	23
	4.2. Conductivity	25
	4.3. Hall Constant	25
5.	INTERPRETATION OF CONDUCTIVITY AND HALL CONSTANT MEASUREMENTS	26
6.	DISCUSSION	31
	6.1. Concentrations of Electrons and Holes	31
	6.2. Mobilities of Electrons and Holes	32
	6.3. Tin-Gallium-Antimony Alloy	32
	6.4. Tin-Lead Alloy	33
	6.5. Variation of Conductivity and Hall Constant in a Magnetic Field	34
7.	CONTACT RECTIFICATION	36
8.	THERMO-ELECTRIC EFFECT	40
9.	TABLES 1 - 58	42
10.	REFERENCES.	103

ELECTRICAL PROPERTIES OF GREY TIN ALLOYS

1. INTRODUCTION

Grey tin has a non-metallic crystal structure, similar to diamond (1,2), i.e. it is the end member of the series C - Si - Ge - αSn. One would therefore expect its electrical properties to be appropriate to its position in this series; but there seemed to be no reliable experimental results available in the literature. It was originally reported that grey tin was a super-conductor, but de Haas (3) and Sharvin (4) showed that this was incorrect, at least above 1.2°K. In a private communication to the author in 1949, Busch reported that he had obtained values for the electrical conductivity of grey tin powder which showed it to be a semi-conductor. On the other hand Moesveld (5) reported that it was a normal metallic conductor.

Some time after the present investigation had commenced Busch, Wieland and Zoller (6) published their results as also did Blum and Goryunova (7). A brief account of the preliminary results obtained by me was published simultaneously (8).

The complete results presented here differ considerably from the above earlier results, particularly in the lower value obtained for the intrinsic activation energy (0.064 eV in place of approximately 0.1eV) and in

the much more coherent picture obtained of the variation of the number of charge carriers and their mobility with temperature.

Electrical conductivity and Hall measurements were made over a temperature range from 77°K to 286°K on a number of grey tin specimens to which known amounts of antimony and gallium had been added. One alloy containing lead was also investigated. Small quantities of antimony enter the crystal lattice to act as a donator impurity. Gallium similarly acts as an acceptor impurity. There is some evidence that lead can act as a donator impurity. The data are analysed to determine the variation of the concentration of current carriers and their mobility with impurity concentration and temperature. The results are interpreted in terms of existing theories of conduction in semi-conductors.

1.1. Energy Levels in Grey Tin

The mechanism of impurity semi-conduction in Group IV elements caused by the addition of small quantities of Group III or Group V elements is well understood. (See, for example, Pearson and Bardeen on conduction in silicon caused by the addition of boron or phosphorus (9)

The main point of difference between silicon and grey tin is that in the former the intrinsic conductivity range occurs at high temperatures and there is an abrupt

transition from the impurity to the intrinsic range. In the case of grey tin the energy gap between the filled and unfilled bands is very small and intrinsic conductivity is observed even at low temperatures. The transition between the two types of conductivity is therefore gradual.

The energy relations are illustrated in Fig.1. There is an energy gap between the filled and unfilled bands of the crystal of 0.064 eV. The acceptor levels lie just above the filled band and the donator levels just below the unfilled band.

The activation energies for the ionization of donators and acceptors can be estimated as approximately 0.005 eV. This follows from the Bohr formula

$$E_I = 2\pi^2 m e^4 / \varkappa^2 h^2 \qquad (1)$$

Setting $\varkappa$ (dielectric constant) equal to 50 gives

$$E_I = 13.5/50^2 = 0.005 \text{ eV} \qquad (2)$$

This corresponds to a temperature of 60^0 Abs. so that we may assume that all the impurity centres are ionized throughout the temperature range investigated.

2. PREPARATION OF SAMPLES

2.1 Review of Previous Work

It has been known from early times that if ordinary

tin is kept at a low temperature for a long time it transforms into a grey friable powder. Coins and early tin ingots which have been kept in museums frequently show patches of grey tin. (See, for example, an ancient tin ingot at present in the Geological Museum at South Kensington). The phase change is ordinarily very slow, but as it is facilitated by innoculation with grey tin it has been called 'tin pest' 'tin disease' or 'museum sickness'. Cohen (10,11) has described this phenomenon in detail. The transition temperature has been measured by Cohen and Decker (12) and more accurately by Cohen and Lieshout (13) as $13.2 \pm 0.1^{\circ}C$. The crystal structure has been determined by Bijl and Kolkmeijer (1) and more accurately, on specimens made by the author , by Brownlee (2), as being the cubic diamond-type lattice with unit cube length $a = 6.4912 \pm 0.0005$A at room temperature, the X-ray density being 5.765 $gm.cm^{-3}$

Although grey tin is the stable allotrope below $13.2^{\circ}C$ the transformation ordinarily takes place extremely slowly. The velocity of transformation is a function of temperature.

Tammann and Dreyer (14) obtained a maximum velocity at $-30^{\circ}C$ for transformation in contact with an aqueous solution of ammonium stannichloride (see Fig.2) Cohen and Lieshout (13) found a maximum velocity at $-50^{\circ}C$

in contact with air (see fig.3). The velocity of transformation is also sensitive to other factors such as the number of previous transformations of a specimen, the medium in which the change takes place, the thermal history of the specimen, mechanical pre-treatment, vibration during transformation, crystal grain size and presence of impurities. The last factor has been studied extensively by Tammann and Dreyer (14), Cohen and Lieshout (15, 16), Mason and Forgeng (17), Cohen and de Meester (18, 19) and Homer and Watkins (20). Although there are some minor inconsistencies in the literature it seems that all alloying elements interfere with the transformation, with the exception of magnesium, aluminium and zinc in the presence of water vapour. Under these conditions a hydroxide appears to be formed, see Heyn and Wetzel (21), which facilitates the initial formation of grey tin nuclei. A very large increase in the initial rate of transformation can be achieved by small additions of these elements in the presence of water. On the other hand certain elements greatly inhibit the transformation even when present in very small amounts; e.g. according to Mason and Forgeng (17) as little as 0.0035% of Bismuth prevents the formation of grey tin nuclei. (Nevertheless a specimen has been transformed here containing ten times as much Bismuth as this).

2.2. Preparation of Pure Grey Tin and Alloys

Spectroscopically pure tin was obtained from

Johnson - Matthey Ltd. and kept in air at -50°C for one month. No change in its appearance was noted at the end of this time. (Note: This bar has subsequently been kept below its transition point, and most of the time at about -50°C, for a further period of three years without change, indicating that the initial formation of a grey tin nucleus is extremely slow and is here the rate controlling factor).

The accelerated method of Cohen, de Meester and Landsmann (19) was therefore adopted by adding 0.1% of aluminium to the tin, exposing to water vapour for two days and then maintaining in air at -50°C. Initial formation of nuclei was apparent within 24 hours, and subsequent innoculation of pure tin with a tiny speck of this material allowed spectroscopically pure grey tin to be prepared on a large scale without further use of the accelerated method. All specimens of grey tin and alloys were subsequently prepared in this way by seeding and the transformation was carried out in sealed Pyrex glass tubes in vacuo. After preparation at -50°C the specimens were stored in a refrigerator at approximately 0°C.

A large number of alloys ~~were~~ was prepared by melting the constituents in vacuo in Pyrex glass tubes,

and the times taken to transform completely to the grey tin modification are given in Table 1, (p. 42).

2.3. Attempted Preparation of Single Crystals

When grey tin is prepared by transformation of white tin at low temperatures it is obtained in the form of a fine grey powder. The large change in specific gravity, from 7.31 to 5.76, is no doubt responsible for this disintegration. It would obviously be very desirable to have grey tin in a massive crystalline form and not merely as a powder, and attempts have been made to this end as follows:-

(a) Electrolytic deposition at temperatures below 13.2°C

Although there are no reports in the literature which refer to the electrical deposition of grey tin it seemed desirable to try some experiments:- (1) using an aqueous solution of stannic chloride and hydrochloric acid as electrolyte with ordinary tin electrodes white tin was deposited at 0°C at current densities from 0.01 to lamp/cm^2; (2) the same result was obtained with an aqueous solution of ammonium stannichloride as electrolyte, (3) the two previous experiments were repeated using a white tin anode and a cathode of pressed grey tin powder; in both cases white tin was deposited on the grey; (4) it was noted that without

any external applied potential an e.m.f. was set up between white and grey tin electrodes immersed in an electrolyte and a current flowed if an external electrical connection was made. The initial magnitude and direction of the e.m.f. was dependent on temperature, the grey tin being the cathode at 0°C and the anode at 25°C. In a particular experiment, using a high resistance (10,000 ohms) in the external circuit to prevent significant current flow the following variation of e.m.f. with temperature was noted:-

Electrolyte:	10% aqueous solution of ammonium stannichloride
1st electrode:	White tin
2nd electrode:	Grey tin
Temp. (°C)	-5°C; 0°C; 5°C; 10°C; 15°C; 20°C; 25°C; 30°C
e.m.f (mV)	- -0.38; -0.32; -0.24; -0.07 +0.06; +0.15; +0.21; +0.25

This relationship is shown graphically in Fig.4.

When a current was allowed to flow (with the external circuit resistance small) the initial e.m.f. at 0°C rapidly fell to zero, and white tin was deposited all over the grey tin cathode.

In view of the negative results obtained in these experiments no further attempts were made to deposit

grey tin electrochemically. Subsequently it has been learned privately from Busch, at Zurich Techniche Hochschule, and Breckenridge, at the National Bureau of Standards, Washington, that similar experiments by them have also given negative results.

(b) Evaporation in vacuo on a cold surface

A Metropolitan-Vickers vacuum-evaporation plant was used, the bell-jar being modified as shown in Fig.5.

The pressure in the evacuated bell-jar was varied from 0.1 to 1 microns, the rate of evaporation of tin from the heater was varied from fast to slow and the following liquids were used in the cold reservoir - water and ice (temperature 0°C), acetone and solid carbon dioxide (temperature -80°C) and liquid nitrogen (temperature -196°C). In all cases white tin was deposited on the cold glass surface. In a further experiment at -80°C and slow evaporation at 0.1 micron white tin was deposited on a surface of pressed grey tin.

(c) Crystallization at low temperature from aqueous solution

The crystallization of tin from an aqueous solution has been described by Kiplinger (22). 30 gm of tin powder was placed in a beaker and covered with 50 cc of concentrated hydrochloric acid. After leaving for 48 hours 50 cc of water was added. After leaving for a

further 24 hours it was noted that a few small needle-shaped crystals of tin (approximately 1 mm long) had been formed adhering to the undissolved original tin. This is the experiment as described by Kiplinger. It was carried out at 20°C and 0°C using both white tin and grey tin powder as the starting material. In all cases tiny needles of white tin were formed.

(d) Crystallization at low temperatures from a liquid alloy

According to the equilibrium diagram of Van Heteren (23) tin amalgum containing 0.3% of tin freezes at 0°C and is in equilibrium with grey tin down to the temperature of -34°C. It might be expected therefore that slow cooling of tin amalgum from 0°C to -34°C should result in the direct deposition of grey tin. Reference to the equilibrium diagram shows that the deposited material should contain approximately 10% of mercury in solid solution.

A low temperature bath was so arranged as to cool slowly at the rate of approximately 1°C per hour over the range 0°C to -30°C. An evacuated Pyrex tube containing 500 gm mercury with 0.3% of tin added was placed in this bath. When the temperature reached -30°C this tube was inverted and allowed to drain while at -30°C. A small amount of solid remained behind and most of this was

successfully scraped away from the sides of the Pyrex tube. The amount of material recovered was 0.105 gm and its specific gravity was approximately 7.5. Its melting point was approximately 200°C. An X-ray powder photograph showed the tetragonal tin structure.

In a further experiment a piece of grey tin weighing 0.274 gm was placed in the amalgum at 0°C. On removal at -30°C at the end of the experiment the piece was found to weigh 0.302 gm. A considerable amount of solidification had taken place on the inside of the Pyrex tube as previously. The specific gravity of the grey tin specimen had increased from approximately 5.7 to approximately 6.4. An X-ray powder photograph showed both the cubic and tetragonal forms to be present.

In view of the above experiments it seems certain that white tin is deposited from the tin amalgum on cooling, even on a grey tin surface.

2.4 Preparation of Pressed-Powder Specimens

If grey tin powder is subjected to pressure it reverts back to white tin. This is in accordance with the principle of le Chatelier, since the specific gravities of grey and white tin are respectively 5.76 and 7.31.

A study of the dependence of the transition temperature on pressure has been made by Komar (24) and he finds that it changes according to -

$$\frac{\partial T}{\partial p} = -5 \times 10^{-2} \quad {}^{\circ}C/\text{Atmosphere}$$

A pressure of 10 tons/sq.in. will thus, for example, lower the transition temperature by 75°C (i.e. to -62°C)

An "Apex" 10-ton laboratory press was modified so that the mould could be cooled by liquid air. Under working conditions a thermocouple measurement of the temperature of the inside of the mould filled with grey tin powder was -125°C. Under these conditions cylindrical specimens of grey tin were pressed, of 0".25 diameter and slightly over 0".5 long, at 10 tons/sq.in pressure.

The specific gravity of the specimens varied from 5.550 to 5.750, and those with the lower specific gravities were rejected as being porous. In all cases some reversion to white tin occurred on the side-surfaces of the specimens. This was easily removed either by dissolving the surface in dilute hydrochloric acid or by keeping the specimen at -50°C overnight

X-ray powder photographs of the final specimens showed only the lines of cubic tin.

Using the last method described above the alloys shown in Table 2 were prepared in the form of cylindrical specimens. (See p. 46).

In column 5 the number of charge carriers per cc has been calculated from the value of the Hall constant at low temperatures. A positive value indicates that the carriers are holes, a negative value that they are electrons.

The pure sample, to which no impurity had been added, contained 3.25×10^{17} free electrons at low temperature. This represents the carriers due to impurities originally present in the "spectroscopically pure" sample.

The value of 3.25×10^{17} is therefore subtracted from the n-type samples in column 5, and added to the p-type samples, to give the values in column 7 which are the carriers due to the added impurities.

It will be noted that the values in columns 7 and 4 are not the same, and their ratio is given in column 8.

If every impurity atom added gave rise to one carrier this ratio would be unity. It is less than unity because a proportion of the added impurity atoms is ineffective

in giving rise to carriers. Presumably this is due to only a proportion of the added impurity atoms going into substitutional positions, the ineffective atoms being precipitated at crystal boundaries or elsewhere and thus not entering the grey tin lattice. It will be noted that the more impure the sample the smaller the proportion of effective impurity atoms. In this, antimony and gallium appear to behave similarly.

In the case of lead, either only a very small proportion enters the lattice substitutionally or some other factor is operating to cut down the effectiveness. It is difficult to understand why lead should give rise to a carrier at all, as it has the same valency as tin. It does not seem likely that the carriers are due to an impurity in the lead as "spectroscopically pure" material was used.

3. EXPERIMENTAL PROCEDURE

The electrical conductivity and Hall constant of the cylindrical specimens of grey tin were measured simultaneously, using the specimen holder shown in fig.6 and the electrical measuring circuit shown in fig.7. There was a considerable variation of both conductivity and Hall Constant with magnetic field strength, especially for the purer alloys at low temperatures. This effect was used to estimate the mobilities of the charge carriers.

The current through the specimen was maintained constant, and values of the potential difference along the length of the specimen and of the Hall e.m.f. were measured as functions of magnetic field strength.

3.1. CONDUCTIVITY

The electrical conductivity was measured by a potential-probe method. The voltage drop along the length of the specimen ~~were~~ was measured independently of the current carrying circuit by the introduction of probe electrodes. The specimen holder is shown in fig.6, and it is seen that the polystyrene tube enclosing the specimen is perforated by two holes through which thin platinum-iridium wires (0.06 mm diameter) are pushed into contact with the grey tin. These holes were placed 0.50 apart and arranged to be near the end surfaces of the grey tin cylinder.

The specimen holder was immersed in a vacuum flask filled with methyl cyclohexane for temperatures down to about $-80^{\circ}C$ and with liquid propane for lower temperatures. This liquid medium was kept stirred with a small motor-stirrer and was cooled by addition of liquid nitrogen. (Note: For the first few measurements small quantities of liquid nitrogen were poured directly into the liquid propane,

but after a minor explosion had occurred the nitrogen was kept out of direct contact with the propane by placing it in a thin-walled copper tube immersed in the liquid. Presumably the explosion occurred owing to the use of liquid nitrogen which had been standing around for some time and had therefore condensed some oxygen from the atmosphere). For the very lowest temperatures the specimen holder was immersed directly in liquid nitrogen.

The temperature was measured by means of an Fe/NiCr thermocouple recessed into the polystyrene cylinder as shown in Fig.6. The thermocouple was calibrated at several fixed temperatures. After addition of liquid nitrogen to the bath an interval of about five minutes was required for the attainment of temperature equilibrium. In practice about ten minutes was allowed.

It was found convenient to carry out measurements at a series of fixed temperatures corresponding to $10^3/T$ = 13, 12, 11, 10, 9, 8, 7, 6.5, 6, 5.5, 5, 4.5, 4, 3.5.

The electrical measuring circuit was as shown in Fig.7. In practice the use of the probe electrodes did not appear to be really necessary as the voltage drop across the current-carrying contacts was always very small compared with the voltage drop along the length of the grey tin specimen.

3.2. Hall Effect

Platinum-iridium probe electrodes were placed on opposite sides of the grey tin specimen as shown in Fig.6. The specimen holder and its container were placed between the poles of an electromagnet, the Hall probes being transverse to the direction of the field. The current through the sample and the direction of the magnetic field were both reversed independently and the four Hall voltages thus obtained generally differed slightly (presumably due to thermo-electric effects). The mean value was taken.

The magnetic field strength was determined by measuring the current through the windings after calibrating by means of a small search coil and ballistic galvanometer.

Since it is the Hall constant at zero field which it is desired to determine, the measurements were extrapolated to H = 0 to give the true values of R. The Hall constant R, in cm^3 /Coulombs, was calculated from the relation

$$R = 10^8 \, Vt/HI \qquad (3)$$

where V is the measured Hall voltage in volts, t is the thickness of the sample in cm, H the magnetic field strength in gauss, and I the current in amperes.

The use of a cylindrical specimen for Hall measurements is unusual; but it is not thought necessary to introduce any geometric factor into the above formula. Isenberg, Russell and Greene[28] have shown that for a rectangular specimen with a ratio of length to width of 2 (as used here) the Hall constant is reduced to 0.93 of its normal value. However, for a cylindrical specimen this reduction will be smaller, and the geometric factor has therefore been taken to be unity in the present case.

4. EXPERIMENTAL RESULTS

4.1. Variation of R and σ with H

The experimental results for Conductivity are given in Tables 3 - 13. In order to obtain reproducible results it was found necessary to limit the power dissipated in the specimen to a maximum of 1mW. The current through the specimen is given in the second column of these tables, and the body of the tables gives the potential drop across the conductivity probes at various values of magnetic field. From these results the conductivity is calculated from the formula -

$$\sigma = \frac{I}{V} \times \frac{l}{\pi r^2}$$

I is the current through the specimen, V is the potential drop across the probes, l is the length of

the specimen between the probes (1.27 cm), r is the radius of the specimen (0.318 cm).

This reduces to -

$$\sigma = 4I/V.$$

From the experimental results the values calculated for the conductivity are set out in Tables 14 - 24.

In the case of alloys (1) and (6) the relative change of conductivity $(\sigma_o - \sigma)/\sigma_o$, where σ_o is the conductivity at zero field, is set out in Tables 25 and 26 and also plotted in Figs. 16 and 17.

The experimental results for the Hall e.m.f. are given in Tables 27 - 37. The e.m.f.s given represent the averages of four different readings, the current and field being reversed independently. These readings did not in general differ by more than 1 - 2 μV provided that they were taken immediately after switching on the field. From the experimental results the values calculated for the Hall constant, from equation (3), are set out in Tables 38 - 48.

In the case of alloys (1) and (6) the relative change of Hall Constant (Ro - R) /Ro, where Ro is the Hall Constant at zero field, is set out in Tables 49 and 50 and also plotted in Figs 16 and 17.

In the case of alloy (1) the values of the Hall Constant are plotted against H^2 for low fields in figs. 10 and 11. This procedure is necessary in order to extrapolate to H = o, as it is the Hall Constant at zero field which we desire to know. The same procedure was followed for the other ten alloys, but the actual graphs are not reproduced here.

4.2. Conductivity

The results obtained for zero magnetic field are given in Table 51 and fig.8. For the straight-line portion of curve (1) (pure grey tin) the conductivity is given by

$$\sigma = \sigma_o \exp(-\varepsilon/2KT) \qquad (4)$$

where $\sigma_o = 1.6 \times 10^4$ ohm^{-1} cm^{-1}, and $\varepsilon = 0.064$ eV.

This value of ε is also obtained from the other curves, except the alloy containing approximately equal amounts of gallium and antimony. Slightly different values of σ_o are obtained, the smallest value being for the purest material.

4.3. Hall Constant

The results, extrapolated to H = o, are given in Table 52 and Fig.9. It will be seen that as the temperature is decreased R increases exponentially until

a saturation value is reached corresponding to the number of impurity charge-carriers.

In the case of alloys (6) - (10) positive values of R were obtained, indicating hole-conduction, except at high temperatures in the case of alloys (6) (7) and (10). In these curves a reversal of sign took place and from the curves a temperature can be found for which R = 0.

5. INTERPRETATION OF CONDUCTIVITY AND HALL CONSTANT MEASUREMENTS

(a) It will be noted that ε does not vary with temperature (within the limits of experimental error).

We may therefore use the relation derived from statistical mechanics (Fowler) :-

$$n_e n_h = 2.4 \times 10^{31} . T^3 . \exp(-\varepsilon/KT) \qquad (5)$$

This relationship will hold whatever the purity of the sample.

In the case of Si a multiplying factor of 32.5 is needed on the right-hand side of this equation, and in the case of Ge a multiplying factor of 3.5.

If this is taken to be due to a linear variation of ε with T,

$$\text{i.e. } \varepsilon_T = \varepsilon_o - \beta T \qquad (6)$$

Then we have,

$$\exp(-\varepsilon_T/KT) = \exp(\beta/K).\ \exp(-\varepsilon_o/KT) \qquad (7)$$

The multiplying factor is thus $\exp(\beta/K)$.

Since in the case of grey tin β must be very small we may take the multiplying factor to be unity.

Calculated values of $n_e n_h$ as a function of $1/T$ are given in Table 53 and plotted in fig.12.

(b) From Fig.9 (Hall constant for tin-gallium alloys) the maximum values of R are:-

(6) ~ 10.6, (7) 6.0

Assuming these alloys are non-degenerate at low temperatures and that $n_e \ll n_h$ then we may calculate the number of charge carriers due to impurities as

$$n_s = -7.4 \times 10^{18}/R = (6)\ 7.0 \times 10^{17}\ (7)\ 1.24 \times 10^{18}$$

Also from Fig.9, R= 0 at $10^3/T$ = (6) 5.65 (7) 4.90.

Using equation (5) we may calculate $n_e n_h$ at the temperature at which R = 0:- $n_e n_h = 2.4 \times 10^{31} T^3 \exp(-0.064/KT)$

$= (6)\ 2.08 \times 10^{36}$, $(7)\ 5.55 \times 10^{36}$

Also, at all temperatures $n_s = n_h - n_e$ (8)

From equation (5) for $n_e n_h$ and (8) for $n_h - n_e$ we may now calculate n_e and n_h separately at all temperatures.

For temperatures at which R = 0 we obtain:-

(6) $n_e = 1.05 \times 10^{18}$, $n_h = 1.75 \times 10^{18}$
(7) $n_e = 1.82 \times 10^{18}$, $n_h = 3.05 \times 10^{18}$

Now at R = 0, the Hall constant is given by

$$R = -7.4 \times 10^{18} (n_e C^2 - n_h) / (n_e C + n_h)^2 = 0 \qquad (9)$$

where $C = \mu e/\mu h$

Therefore, at these temperatures, $C = \sqrt{n_h/n_e}$ = (6) 1.29 (7) 1.30

We will take C = 1.3.

(c) The critical temperature (T_c) for the transition from non-degenerate to degenerate conditions is that for which the energy of an electron or hole corresponding to the energy at the surface of the Fermi distribution is equal to KT_c.

We thus have:-

$$T_c = (h^2/8\ Km)\ (3/\pi)^{2/3}\ n^{2/3} = 4.2 \times 10^{-11}\ n^{2/3} \qquad (10)$$

A plot of T_c against n is given in Fig.13.

(d) Using the relationships

$$R = -7.4 \times 10^{18}\ (n_e C^2 - n_h)/(n_e C + n_h)^2 \qquad (11)$$

and $n_e - n_h = n_s$

We may now calculate n_e and n_h separately at all temperatures for the non-degenerate samples.

For the degenerate samples we may substitute the numerical factor 6.25 in place of 7.4 in equation (9)

For samples which are on the border-line between degenerate and non-degenerate we may use a weighted mean of the two numerical factors.

In the lattice scattering range we take C = 1.3

In the impurity scattering range we take C = 1

In the transitional range a weighted mean (obtained graphically) must be used. In practice this variation of C makes only a slight difference in the cases of some of the alloys over a range where $n_e \approx n_h$ corresponds with the transitional region.

The values obtained for n_e and n_h are given in Tables 54 and 55. The values of $n_e + n_h$ are given in

Table 56 and in fig.12. The boundary between the degenerate and non-degenerate samples is shown by plotting T_c.

It is seen that the number of charge carriers increases exponentionally in the intrinsic range and is constant in the impurity range.

(e) Using the relationships

$$\sigma = en_e\mu_e + en_h\mu_h \qquad (13)$$

and $$\mu_e = 1.3 \times \mu_h \qquad (14)$$

we may now calculate values for μ_e and μ_h in the lattice-scattering range.

In the impurity-scattering range we must take $\mu_e = \mu_h$.

For intermediate ranges we must take a weighted mean of the numerical ratios 1.3 and 1.0. (Found graphically). (In practice this makes only a slight difference and then only when $n_e \approx n_h$ in the intermediate range). The results are given in Table 57 and in Fig.15.

It is seen that in the lattice-scattering range μ_e and μ_h are given by the equations:-

$$\mu_{eL} = 11.6 \times 10^6 T^{-3/2} \qquad (15)$$

$$\mu_{hL} = 8.9 \times 10^6 T^{-3/2} \qquad (16)$$

Impurity scattering gives rise to lower mobilities and the greater the number of impurity atoms the smaller the mobility.

6. DISCUSSION

6.1. Concentrations of Electrons and Holes

The values of n_e and n_h as functions of temperature given in Tables 54 and 55 were calculated from the Hall constant and the requirement for electrical neutrality, namely that the difference of n_e and n_h must be equal to the number of charge carriers introduced by the addition of impurity atoms in substitutional positions in the grey tin lattice.

They may also be calculated without knowing the Hall constant by making use of the theoretical equation (5) for the product $n_e n_h$. The values so calculated come out to be within the limits of experimental error in the measurement of the Hall constant throughout the entire range of temperature.

In the case of silicon, Pearson and Bardeen (9) did not obtain such close agreement and therefore cast doubt on the adequacy of the theory of the Hall effect in the intrinsic range. In the case of grey tin the theory seems to be quite adequate.

6.2. Mobilities of Electrons and Holes

For the non-degenerate samples the mobilities of electrons and holes approach the same values at high temperatures for all impurity concentrations. This is due to lattice scattering and it is found that μ varies as $T^{-3/2}$.

At lower temperatures impurity scattering becomes important, although the temperature range investigated did not extend sufficiently low for an accurate evaluation to be made of this effect. Making a rough comparison with the impurity scattering observed in silicon alloys by Pearson and Bardeen (9) it is remarkable that in grey tin the scattering by impurity atoms seems to be less effective by a factor of about 100. The reason for this is not at all apparent.

For the degenerate samples the mobility should be relatively insensitive to temperature, and this is seen to be generally true, although alloy (3) which should be degenerate at low temperatures shows a significant decrease in mobility at low temperatures i.e. it seems to behave as though it were non-degenerate.

6.3. Tin-Gallium-Antimony Alloy

This alloy has a comparatively large impurity

content, but only a small number of charge carriers owing to the mutual neutralization of n- and p-type impurity centres. The p-type impurities are in slight excess.

The conductivity-temperature relation is unusual in that the slope of $\log \sigma / T^{-1}$ is not constant in the intrinsic range (fig.8).

The Hall constant has the value one would expect from the difference in the Sb and Ga contents. The mobility approximates to the value one would expect from the sum of the Sb and Ga contents. It would thus appear that neutral scattering atoms are just as effective as ionized ones.

6.4 Tin-Lead Alloy

Although the impurity concentration is comparatively large the number of free charge carriers produced is small and the Hall constant is therefore large. The mobility corresponds to approximately what one would expect from the added impurity concentration, so that a much larger proportion of the lead must go into substitutional positions than is effective as a carrier producer.

The simplest assumption to make would be that lead itself contained an impurity (e.g. antimony) which

was the effective electron-producing agent, while the lead remained only a neutral scattering agent. However about 10% of impurity in the lead would be required, and in fact spectroscopically pure lead was used.

6.5. Variation of Conductivity and Hall Constant in a Magnetic Field

(a) Conductivity

At low fields we have (26,27)

$$(\sigma_o - \sigma)/\sigma_o = \frac{9\pi}{64} \cdot (4 - \pi).\mu^2 H^2 \qquad (17)$$

Values of $(\sigma_o - \sigma)/\sigma_o$ are given in Tables 25 and 26 for alloys (1) and (6) and are plotted against H in Figs. 16 and 17. It is seen that at low fields the H^2 law is obeyed but at higher fields the relationship falls to a lower power of H.

From the values in the low-field region an estimate of the mobility of the charge carriers may be obtained. Introducing numerical values into equation (17) and changing from e.s.u. to practical units, we obtain

$$(\sigma_o - \sigma)/\sigma_o = 0.38\ \mu^2 H^2 \times 10^{-16} \qquad (18)$$

Values of mobility calculated from this equation are given in Table 58. It is seen that much

higher values of mobility are obtained by this method, especially at low temperatures. Also that the mobility of holes appears to be higher than that of electrons. These effects have also been observed by Pearson and Suhl (26) in germanium. They are due to the anisotropic nature of the magneto-resistance effect. In place of σ_o in the above equations we should really have σ_1 where σ_1 is the conductivity in a longitudinal magnetic field. In certain directions in the crystal this is nearly the same as σ_o, but in some directions it is significantly different (comparable with σ) Equation (18) will thus lead to a too high value for the mobility.

(b) Hall constant

Electronic theory gives a similar formula for the variation of the Hall constant with transverse magnetic field

$$(R_o - R)/R_o = \frac{9\pi^2}{64} \mu^2 H^2 \qquad (19)$$

or in practical units

$$(R_o - R)/R_o = 1.38 \mu^2 H^2 \times 10^{-16} \qquad (20)$$

Values of $(R_o - R)/R_o$ are given in Tables 49 and 50 for alloys (1) and (6) and are plotted against H in

Figs. 16 and 17. It is seen that at low field an H^2 law is obeyed, but at higher fields the relationship falls to a lower power of H (even lower than in the case of the megneto-resistance effect).

From the values in the low-field region an estimate of the mobility of the charge-carriers may be obtained, and these are given in Table 58. It is seen that the values in general agree with those estimated from the magneto-resistance effect.

7. CONTACT RECTIFICATION

The elements silicon and germanium show contact rectification, and germanium exhibits transistor action, it therefore seemed possible that grey tin would also exhibit these properties and the following investigation was carried out to determine the current/voltage characteristics of a contact between grey tin and a metal.

EXPERIMENTAL

A crystalline piece of spectroscopically pure grey tin (approximately 30mm^3.) was held in a brass cup and a cat's-whisker contact was made to it with copper wire 0.2 mm. diameter. This wire was pressed on to the tin by a weak spring. Current was passed through the combination and the voltage drop measured, by means of a potentiometer, from the cat's-whisker to the copper cup.

This gives the voltage drop across two grey tin-metal contacts in series, but since the area of the cat's-whisker contact was much smaller than the cup contact the bulk of the resistance was concentrated there. See fig.18 for the experimental arrangement.

The resistance of the combination was very dependent on contact pressure. Without the grey tin (i.e. with the cat's-whisker pressing directly on the brass cup) the following results were obtained:-

		mA	mV	Resistance (ohms)
(1)	Very light pressure	5.20	90.00	17
(2)	Pressure approximately as used on grey tin	5.60	20.00	3.58
(3)	Heavy pressure	5.65	7.425	1.30
(4)	Cat's-whisker wire soldered to cup.	5.75	0.80	0.14

With the grey tin in place the following results were obtained:-

A. EXPERIMENTAL RESULTS: TEMPERATURE = 15°C

1. Probe positive			2. Probe negative		
μA.	μV	Resistance (ohms)	μA	μV	Resistance (ohms)
4.2	11	2.62	4.0	10	2.50
9.0	24	2.66	9.25	25	2.70
12.4	30	2.42	17.6	43	2.44

1. Probe positive			2. Probe negative		
μA	μV	Resistance (ohms)	μA	μV	Resistance (ohms)
31.2	82	2.63	43.5	117	2.69
96.2	252	2.62	97.5	258	2.65
142	368	2.59	144	375	2.61
388	1043	2.69	380	1005	2.65
670	1775	2.65	650	1720	2.65
1200	3200	2.67	1050	2780	2.65
2540	6700	2.64	2500	6600	2.64

B. EXPERIMENTAL RESULTS: TEMPERATURE = -196°C

1. Probe positive			2. Probe negative		
μA	μV	Resistance (ohms)	μA	μV	Resistance (ohms)
3.0	10.0	3.33	2.4	8.0	3.34
4.8	16.5	3.44	5.1.	17.0	3.33
9.35	32.0	3.42	9.5	32.0	3.37
14.1	47.5	3.37	14.7	49.5	3.37
18.6	62.5	3.36	19.5	65	3.34
23.3	79	3.39	24.2	82	3.39
55.8	190	3.40	57.5	195	3.39
82.0	278	3.39	90.0	305	3.39
220	738	3.36	240	815	3.39
418	1420	3.40	435	1480	3.40
685	2325	3.39	705	2400	3.40
1210	4120	3.40	1410	4780	3.39
2520	8550	3.39	2550	8650	3.39

CONCLUSIONS

The change in resistance on going from room temperature to -196°C. is probably to be ascribed to a consequent change in contact pressure and has no other significance. It is not necessary to plot out the results on a graph to see that

there is no non-linearity of current/voltage. It was hoped that at low temperature and small voltage drop across the contact some non-linearity might have been apparent, but this is not the case.

It is concluded that grey tin is too nearly metallic to show non-linearity under the experimental conditions used. Non-linearity might however be observed if even purer grey tin could be obtained and if the measurements were carried out at liquid hydrogen temperature. It is also concluded that there is in these circumstances little point in attempting to construct a transistor with grey tin at present.

8. THERMO-ELECTRIC EFFECT

No quantitative measurements of the Thermo-electric co-efficient of grey tin alloys were attempted; but a brief qualitative confirmation was made of the sign of the co-efficient in n and p type alloys respectively.

The experimental arrangement is shown in figure 19. The cylindrical specimen of grey tin was placed between two copper blocks as shown and the bottom block was cooled by pouring liquid nitrogen into the containing vessel. The temperature difference across the grey tin specimen was not measured, and the results given in the table below therefore have no quantitative significance.

The e.m.f. was measured with a potentiometer.

	Specimen	Thermo-electric e.m.f (mV)
(1)	Pure tin	+ 2.8
(3)	.028% Sb	+ 8.3
(4)	.074% Sb	+ 7.8
(8)	.081% Ga	- 2.6
(9)	.322% Ga	- 1.9
(10)	.063% Ga) .056% Sb)	- 3.0

TABLE 1

ALLOYS PREPARED

Alloy specimen:	Impurity	Atomic %	Time for transformation (days)
A	"Spectroscopically pure" (Unseeded)	0.0	No change
B	Aluminium (Accelerated method)	0.11	15
C	"Spectroscopically pure" (Seeded)	0.0	6
D	"Chempur" tin (Capper-Pass) (Seeded)	0.0	14
	(All subsequent specimens seeded)		
24	"Spectroscopically pure"	0.0	5
32	-do-	0.0	5
62	-do-	0.0	6
4	Aluminium	19.5	No change
56	-do-	1.54	-do-
15	-do-	0.45	7
25	-do-	0.16	6
52	Gallium	0.57	28
51	-do-	0.40	20
67	-do-	0.322	21
37	-do-	0.150	7
68	-do-	0.0806	10
69	-do-	0.0119	7

TABLE 1 (Continued)

Alloy specimen:	Impurity :	Atomic %	: Time for transformation (days)
70	Gallium	0.0060	6
44	Indium	0.44	No change
45	-do-	0.19	-do-
35	Thallium	0.091	No change
55	-do-	0.0154	-do-
41	-do-	0.0100	~120
54	-do-	0.0052	40
53	-do-	0.0017	8
1	Arsenic	2.85	No change
13	-do-	0.60	-do-
23	-do-	0.043	30
5	Antimony	1.92	No change
7	-do-	1.67	-do-
11	-do-	0.71	~ 365
50	-do-	0.310	~ 100
48	-do-	0.0740	29
20	-do-	0.046	14
46	-do-	0.0279	15
65	-do-	0.0143	14
49	-do-	0.013	10
47	-do-	0.0059	10
6	Bismuth	1.33	No change

TABLE 1 (Continued)

Alloy specimen	Impurity	Atomic %	Time for transformation (days
16	Bismuth	0.42	No change
22	-do-	0.029	44
3	Lead	1.26	No change
12	-do-	0.79	-do-
21	-do-	0.047	-do-
66	-do-	0.025	~ 365
42	-do-	0.0056	~ 175
14	Copper	0.66	14
36	Nickel	0.175	14
31	Cadmium	0.092	21 *
33	Zinc	0.163	16 *
34	Magnesium	0.175	18 *
38	Silver	0.083	18 *
61	(Gallium (Antimony	0.12) 0.12)	15
64	(Gallium (Antimony	0.063) 0.056)	7

* These alloys remained unchanged for one year. They were then unsealed and subsequent transformation after exposure to the air took place in the time stated. Possibly the initial "seeding" was ineffective due to

the alloy specimen being inadvertently warmed. It was noted that a while after grey tin had first been made in the laboratory simple exposure to the air was thereafter quite sufficient as a seeding process.

Note: Chemical analysis by the suppliers of the "spectroscopically pure" tin gave the following results:

Lead	0.0012%	Antimony	0.001%
Iron	0.00027%	Copper	0.0002%
Arsenic	0.0002%	Bismuth	0.0001%
Sulphur	0.0003%	Tin	99.997% (By difference)

TABLE 2

ALLOYS STUDIED

1 Sample	2 Impurity	3 Atomic % Added	4 Atoms/cc added	5 Carriers/cc at low temp.	6 Sign of Carriers	7 Carriers due to added impurity	8 Carriers/Atoms
			COMPOSITIONS OF TIN ALLOYS				
(1)	-	0	0	3.25×10^{17}	-	0	-
(2)	Sb	0.0143	4.18×10^{18}	2.52×10^{18}	-	2.20×10^{18}	0.53
(3)	Sb	0.0279	8.17	4.08	-	3.76	0.46
(4)	Sb	0.0740	2.16×10^{19}	8.47	-	8.15	0.38
(5)	Sb	0.310	9.07	2.16×10^{19}	-	2.13×10^{19}	0.24
(6)	Ga	0.0060	1.76×10^{18}	7.0×10^{17}	+	1.02×10^{18}	0.58
(7)	Ga	0.0119	3.48	1.24×10^{18}	+	1.56	0.45
(8)	Ga	0.0806	2.36×10^{19}	8.15	+	8.48	0.36
(9)	Ga	0.322	9.42	2.70×10^{19}	+	2.73×10^{19}	0.29
(10)	Ga	0.063	1.84×10^{19}				
	Sb	0.056	1.63×10^{19}				
Difference			2.1×10^{18}	4.40×10^{17}	+	7.65×10^{17}	0.36
(11)	Pb	0.025	7.32×10^{18}	8.00×10^{17}	-	4.75×10^{17}	0.065

TABLE 3

CONDUCTIVITY - EXPERIMENTAL RESULTS - ALLOY (1)

		H=0	500	700	1000	1500	2000	3000	4000	5000	6000	8000 (Gauss)
$10^3/T$	Current (amps)	Voltage (mV)										
13	.352	1.665	1.682	1.708	1.760	1.862	1.985	2.225	2.440	2.660	2.825	3135
12	.352	1.770	1.795	1.820	1.850	1.964	2.125	2.340	2.560	2.770	2.912	3.280
11	.352	1.875	1.850	1.832	1.805	2.065	2.175	2.410	2.598	2.785	2.985	3.355
10	.352	1.860	1.880	1.892	1.925	2.005	2.102	2.265	2.438	2.600	2.770	3.102
9	.352	1.755	1.762	1.775	1.792	1.850	1.915	2.038	2.185	2.310	2.405	2.650
8	.450	1.782	1.790	1.800	1.818	1.845	1.885	1.975	2.045	2.150	2.220	2.360
7	.505	1.528	1.532	1.540	1.550	1.572	1.590	1.638	1.700	1.760	1.805	1.965
6.5	.600	1.545	1.552	1.555	1.562	1.578	1.600	1.642	1.682	1.718	1.752	1.820
6	.600	1.332	1.335	1.338	1.340	1.345	1.360	1.385	1.410	1.435	1.468	1.512
5.5	.704	1.320	1.322	1.325	1.328	1.332	1.338	1.348	1.362	1.378	1.392	1.425
5	.755	1.185	1.185	1.185	1.188	1.190	1.192	1.195	1.208	1.218	1.225	1.245
4.5	.850	1.122	1.122	1.122	1.125	1.125	1.128	1.130	1.140	1.148	1.155	1.172
4	.950	1.032	1.032	1.032	1.032	1.032	1.035	1.038	1.042	1.048	1.050	1.065
3.5	1.005	.911	.911	.911	.911	.912	.912	.913	.915	.917	.921	.928

TABLE 4

CONDUCTIVITY - EXPERIMENTAL RESULTS - ALLOY (2)

		H=0	500	700	1000	1500	2000	3000	4000	5000	6000	8000 (gauss)
$10^3/T$	Current (amp)	Voltage (mV)										
13	.800	.942	.944	.948	.956	.975	.997	1.022	1.050	1.074	1.096	1.129
12	.800	.936	.938	.943	.950	.969	.992	1.017	1.044	1.070	1.092	1.128
11	.800	.942	.945	.949	.956	.975	.998	1.025	1.055	1.080	1.100	1.140
10	.800	.951	.954	.957	.966	.984	1.000	1.030	1.061	1.082	1.106	1.145
9	.800	.968	.972	.975	.985	1.002	1.016	1.042	1.072	1.093	1.119	1.148
8	.800	1.009	1.011	1.015	1.019	1.035	1.049	1.077	1.095	1.114	1.132	1.158
7	.800	1.059	1.061	1.068	1.066	1.072	1.085	1.107	1.129	1.150	1.165	1.190
6.5	.800	1.096	1.095	1.098	1.102	1.109	1.118	1.139	1.155	1.175	1.190	1.223
6	.800	1.121	1.122	1.125	1.128	1.131	1.138	1.153	1.170	1.183	1.197	1.220
5.5	.800	1.122	1.124	1.125	1.127	1.129	1.133	1.145	1.158	1.170	1.175	1.195
5	.800	1.055	1.055	1.056	1.058	1.060	1.062	1.068	1.076	1.085	1.095	1.108
4.5	.905	1.082	1.084	1.085	1.085	1.086	1.089	1.092	1.100	1.106	1.115	1.128
4	.950	.974	.974	.975	.975	.976	.978	.980	.983	.987	.993	1.004
3.5	1.055	.900	.901	.901	.902	.902	.903	.905	.907	.910	.912	.916

TABLE 5

CONDUCTIVITY - EXPERIMENTAL RESULTS - ALLOY (3)

		H=0	500	700	1000	1500	2000	3000	4000	5000	6000	8000 (Gauss)
$10^2/T$	Current (amps)	Voltage (mV)										
13	.945	.935	.936	.937	.939	.944	.954	.968	.978	.987	.996	1.010
12	.945	.890	.891	.894	.896	.903	.914	.928	.942	.953	.960	.975
11	.945	.882	.883	.884	.886	.894	.907	.920	.935	.942	.949	.968
10	.945	.876	.878	.881	.883	.892	.903	.918	.935	.944	.954	.978
9	.945	.888	.890	.892	.900	.903	.914	.932	.946	.958	.975	.998
8	.945	.902	.904	.905	.907	.915	.926	.944	.958	.970	.980	1.005
7	.945	.934	.935	.937	.940	.945	.957	.983	.990	1.000	1.009	1.026
6.5	.945	.969	.970	.972	.974	.978	.985	1.002	1.018	1.030	1.042	1.060
6	.945	.994	.995	.997	.998	1.002	1.007	1.020	1.035	1.047	1.060	1.075
5.5	.945	1.008	1.009	1.010	1.011	1.013	1.015	1.029	1.038	1.050	1.058	1.070
5	.945	1.005	1.005	1.006	1.007	1.008	1.010	1.018	1.028	1.035	1.045	1.055
4.5	.945	.982	.982	.983	.983	.984	.985	.988	.995	1.002	1.010	1.023
4.[illegible]	1.000	.940	.941	.942	.942	.942	.944	.946	.949	.953	.960	.972
3.5	1.090	.907	.907	.907	.908	.908	.908	.910	.912	.915	.918	.925

TABLE 6

CONDUCTIVITY - EXPERIMENTAL RESULTS - ALLOY (4)

		H=0	1500	2000	3000	4000	5000	6000	8000 (gauss)
$10^3/T$	Current (amps)	Voltage (mV)							
13	1.150	.852	.854	.856	.862	.866	.872	.880	.890
12	1.150	.860	.862	.864	.870	.876	.882	.886	.898
11	1.150	.870	.872	.874	.878	.885	.890	.895	.906
10	1.150	.885	.886	.888	.894	.900	.905	.910	.920
9	1.075	.884	.845	.846	.849	.856	.861	.866	.876
8	1.075	.869	.871	.873	.876	.882	.885	.890	.901
7	1.075	.900	.900	.901	.905	.912	.916	.921	.932
6.5	1.050	.894	.894	.895	.899	.903	.908	.914	.923
6	1.050	.913	.914	.915	.918	.923	.927	.932	.942
5.5	1.050	.933	.934	.935	.936	.940	.945	.952	.962
5	1.050	.903	.904	.905	.907	.911	.915	.920	.930
4.5	1.075	.882	.882	.883	.885	.887	.890	.894	.903
4	1.150	.894	.894	.895	.896	.898	.902	.906	.915
3.5	1.150	.868	.868	.869	.870	.872	.874	.874	.880

TABLE 7

CONDUCTIVITY - EXPERIMENTAL RESULTS - ALLOY (5)

		H=0	2000	3000	4000	5000	6000	8000 (gauss)
$10^3/T$	Current (amps)	Voltage (mV)						
13	1.400	.709	.710	.711	.712	.714	.716	.721
12	1.400	.723	.724	.725	.726	.727	.729	.735
11	1.400	.737	.737	.739	.740	.741	.744	.747
10	1.400	.747	.747	.748	.750	.751	.753	.757
9	1.400	.762	.762	.763	.764	.766	.768	.772
8	1.400	.778	.778	.779	.780	.782	.784	.788
7	1.300	.743	.743	.744	.745	.746	.748	.752
6.5	1.300	.760	.760	.761	.762	.763	.764	.767
6	1.300	.776	.776	.777	.778	.780	.781	.784
5.5	1.250	.775	.775	.776	.777	.777	.778	.782
5	1.250	.794	.794	.795	.795	.796	.798	.800
4.5	1.250	.794	.794	.794	.795	.796	.798	.800
4	1.300	.776	.776	.776	.777	.778	.780	.782
3.5	1.400	.788	.788	.788	.789	.790	.792	.795

TABLE 8

CONDUCTIVITY - EXPERIMENTAL RESULTS - ALLOY (6)

		H=0	500	700	1000	1500	2000	3000	4000	5000	6000	8000 (gauss)
$10^3/T$	Current (amps)	Voltage (mV)										
13	.400	1.095	1.115	1.135	1.170	1.250	1.335	1.525	1.650	1.800	1.925	2.110
12	.400	1.210	1.230	1.250	1.290	1.370	1.470	1.630	1.800	1.925	2.080	2.280
11	.400	1.345	1.360	1.380	1.420	1.510	1.600	1.775	1.930	2.080	2.200	2.460
10	.400	1.500	1.510	1.530	1.560	1.650	1.740	1.910	2.050	2.200	2.320	2.580
9	.400	1.590	1.595	1.605	1.630	1.685	1.790	1.900	1.950	2.100	2.230	2.430
8	.400	1.480	1.490	1.500	1.510	1.545	1.585	1.675	1.755	1.850	1.940	2.050
7	.500	1.540	1.540	1.545	1.550	1.575	1.605	1.675	1.750	1.840	1.890	2.020
6.5	.550	1.520	1.520	1.525	1.530	1.540	1.560	1.600	1.640	1.670	1.710	1.815
6	.600	1.430	1.430	1.435	1.440	1.445	1.460	1.490	1.525	1.560	1.590	1.650
5.5	.650	1.300	1.300	1.300	1.302	1.305	1.310	1.322	1.340	1.360	1.375	1.420
5	.750	1.250	1.250	1.250	1.250	1.258	1.255	1.265	1.275	1.290	1.300	1.320
4.5	.800	1.085	1.085	1.085	1.085	1.090	1.092	1.095	1.102	1.108	1.118	1.135
4	.925	1.022	1.022	1.022	1.022	1.025	1.025	1.028	1.030	1.035	1.040	1.050
3.5	1.000	.900	.900	.900	.900	.901	.901	.902	.904	.906	.910	.918

TABLE 9

CONDUCTIVITY - EXPERIMENTAL RESULTS - ALLOY (7)

		H=0	500	700	1000	1500	2000	3000	4000	5000	6000	8000 (gauss)
10 /T	Current (amps)	Voltage (mV)										
13	.500	1.020	1.030	1.050	1.070	1.135	1.205	1.325	1.455	1.540	1.620	1.725
12	.500	1.005	1.015	1.030	1.055	1.125	1.185	1.330	1.440	1.550	1.620	1.730
11	.500	1.030	1.045	1.055	1.080	1.140	1.195	1.320	1.435	1.540	1.615	1.750
10	.500	1.125	1.135	1.145	1.170	1.225	1.290	1.415	1.515	1.625	1.785	1.870
9	.500	1.235	1.245	1.255	1.275	1.315	1.370	1.480	1.530	1.640	1.740	1.900
8	.500	1.340	1.350	1.355	1.370	1.400	1.435	1.520	1.600	1.680	1.740	1.770
7	.500	1.300	1.305	1.310	1.310	1.315	1.330	1.370	1.410	1.430	1.470	1.560
6.5	.600	1.470	1.475	1.478	1.480	1.490	1.515	1.550	1.595	1.620	1.670	1.765
6	.600	1.298	1.298	1.300	1.305	1.308	1.325	1.355	1.385	1.410	1.440	1.490
5.5	.700	1.320	1.320	1.322	1.325	1.328	1.330	1.342	1.360	1.380	1.400	1.445
5	.800	1.265	1.265	1.268	1.265	1.270	1.275	1.280	1.290	1.302	1.315	1.335
4.5	.900	1.155	1.155	1.155	1.158	1.158	1.160	1.165	1.170	1.178	1.188	1.210
4	1.000	1.050	1.050	1.050	1.050	1.052	1.055	1.055	1.058	1.062	1.068	1.080
3.5	1.100	.947	.947	.947	.947	.948	.948	.949	.951	.953	.958	.965

TABLE 10

CONDUCTIVITY - EXPERIMENTAL RESULTS - ALLOY (8)

		H=0	700	1000	1500	2000	3000	4000	5000	6000	8000	(gauss)
$10^3/T$	Current (amps)	Voltage (mV)										
13	1.100	.847	.848	.850	.853	.858	.868	.880	.889	.897	.908	
12	1.100	.846	.847	.850	.854	.860	.872	.883	.892	.899	.911	
11	1.100	.847	.847	.849	.852	.858	.868	.880	.891	.897	.910	
10	1.100	.864	.865	.866	.868	.873	.885	.897	.905	.913	.926	
9	1.100	.872	.873	.875	.877	.883	.895	.906	.914	.921	.934	
8	1.100	.898	.899	.901	.904	.907	.921	.932	.943	.950	.964	
7	1.100	.918	.918	.920	.923	.927	.937	.951	.960	.968	.980	
6.5	1.100	.927	.928	.930	.932	.935	.948	.960	.968	.975	.986	
6	1.100	.947	.948	.950	.952	.954	.963	.973	.983	.993	1.002	
5.5	1.100	.979	.979	.980	.982	.984	.993	1.002	1.011	1.021	1.034	
5	1.100	1.020	1.020	1.020	1.022	1.024	1.029	1.040	1.051	1.059	1.073	
4.5	1.100	1.024	1.024	1.024	1.025	1.030	1.032	1.039	1.047	1.052	1.070	
4	1.100	.978	.978	.978	.979	.980	.981	.984	.990	.995	1.008	
3.5	1.100	.908	.908	.908	.908	.908	.910	.912	.914	.919	.926	

TABLE 11

CONDUCTIVITY - EXPERIMENTAL RESULTS - ALLOY (9)

		H=0	3000	4000	5000	6000	8000 (gauss)
$10^3/T$	Current (amps)	Voltage (mV)					
13	1.400	.700	.702	.704	.706	.708	.711
12	1.400	.705	.707	.710	.712	.714	.717
11	1.400	.710	.712	.714	.715	.717	.720
10	1.400	.714	.715	.717	.718	.720	.724
9	1.400	.718	.720	.721	.722	.725	.728
8	1.400	.728	.729	.731	.733	.735	.738
7	1.400	.747	.748	.749	.751	.753	.757
6.5	1.400	.756	.757	.759	.762	.762	.766
6	1.350	.778	.778	.779	.782	.784	.788
5.5	1.350	.794	.795	.797	.798	.800	.804
5	1.350	.805	.805	.807	.809	.811	.815
4.5	1.350	.817	.818	.820	.821	.823	.826
4	1.350	.823	.824	.825	.827	.829	.833
3.5	1.350	.817	.817	.818	.821	.823	.826

TABLE 12

CONDUCTIVITY - EXPERIMENTAL RESULTS - ALLOY (10)

		H=0	1500	2000	3000	4000	5000	6000	8000 (gau
$10^3/T$	Current (amps)	Voltage (mV)							
13	.275	3.860	3.875	3.920	3.975	4.025	4.060	4.110	4.180
12	.275	3.775	3.820	3.870	3.910	4.950	4.975	4.020	4.080
11	.275	3.650	3.690	3.750	3.790	3.840	3.860	3.880	3.910
10	.275	3.410	3.450	3.500	3.550	3.580	3.620	3.675	3.700
9	.300	3.130	3.170	3.210	3.250	3.290	3.310	3.360	3.390
8	.350	2.720	2.750	2.775	2.800	2.825	2.860	2.880	2.925
7	.400	2.025	2.040	2.050	2.075	2.105	2.120	2.135	2.175
6.5	.500	2.020	2.030	2.040	2.060	2.090	2.115	2.130	2.160
6	.550	1.670	1.675	1.680	1.690	1.715	1.740	1.755	1.770
5.5	.650	1.530	1.535	1.540	1.550	1.565	1.580	1.595	1.615
5	.700	1.275	1.280	1.280	1.285	1.300	1.312	1.320	1.340
4.5	.800	1.122	1.125	1.128	1.132	1.140	1.145	1.155	1.172
4	.900	1.000	1.000	1.000	1.002	1.005	1.010	1.015	1.028
3.5	1.050	.955	.956	.955	.957	.959	.961	.968	.975

TABLE 13

CONDUCTIVITY - EXPERIMENTAL RESULTS - ALLOY (11)

		H=0	1000	1500	2000	3000	4000	5000	6000	8000	(gauss)
$10^3/T$	Current (amps)	Voltage (mV)									
13	.400	2.580	2.585	2.590	2.615	2.640	2.680	2.702	2.720	2.765	
12	.400	2.515	2.520	2.535	2.555	2.590	2.620	2.640	2.660	2.690	
11	.400	2.455	2.460	2.675	2.500	2.530	2.565	2.580	2.605	2.650	
10	.400	2.350	2.355	2.365	2.390	2.420	2.460	2.475	2.490	2.525	
9	.400	2.220	2.230	2.240	2.260	2.280	2.310	2.330	2.350	2.380	
8	.450	2.140	2.140	2.150	2.165	2.200	2.230	2.250	2.270	2.300	
7	.500	1.755	1.760	1.765	1.775	1.795	1.815	1.835	1.850	1.875	
6.5	.550	1.595	1.600	1.605	1.615	1.635	1.655	1.670	1.685	1.700	
6	.600	1.450	1.455	1.460	1.465	1.480	1.495	1.510	1.520	1.540	
5.5	.700	1.385	1.390	1.395	1.400	1.415	1.430	1.440	1.450	1.470	
5	.750	1.220	1.220	1.225	1.225	1.235	1.245	1.255	1.265	1.290	
4.5	.850	1.135	1.135	1.135	1.140	1.145	1.155	1.160	1.170	1.185	
4	.950	1.025	1.025	1.028	1.030	1.032	1.035	1.040	1.045	1.060	
3.5	1.050	.934	.934	.935	.935	.936	.938	.940	.945	.950	

TABLE 14

CONDUCTIVITY OF ALLOY (1) ($ohm^{-1} cm^{-1}$)

$10^3/T$	H=0	500	700	1000	1500	2000	3000	4000	5000	6000	8000 (gauss)
13	845	835	825	800	755	710	630	575	530	500	450
12	795	785	780	760	715	660	600	550	510	485	430
11	750	740	735	720	680	650	585	540	505	470	420
10	755	750	745	730	700	670	620	575	540	510	455
9	805	800	795	785	760	735	690	645	610	585	530
8	1010	1010	1000	990	975	955	915	880	840	815	760
7	1320	1320	1310	1305	1290	1270	1230	1190	1150	1120	1025
6.5	1550	1550	1545	1540	1520	1500	1460	1430	1400	1370	1320
6	1800	1800	1800	1790	1780	1760	1730	1700	1670	1640	1590
5.5	2130	2130	2130	2130	2120	2110	2080	2060	2040	2020	1970
5	2550	2550	2550	2550	2540	2540	2520	2500	2480	2460	2420
4.5	3030	3030	3030	3030	3030	3020	3010	2980	2960	2940	2900
4	3680	3680	3680	3680	3680	3670	3670	3650	3630	3620	3570
3.5	4410	4410	4410	4410	4410	4410	4400	4390	4380	4360	4330

TABLE 15

CONDUCTIVITY OF ALLOY (2)

$10^3/T$:	H=0 :	500 :	700 :	1000 :	1500 :	2000 :	3000	4000 :	5000 :	6000 :	8000 (gauss)
13	3400	3390	3370	3340	3280	3210	3130	3050	2980	2920	2830
12	3420	3410	3390	3360	3300	3220	3140	3060	2990	2930	2830
11	3400	3390	3370	3340	3280	3210	3120	3030	2960	2900	2800
10	3360	3350	3340	3310	3250	3200	3100	3020	2960	2890	2800
9	3300	3290	3280	3250	3200	3150	3070	2980	2930	2860	2790
8	3170	3160	3150	3140	3090	3050	2970	2920	2870	2830	2760
7	3020	3020	3010	3000	2980	2950	2890	2840	2780	2750	2690
6.5	2920	2920	2920	2910	2885	2860	2810	2770	2720	2690	2620
6	2850	2850	2850	2840	2830	2815	2775	2740	2705	2675	2630
5.5	2850	2850	2850	2845	2835	2825	2795	2765	2740	2720	2680
5	3030	3030	3030	3030	3025	3015	2995	2970	2950	2920	2890
4.5	3340	3340	3340	3340	3340	3330	3315	3300	3270	3250	3210
4	3900	3900	3900	3900	3900	3890	3880	3970	3850	3830	3780
3.5	4680	4680	4680	4680	4680	4680	4670	4660	4650	4630	4600

TABLE 16

CONDUCTIVITY OF ALLOY (3)

10^{5}/T	H=0	500	700	1000	1500	2000	3000	4000	5000	6000	8000 (gauss)
13	4050	4050	4040	4030	4000	3960	3910	3870	3830	3800	3740
12	4250	4240	4240	4220	4190	4140	4075	4020	3970	3940	3880
11	4300	4290	4285	4270	4230	4175	4110	4050	4020	3990	3910
10	4320	4310	4300	4290	4240	4190	4120	4050	4010	3970	3870
9	4260	4250	4245	4230	4190	4140	4060	4000	3950	3880	3790
8	4200	4190	4190	4175	4130	4080	4010	3950	3900	3860	3770
7	4050	4050	4040	4030	4000	3950	3890	3820	3780	3750	3680
6.5	3900	3900	3890	3885	3865	3840	3775	3720	3670	3630	3570
6	3800	3800	3790	3790	3775	3755	3700	3650	3610	3570	3510
5.5	3750	3750	3750	3740	3730	3720	3675	3640	3600	3580	3530
5	3760	3760	3760	3760	3750	3740	3710	3680	3655	3620	3580
4.5	3850	3850	3850	3850	3840	3840	3825	3800	3770	3750	3700
4	4250	4250	4250	4250	4250	4240	4230	4220	4200	4170	4120
3.5	4800	4800	4800	4800	4800	4800	4790	4780	4770	4750	4710

TABLE 17

CONDUCTIVITY OF ALLOY (4)

$10^3/T$	H=0	1500	2000	3000	4000	5000	6000	800
13	5400	5390	5370	5340	5300	5270	5230	5170
12	5350	5340	5325	5290	5250	5220	5190	5130
11	5290	5280	5270	5240	5200	5170	5140	5080
10	5200	5190	5180	5150	5120	5090	5060	5000
9	5100	5090	5080	5060	5025	5000	4970	4910
8	4950	4940	4930	4910	4880	4860	4830	4770
7	4780	4775	4770	4750	4720	4700	4675	4620
6.5	4700	4700	4690	4670	4650	4625	4600	4550
6	4600	4600	4590	4575	4550	4530	4510	4460
5.5	4500	4500	4490	4480	4460	4440	4410	4370
5	4650	4650	4640	4630	4610	4590	4570	4520
4.5	4880	4880	4870	4860	4850	4830	4810	4760
4	5150	5150	5140	5130	5120	5100	5080	5030
3.5	5300	5300	5300	5290	5280	5270	5260	5230

TABLE 18

CONDUCTIVITY OF ALLOY (5)

$10^3/T$:	H=0 :	2000 :	3000 :	4000 :	5000 :	6000 :	8000 (gauss)
13	7900	7890	7880	7870	7840	7820	7760
12	7750	7740	7730	7720	7700	7680	7620
11	7600	7600	7580	7570	7560	7540	7500
10	7500	7500	7490	7470	7460	7440	7400
9	7350	7350	7340	7330	7310	7290	7250
8	7200	7200	7190	7180	7160	7150	7110
7	7000	7000	6990	6980	6970	6950	6920
6.5	6850	6850	6840	6830	6820	6810	6770
6	6700	6700	6690	6680	6670	6660	6630
5.5	6450	6450	6440	6430	6430	6420	6390
5	6300	6300	6290	6290	6280	6270	6250
4.5	6300	6300	6300	6290	6280	6270	6250
4	6700	6700	6700	6690	6680	6670	6650
3.5	7100	7100	7100	7090	7080	7070	7050

TABLE 19

CONDUCTIVITY OF ALLOY (6)

$10^3/T$	H = 0	500	700	1000	1500	2000	3000	4000	5000	6000	8000 (gauss)
13	1460	1435	1410	1370	1275	1200	1050	970	890	835	760
12	1320	1300	1280	1240	1170	1090	975	890	830	775	700
11	1190	1175	1160	1130	1060	1000	905	830	775	725	655
10	1070	1060	1045	1025	980	920	840	780	725	690	620
9	1010	1005	995	980	950	915	845	800	760	720	655
8	1080	1075	1070	1060	1035	1010	955	905	865	835	780
7	1300	1300	1295	1290	1270	1245	1195	1140	1095	1060	985
6.5	1450	1450	1445	1440	1430	1410	1375	1340	1320	1285	1210
6	1680	1680	1675	1670	1660	1645	1610	1575	1545	1510	1460
5.5	2000	2000	2000	1995	1990	1985	1965	1940	1915	1890	1830
5	2400	2400	2400	2400	2390	2390	2375	2350	2330	2310	2280
4.5	2950	2950	2950	2950	2940	2940	2930	2905	2890	2865	2820
4	3620	3620	3620	3620	3620	3620	3610	3600	3580	3560	3520
3.5	4450	4450	4450	4450	4450	4450	4440	4430	4420	4390	4340

TABLE 20

CONDUCTIVITY OF ALLOY (7)

$10^3/T$	H=0	500	700	1000	1500	2000	3000	4000	5000	6000	8000 (gauss)
13	1960	1940	1910	1870	1760	1660	1510	1375	1300	1235	1160
12	1990	1965	1940	1895	1780	1690	1510	1390	1290	1235	1155
11	1940	1920	1895	1855	1760	1670	1515	1395	1300	1240	1145
10	1780	1760	1745	1710	1630	1550	1410	1320	1230	1120	1070
9	1620	1610	1595	1570	1520	1460	1350	1310	1220	1150	1050
8	1490	1480	1475	1460	1430	1395	1320	1250	1190	1150	1075
7	1540	1535	1530	1530	1520	1500	1460	1420	1400	1360	1285
6.5	1630	1625	1625	1620	1605	1585	1545	1505	1485	1440	1360
6	1850	1850	1845	1840	1835	1810	1770	1735	1700	1665	1610
5.5	2120	2120	2120	2115	2110	2105	2085	2055	2030	2000	1940
5	2530	2530	2530	2530	2520	2510	2500	2480	2455	2435	2400
4.5	3120	3120	3120	3120	3120	3110	3095	3085	3060	3030	2980
4	3810	3810	3810	3810	3810	3800	3800	3790	3770	3750	3700
3.5	4650	4650	4650	4650	4650	4650	4640	4630	4620	4590	4560

TABLE 21

CONDUCTIVITY OF ALLOY (8)

$10^3/T$	H=0	700	1000	1500	2000	3000	4000	5000	6000	8000 (gauss)
13	5200	5190	5180	5160	5130	5060	5000	4950	4910	4850
12	5200	5190	5180	5160	5120	5050	4990	4940	4900	4830
11	5200	5190	5180	5160	5130	5060	5000	4940	4910	4830
10	5100	5090	5080	5060	5030	4970	4900	4860	4820	4750
9	5050	5050	5030	5020	4990	4920	4860	4820	4780	4710
8	4900	4900	4890	4870	4850	4780	4720	4670	4640	4570
7	4800	4800	4790	4770	4750	4700	4630	4590	4550	4490
6.5	4750	4750	4740	4730	4710	4650	4590	4550	4520	4470
6	4650	4650	4640	4630	4620	4575	4525	4480	4440	4390
5.5	4500	4500	4500	4480	4470	4430	4390	4350	4310	4260
5	4320	4320	4320	4310	4300	4280	4230	4190	4160	4100
4.5	4300	4300	4300	4300	4280	4270	4240	4210	4180	4110
4	4500	4500	4500	4500	4500	4490	4475	4450	4425	4370
3.5	4850	4850	4850	4850	4850	4840	4830	4820	4790	4750

TABLE 22

CONDUCTIVITY OF ALLOY (9)

$10^3/T$	H=0	3000	4000	5000	6000	8000 (gauss)
13	8000	7980	7960	7940	7920	7880
12	7950	7930	7900	7880	7860	7820
11	7900	7880	7860	7840	7820	7780
10	7850	7840	7800	7780	7780	7740
9	7800	7780	7760	7750	7720	7700
8	7700	7680	7660	7650	7620	7580
7	7500	7480	7470	7450	7540	7400
6.5	7400	7400	7370	7350	7350	7300
6	7200	7200	7180	7150	7140	7100
5.5	7050	7050	7020	7020	7000	6960
5	6950	6950	6930	6910	6900	6870
4.5	6850	6850	6830	6820	6800	6770
4	6800	6800	6780	6760	6750	6720
3.5	6850	6850	6850	6820	6800	6770

TABLE 23

CONDUCTIVITY OF ALLOY (10)

$10^3/T$	H=0	1500	2000	3000	4000	5000	6000	8000
13	285	285	280	275	275	270	270	265
12	290	290	285	280	275	275	275	270
11	300	300	295	290	285	285	285	280
10	320	320	315	310	305	305	300	300
9	380	380	375	370	365	360	355	355
8	515	510	505	500	495	490	485	480
7	790	785	780	770	760	755	750	735
6.5	990	985	980	970	955	945	940	925
6	1320	1315	1310	1300	1280	1265	1255	1245
5.5	1700	1695	1690	1675	1660	1640	1630	1610
5	2200	2190	2190	2180	2155	2135	2120	2090
4.5	2850	2850	2840	2830	2810	2795	2770	2730
4	3600	3600	3600	3590	3580	3560	3540	3500
3.5	4400	4400	4400	4390	4380	4370	4340	4310

TABLE 24

CONDUCTIVITY OF ALLOY (11)

$10^3/T$	H=0	1000	1500	2000	3000	4000	5000	6000	8000 (gauss)
13	620	620	615	610	605	595	590	590	580
12	635	635	630	625	615	610	605	600	595
11	650	650	645	640	630	625	620	615	605
10	680	680	675	670	660	650	645	640	635
9	720	720	715	710	700	690	685	680	670
8	840	840	835	830	815	805	800	795	785
7	1140	1135	1135	1125	1110	1100	1090	1080	1070
6.5	1380	1375	1370	1365	1345	1330	1320	1310	1295
6	1660	1655	1650	1640	1620	1605	1590	1580	1560
5.5	2020	2020	2010	2005	1980	1960	1945	1930	1905
5	2460	2460	2450	2450	2430	2410	2390	2375	2330
4.5	3000	3000	3000	2990	2975	2950	2930	2910	2870
4	3700	3700	3700	3690	3685	3670	3650	3640	3590
3.5	4500	4500	4500	4500	4490	4480	4470	4450	4420

TABLE 25

VARIATION OF $(\sigma_o - \sigma)/\sigma_o$ WITH FIELD ALLOY (1)

$10^3/T$: H = 0 :	500 :	700 :	1000 :	1500 :	2000 :	3000 :	4000 :	5000 :	6000 :	8000 (gauss)
13	0.012	0.024	0.053	0.106	0.160	0.254	0.32	0.37	0.41	0.47
12	0.0125	0.019	0.044	0.100	0.170	0.245	0.31	0.36	0.39	0.46
11	0.013	0.020	0.040	0.093	0.133	0.220	0.28	0.325	0.37	0.44
10	0.007	0.013	0.033	0.073	0.113	0.180	0.24	0.285	0.325	0.40
9	0.006	0.0125	0.025	0.056	0.087	0.143	0.20	0.24	0.27	0.34
8		0.010	0.020	0.035	0.055	0.094	0.13	0.17	0.195	0.25
7		0.0075	0.011	0.023	0.038	0.068	0.10	0.13	0.15	0.225
6.5		0.003	0.0065	0.019	0.032	0.058	0.077	0.10	0.115	0.15
6			0.0055	0.011	0.022	0.039	0.056	0.072	0.09	0.117
5.5				0.005	0.0095	0.0235	0.033	0.042	0.052	0.075
5				0.004	0.004	0.012	0.020	0.0275	0.035	0.051
4.5					0.003	0.0065	0.0165	0.023	0.030	0.043
4					0.003	0.003	0.008	0.0135	0.016	0.030
3.5						0.002	0.0045	0.007	0.011	0.018

TABLE 26

VARIATION OF $(\sigma_0 - \sigma)/\sigma_0$ WITH FIELD ALLOY (6)

$10^3/T$: H =500	700	1000	1500	2000	3000	4000	5000	6000	8000
13	0.017	0.034	0.062	0.125	0.18	0.28	0.335	0.39	0.43	0.48
12	0.015	0.030	0.060	0.114	0.175	0.26	0.325	0.37	0.415	0.47
11	0.0125	0.025	0.050	0.109	0.16	0.24	0.30	0.35	0.39	0.45
10	0.0095	0.023	0.042	0.084	0.14	0.215	0.27	0.32	0.355	0.42
9	0.005	0.015	0.030	0.060	0.095	0.165	0.19	0.25	0.29	0.35
8	0.0045	0.0093	0.0185	0.042	0.065	0.115	0.16	0.20	0.225	0.28
7		0.004	0.0077	0.023	0.042	0.081	0.123	0.16	0.185	0.24
6.5		0.0035	0.007	0.014	0.0275	0.052	0.076	0.090	0.115	0.165
6		0.003	0.006	0.009	0.021	0.042	0.0625	0.080	0.100	0.13
5.5			0.0025	0.005	0.0075	0.0175	0.030	0.0425	0.055	0.085
5				0.004	0.004	0.010	0.021	0.029	0.0375	0.050
4.5				0.0035	0.0035	0.007	0.015	0.020	0.029	0.044
4						0.0028	0.0055	0.011	0.0165	0.028
3.5						0.0022	0.0045	0.007	0.0125	0.020

TABLE 27

HALL E.M.F - EXPERIMENTAL RESULTS - ALLOY (1)

$10^3/T$:	H =400 E.M.F μV	: 500	: 600	: 700	: 1000	: 1500	: 2000	: 3000	: 4000	: 5000	: 6000	: 8000
13	48.0	58.0	68.5	78.5	107	152	194	269	338	400	455	568
12	47.5	57.0	67.5	78.0	107	151	187	264	342	410	470	585
11	43.0	52.0	61.5	71.0	98	139	177	249	320	382	442	560
10	35.0	42.5	50.5	58.0	80	115	146	208	264	320	370	470
9	23.5	28.5	33.5	39.0	54.0	77.5	100	144	185	222	260	330
8	14.3	19.0	22.5	26.5	37.0	55.0	71.5	103	132	160	188	244
7	8.5	10.5	12.5	15.0	21.0	30.5	40.0	59.0	77.0	94	110	140
6.5	7.0	9.0	11.0	12.5	17.5	26.0	34.0	50.0	65.0	80	95	120
6	4.5	5.5	7.0	8.0	11.0	16.5	22.0	33.0	42.0	52.0	61.0	80
5.5	3.5	4.5	5.5	6.0	8.5	13.0	17.0	25.5	33.5	42.0	50.0	64.5
5	2.5	3.5	4.0	4.5	6.5	10.0	12.5	19.0	25.0	31.0	37.0	48.0
4.5	2.0	2.5	3.0	3.0	4.5	7.0	9.0	13.5	18.0	22.5	27.0	35.0
4	1.5	2.0	2.5	2.5	4.0	5.5	7.5	11.0	15.0	18.5	22.0	29.0
3.5	1.0	1.0	1.5	2.0	2.5	3.5	5.0	7.0	9.5	12.0	14.5	19.0

TABLE 28

HALL E.M.F. - EXPERIMENTAL RESULTS - ALLOY (2)

$10^3/T$:	H = 500 E.M.F. (μV)	: 700	: 1000	: 1500	: 2000	: 3000	: 4000	: 5000	: 6000	: 8000 (gauss)
13	18.5	25.0	35.0	50.5	65	94	122	145	170	218
12	18.5	25.0	35.0	50.0	65	94	119	144	170	212
11	18.5	25.0	35.0	51.0	64	93	121	145	172	215
10	18.5	25.0	35.0	50.5	65	93	122	148	175	215
9	18.5	25.5	35.5	50.5	65	95	122	150	175	225
8	18.0	24.5	34.0	50.0	66	95	123	148	174	215
7	16.0	22.0	31.0	46.0	61	88	113	138	160	202
6.5	14.0	19.5	28.0	40.0	53	78	101	125	144	182
6	11.5	16.0	23.0	34.0	44	67	83	104	123	160
5.5	9.0	12.5	18.0	27.0	35.0	51	67	85	101	128
5	6.0	8.0	11.5	17.0	23.0	34.0	42	53	63	80
4.5	4.5	6.0	8.5	13.0	17.5	26.5	35.0	42	50	65
4	3.0	4.0	6.0	9.0	12.0	18.0	25.0	30.0	37	48
3.5	2.0	3.0	4.0	6.0	8.0	12.5	17.0	21.0	25.0	34.0

TABLE 29

HALL E.M.F - EXPERIMENTAL RESULTS - ALLOY (3)

$10^3/T$	H=500 E.M.F (μV)	700	1000	1500	2000	3000	4000	5000	6000	8000 (gauss)
13	13.0	18.5	26.0	38.0	50	73	95	118	138	180
12	13.5	19.0	27.0	39.0	51	74	96	120	140	182
11	13.5	19.0	27.0	39.5	51.5	75	96	122	140	180
10	13.5	19.0	27.0	39.0	51.5	75	97	120	140	180
9	13.5	19.0	27.0	39.0	51	73	95	120	138	182
8	13.0	18.5	26.5	38.0	50	73	95	116	138	178
7	12.5	17.5	25.0	36.0	47.5	69	91	110	134	170
6.5	12.0	17.0	24.0	35.0	46	67	87	108	128	165
6	11.0	15.0	21.5	32.0	42.5	62	80	99	115	152
5.5	10.0	13.5	19.5	29.0	38.5	57	74	91	106	140
5	7.5	10.5	15.0	22.0	30.0	44	58	71	84	110
4.5	5.5	7.5	10.5	15.5	21.0	31.0	41	51	60	75
4	3.0	4.5	6.5	9.5	12.5	19.0	25	31	37	50
3.5	2.0	3.0	4.5	6.5	8.5	13.0	17.0	21	25	34

TABLE 30

HALL E.M.F - EXPERIMENTAL RESULTS - ALLOY (4)

$10^3/T$	H = 500 E.M.F (μV)	700	1000	1500	2000	3000	4000	5000	6000	8000 (gauss)
13	7.0	9.5	14.0	21	28	42	55	64	78	105
12	7.0	9.5	13.5	20.5	27.5	41	54	63	75	102
11	7.0	9.5	13.5	20	27	40	54	64	75	100
10	7.0	9.5	13.5	20	27	40	52	64	76	100
9	6.5	9.0	13.0	19.5	26	39	51	63	74	98
8	6.5	9.0	13.0	19.0	26	38	50	62	72	95
7	6.5	9.0	12.5	19.0	25.5	38	50	62	70	92
6.5	6.5	9.0	12.5	18.5	25.0	37	50	62	72	92
6	6.0	9.0	12.0	18.0	24.0	36	49	61	72	90
5.5	6.0	8.5	12.0	17.5	23.5	35	47	59	70	88
5	6.0	8.0	11.5	17.0	23.0	35	46	57	68	85
4.5	5.0	7.0	10.0	15.0	20.5	31	41	50	61	80
4	4.5	6.5	9.0	13.5	18	27	36	45	55	70
3.5	3.0	4.5	6.5	9.5	12.5	19	25	32	38	50

TABLE 31

HALL E.M.F - EXPERIMENTAL RESULTS - ALLOY (5)

$10^3/T$:	H= 1000 : E.M.F (μ.V)	2000 :	4000 :	8000 (gauss)
13	6.5	14.0	27.5	53
12	6.5	13.0	27	54
11	7.0	14.0	27	54
10	6.5	13.5	27	53
9	6.5	13.0	26	55
8	7.0	13.0	27	52.5
7	6.0	12.0	25	50
6.5	6.0	12.5	24	50
6	6.0	12.0	24	48
5.5	6.0	12.0	24	47
5	6.0	11.5	23	46
4.5	5.5	11.0	22	43
4	5.0	10.5	20.0	42
3.5	5.0	10.0	19.5	40

TABLE 32

HALL E.M.F - EXPERIMENTAL RESULTS - ALLOY (6)

$10^3/T$: H = E.M.F (μV) : 500	700	1000	1500	2000	3000	4000	5000	6000	8000 (gauss)
13	31.5	42.0	57.0	80	99	138	178	214	242	305
12	31.0	42.0	57.5	81	103	143	180	216	249	315
11	31.0	42.0	58.0	81.5	104	146	184	222	256	322
10	28.0	38.5	55.0	75	92	136	173	210	242	305
9	21.5	29.5	42.0	58.0	75	107	137	166	195	245
8	12.5	17.5	25.0	35.0	46.0	67	86	106	125	160
7	5.0	7.0	10.0	15.0	20.0	28.5	37.5	45.5	54.0	70
6.5	2.0	3.0	4.5	6.5	8.5	12.5	16.0	19.5	23.5	30.5
6	.5	1.0	1.0	2.0	2.5	3.5	4.5	5.5	6.5	8.5
5.5					-1.0	-2.0	-2.0	-2.5	-3.0	-4.0
5	-1.0	-1.5	-2.0	-3.0	-3.5	-5.5	-7.0	-9.0	-10.0	-13.5
4.5	-1.0	-1.5	-2.0	-3.0	-4.0	-6.5	-8.5	-10.0	-13.0	-16.0
4	-1.0	-1.5	-2.0	-3.0	-4.5	-6.5	-9.0	-11.0	-13.0	-17.5
3.5	-1.0	-1.5	-2.0	-3.0	-4.0	-5.5	-7.5	-9.5	-11.5	-15.0

TABLE 33

HALL E.M.F - EX ERIMENTAL RESULTS - ALLOY (7)

$10^3/T$	H = 500 E.M.F (μ.V)	700	1000	1500	2000	3000	4000	5000	6000	8000 (gauss)
13	24.0	32.0	44	62	80	112	144	170	200	255
12	24.0	32.0	44	62	79	112	144	166	200	252
11	23.5	31.5	44	62	80	112	142	165	196	250
10	22.5	30.5	42	60	76	110	140	165	194	247
9	20.0	27.5	37	54	70	100	126	155	180	230
8	16.0	21.5	30	44	57	83	110	133	156	215
7	9.0	12.5	18.0	26.0	34	50	65	81	95	125
6.5	6.5	9.5	13.5	19.5	25.5	37	49	61	72	95
6	3.5	4.5	6.5	10.0	13.5	19.5	26.0	31.0	37	48
5.5	1.5	2.5	3.5	5.0	6.5	10.0.	13.0	16.0	19.0	24.5
5					1.0	2.0	2.5	3.0	4.0	5.0
4.5			-1.0	-1.5	-2.0	-3.0	-4.0	-5.0	-6.0	-8.0
4		-1.0	-1.5	-2.5	-3.0	-5.0	-6.5	-8.0	-9.5	-12.5
3.5		-1.0	-1.5	-2.0	-3.0	-4.0	-6.0	-7.0	-8.5	-11.0

TABLE 34

HALL E.M.F - EXPERIMENTAL RESULTS - ALLOY (8)

$10^3/T$:	H=700 E.M.F (μV) :	1000 :	1500 :	2000 :	3000 :	4000 :	5000 :	6000 :	8000 (gauss)
13	9.0	13.0	19.5	25.0	36	48	61	70	
12	9.0	13.5	19.5	25.5	37	48	61	70	
11	9.0	13.0	20.0	25.5	37	49	62	72	
10	9.5	13.5	20.0	26.0	38	48	62	72	
9	9.0	13.5	20.0	26.0	38.5	50	62	73	
8	9.5	13.0	19.5	27.0	38	50	62	74	
7	9.0	13.0	19.0	26.0	38	51	61	74	
6.5	8.5	12.5	19.5	25.5	39	50	63	73	
6	9.0	12.5	19.0	25.0	38	48	61	70	
5.5	8.5	12.0	18.5	24.0	36	47	60	68	
5	7.5	11.0	16.0	21.0	32	42	52	61	
4.5	6.0	9.0	13.0	17.5	26	34	43	52	
4	4.0	5.5	8.0	10.0	15.5	21	26	31	
3.5	2.0	2.5	4.0	5.0	8.0	10.0	13.0	15.5	

TABLE 35

HALL E.M.F - EXPERIMENTAL RESULTS - ALLOY (9)

$10^3/T$:	H = 1000 : E.M.F (m.V)	2000 :	4000 :	8000 (gauss)
13	5.0	10.0	20.0	40. 0.
12	5.0	10.0	20.0	40.5
11	5.0	10.5	21.0	41.5
10	5.5	10.5	21.0	41.0
9	5.0	10.0	21.5	42.0
8	5.0	10.0	21.0	41.0
7	5.5	9.5	20.5	40.0
6.5	5.0	10.0	20.0	40.5
6	5.0	10.0	20.0	39.0
5.5	5.0	10.0	19.5	39.0
5	5.0	9.5	19.5	38.5
4.5	5.0	9.5	19.0	37.5
4	4.5	8.5	17.0	34.0
3.5	4.0	8.0	15.5	31.0

TABLE 36

HALL E.M.F - EXPERIMENTAL RESULTS - ALLOY (10)

$10^3/T$	H =500 E.M.F. (μV)	700	1000	1500	2000	3000	4000	5000	6000	8000 (gauss)
13	36	50	72	107	140	207	268	332	390	512
12	35	49	70	104	136	200	260	320	380	495
11	33	46	65	97	128	188	244	300	355	465
10	28	39	56	83	109	160	209	258	305	398
9	25	29.5	41.5	62	82	119	157	193	228	300
8	13.0	18.0	25.5	38	50	73	97	120	140	185
7	5.5	8.0	11.5	17.0	22.0	32.5	43	54	63	81
6.5	4.5	6.5	9.0	13.5	17.5	26	34	43	50	66
6	2.5	3.5	5.5	8.0	10.5	15.0	20.0	24.5	29.5	38
5.5	1.5	2.5	3.5	5.0	6.5	10.0	13.0	16.0	18.5	24.5
5	1.0	1.5	2.0	3.0	4.0	6.0	7.5	9.0	10.5	14.0
4.5							-1.0	-1.0	-1.5	-2.0
4		-1.0	-1.5	-2.0	-3.0	-4.0	-5.5	-7.0	-8.5	-11.5
3.5	-1.0	-1.5	-2.0	-3.0	-4.0	-6.0	-7.5	-10.0	-12.5	-16.0

TABLE 37

HALL E.M.F - EXPERIMENTAL RESULTS - ALLOY (11)

$10^3/T$:	H=500 E.M.F (μV)	700	1000	1500	2000	3000	4000	5000:	6000	8000 (gauss)
13	29.5	41.5	59	88	115	170	222	272	322	420
12	29.0	41.0	58	87	114	168	220	268	318	415
11	29.0	40.5	57	86	113	166	216	265	315	410
10	27.5	38.5	55	82	107	158	207	255	300	395
9	24.0	33.5	48	72	95	140	181	222	262	345
8	20.5	28.5	41	60	80	118	153	188	222	290
7	13.5	19.0	27.0	39.0	53	79	105	125	150	195
6.5	11.0	15.0	22.0	33.0	43	63	83	102	120	158
6	8.0	11.5	16.0	24.0	32.0	47	62	76	90	118
5.5	6.0	8.5	12.0	18.5	24.5	36	47	58	70	90
5	4.0	5.5	8.0	12.5	16.5	25.0	32.5	40	48	62
4.5	3.5	4.5	6.5	10.0	13.5	20.0	27.0	33.5	39	51
4	2.5	3.0	4.5	7.0	9.0	13.5	18.0	22.5	27.0	35.0
3.5	1.0	2.0	3.0	4.5	6.0	9.5	12.0	15.5	18.0	24.0

TABLE 38

HALL CONSTANT OF ALLOY (1)

10^3 /T	H =400	500	600	700	1000	1500	2000	3000	4000	5000	6000	8000 (gauss)
13	21.5	21.1	20.7	20.4	19.4	18.4	17.6	16.3	15.4	14.5	13.8	12.9
12	21.2	20.8	20.4	20.2	19.4	18.3	17.0	16.0	15.6	14.9	14.2	13.3
11	19.2	19.0	18.7	18.4	17.9	16.8	16.1	15.1	14.5	13.9	13.4	12.7
10	15.7	15.5	15.3	15.1	14.5	13.9	13.3	12.6	12.0	11.6	11.2	10.7
9		10.3	10.2	10.1	9.8	9.4	9.1	8.7	8.4	8.1	7.85	7.5
8					5.2	5.1	5.0	4.8	4.6	4.5	4.4	4.25
7					2.6	2.55	2.5	2.45	2.4	2.35	2.3	2.2
6.5							1.8	1.75	1.7	1.7	1.65	1.6
6								1.15	1.1	1.1	1.07	1.05
5.5									0.75	0.75	0.74	0.72
5										0.52	0.51	0.50
4.5											0.33	0.33
4												0.24
3.5												0.15

TABLE 39

HALL CONSTANT OF ALLOY (2)

$10^3/T$:	H=500 :	700 :	1000 :	1500 :	2000 :	3000 :	4000 :	5000 :	6000 :	8000 (gauss)
13	2.9	2.8	2.75	2.65	2.55	2.45	2.4	2.3	2.25	2.2
12	2.9	2.8	2.75	2.6	2.55	2.45	2.35	2.3	2.25	2.15
11	2.9	2.8	2.75	2.65	2.55	2.45	2.4	2.3	2.25	2.2
10	2.9	2.8	2.75	2.65	2.55	2.45	2.4	2.35	2.3	2.2
9	2.9	2.85	2.8	2.65	2.55	2.5	2.4	2.35	2.3	2.3
8	2.8	2.75	2.7	2.6	2.6	2.5	2.4	2.35	2.3	2.2
7	2.5	2.5	2.45	2.4	2.4	2.3	2.2	2.15	2.1	2.05
6.5		2.2	2.2	2.1	2.1	2.05	2.0	1.95	1.9	1.8
6			1.8	1.8	1.75	1.75	1.65	1.65	1.6	1.6
5.5				1.4	1.4	1.35	1.35	1.35	1.35	1.25
5					.90	.90	.85	.85	.85	.80
4.5						.60	.60	.60	.60	.55
4									.40	.40
3.5										.25

TABLE 40

HALL CONSTANT OF ALLOY (3)

$10^3/T$:	H =500 :	700 :	1000 :	1500 :	2000 :	3000 :	4000 :	5000 :	6000 :	8000 (gauss)
13	1.75	1.75	1.75	1.70	1.65	1.65	1.60	1.55	1.55	1.50
12		1.80	1.80	1.75	1.70	1.65	1.60	1.60	1.55	1.55
11		1.80	1.80	1.75	1.70	1.65	1.60	1.60	1.55	1.50
10		1.80	1.80	1.75	1.70	1.65	1.60	1.60	1.55	1.50
9		1.80	1.80	1.75	1.70	1.65	1.60	1.60	1.55	1.55
8		1.75	1.75	1.70	1.65	1.65	1.60	1.55	1.55	1.50
7		1.65	1.65	1.60	1.60	1.55	1.50	1.45	1.45	1.40
6.5		1.60	1.60	1.55	1.55	1.50	1.45	1.45	1.40	1.40
6			1.45	1.45	1.40	1.40	1.35	1.30	1.30	1.25
5.5				1.30	1.30	1.25	1.25	1.20	1.20	1.15
5					1.00	1.00	.95	.95	.95	.90
4.5							.70	.70	.65	.65
4									.40	.40
3.5									.25	.25

TABLE 41

HALL CONSTANT OF ALLOY (4)

$10^3/T$:	H =500 :	700 :	1000 :	1500 :	2000 :	3000 :	4000 :	5000 :	6000 :	8000 (gauss)
13					.75	.75	.70	.70	.70	.70
12						.75	.75	.70	.70	.70
11						.75	.75	.70	.70	.70
10						.75	.75	.70	.70	.70
9						.75	.75	.70	.70	.70
8						.75	.75	.70	.70	.70
7							.75	.75	.70	.70
6.5							.75	.75	.70	.70
6								.75	.70	.70
5.5								.70	.70	.65
5								.70	.70	.65
4.5									.60	.60
4									.50	.50
3.5									.35	.35

TABLE 42

HALL CONSTANT OF ALLOY (5)

$10^3/T$	R	No observable change with field
13	.30	
12	.30	
11	.30	
10	.30	
9	.30	
8	.30	
7	.30	
6.5	.30	
6	.30	
5.5	.30	
5	.30	
4.5	.27	
4	.25	
3.5	.22	

TABLE 43

HALL CONSTANT OF ALLOY (6)

$10^3/T$:	H=500	700	1000	1500	2000	3000	4000	5000	6000	8000 (gauss)
13	9.9	9.5	8.95	8.4	7.8	7.25	7.0	6.75	6.35	6.0
12	9.8	9.5	9.0	8.5	8.1	7.5	7.1	6.8	6.55	6.2
11	9.8	9.5	9.1	8.55	8.2	7.65	7.25	7.0	6.75	6.35
10	8.9	8.7	8.3	7.9	7.6	7.15	6.8	6.6	6.35	6.0
9	6.7	6.6	6.4	6.1	5.9	5.6	5.4	5.25	5.1	4.85
8		3.9	3.8	3.7	3.65	3.5	3.4	3.35	3.3	3.15
7				1.25	1.25	1.2	1.18	1.15	1.13	1.10
6.5					0.50	0.47	0.45	0.45	0.45	0.44
6								0.12	0.11	0.11
5.5										-0.05
5								-0.15	-0.14	-0.14
4.5									-0.17	-0.16
4										-0.15
3.5										-0.12

TABLE 44

HALL CONSTANT OF ALLOY (7)

$10^3/T$:	H=500 :	700 :	1000 :	1500 :	2000 :	3000 :	4000 :	5000 :	6000 :	8000 (gauss)
13	6.0	5.8	5.5	5.2	5.0	4.7	4.5	4.3	4.2	4.0
12	6.0	5.8	5.5	5.2	5.0	4.7	4.5	4.2	4.2	4.0
11	5.9	5.7	5.5	5.2	5.0	4.7	4.5	4.2	4.1	3.9
10	5.7	5.5	5.3	5.0	4.8	4.6	4.4	4.2	4.1	3.9
9	5.1	4.9	4.7	4.5	4.4	4.2	4.0	3.9	3.8	3.6
8	4.0	3.9	3.8	3.7	3.6	3.5	3.45	3.35	3.3	3.2
7	2.3	2.3	2.25	2.2	2.15	2.1	2.05	2.05	2.0	1.95
6.5		1.4	1.4	1.35	1.35	1.3	1.3	1.3	1.25	1.25
6			.70	.70	.70	.68	.68	.65	.65	.65
5.5					.30	.30	.30	.30	.28	.28
5										.05
4.5										-.07
4										-.10
3.5										-.08

TABLE 45

HALL CONSTANT OF ALLOY (8)

$10^3/T$:	H=700 :	1000 :	1500 :	2000 :	3000:	4000 :	5000 :	6000	8000 (gauss)
13	.75	.75	.75	.72	.70	.70	.70	.68	.65
12		.75	.75	.72	.70	.70	.70	.68	.65
11		.75	.75	.72	.70	.70	.70	.68	.65
10			.75	.75	.72	.70	.70	.68	.65
9			.75	.75	.72	.72	.70	.70	.68
8			.75	.75	.72	.72	.70	.70	.68
7			.75	.75	.72	.72	.70	.70	.68
6.5				.75	.75	.72	.72	.70	.70
6				.72	.72	.70	.70	.68	.68
5.5				.70	.70	.68	.68	.65	.65
5						.60	.60	.58	.55
4.5							.50	.50	.48
4								.30	.30
3.5								.15	.15

TABLE 46

HALL CONSTANT OF ALLOY (9)

$10^3/T$:	R :	No observable change with field
13	.23	
12	.23	
11	.23	
10	.23	
9	.23	
8	.23	
7	.23	
6.5	.23	
6	.23	
5.5	.23	
5	.23	
4.5	.22	
4	.20	
3.5	.18	

TABLE 47

HALL CONSTANT OF ALLOY (10)

10^3/T	H=500	700	1000	1500	2000	3000	4000	5000	6000	8000 (gauss)
13	16.5	16.5	16.4	16.25	16.0	15.8	15.4	15.2	14.9	14.7
12	16.0	16.0	15.9	15.75	15.55	15.3	14.95	14.7	14.5	14.2
11	15.0	15.0	14.9	14.8	14.6	14.35	14.0	13.8	13.6	13.35
10	12.8	12.8	12.7	12.6	12.45	12.25	12.0	11.8	11.6	11.4
9	8.8	8.8	8.75	8.7	8.6	8.45	8.25	8.1	8.0	7.85
8		4.6	4.6	4.55	4.5	4.4	4.35	4.3	4.2	4.15
7			1.8	1.8	1.75	1.7	1.7	1.7	1.65	1.6
6.5			1.15	1.15	1.10	1.10	1.08	1.08	1.05	1.05
6				.60	.60	.58	.57	.56	.56	.55
5.5					.32	.32	.31	.31	.30	.30
5						.17	.17	.16	.16	.16
4.5									-.02	-.02
4									-.10	-.10
3.5									-.12	-.12

TABLE 48

HALL CONSTANT OF ALLOY (11)

$10^3/T$:	H=500 :	700 :	1000 :	1500 :	2000 :	3000 :	4000 :	5000 :	6000 :	8000 (gauss)
13	9.3	9.3	9.3	9.2	9.1	8.9	8.75	8.55	8.45	8.3
12	9.2	9.2	9.15	9.1	9.0	8.8	8.65	8.45	8.35	8.2
11	9.1	9.1	9.0	9.0	8.9	8.7	8.5	8.35	8.3	8.1
10	8.7	8.7	8.65	8.6	8.45	8.25	8.15	8.0	7.9	7.75
9	7.6	7.6	7.6	7.55	7.45	7.3	7.15	7.0	6.9	6.8
8	5.7	5.7	5.7	5.6	5.6	5.5	5.35	5.25	5.2	5.1
7			3.4	3.4	3.35	3.3	3.2	3.15	3.15	3.05
6.5			2.5	2.5	2.45	2.4	2.4	2.35	2.3	2.25
6				1.7	1.7	1.65	1.6	1.6	1.6	1.55
5.5				1.1	1.1	1.08	1.06	1.05	1.05	1.01
5					.70	.70	.68	.67	.67	.65
4.5							.50	.50	.48	.47
4								.30	.30	.29
3.5									.18	.18

TABLE 49

VARIATION OF $(R_o - R)/R_o$ WITH FIELD ALLOY (1)

$10^3/T$:	H=400	500	600	700	1000	1500	2000	3000	4000	5000	6000	8000 (gauss)
13	0.027	0.045	0.063	0.077	0.124	0.167	0.20	0.26	0.30	0.34	0.375	0.415
12	0.027	0.046	0.064	0.072	0.110	0.160	0.22	0.27	0.28	0.32	0.35	0.39
11	0.025	0.035	0.051	0.066	0.091	0.147	0.18	0.23	0.26	0.295	0.32	0.355
10	0.019	0.031	0.044	0.056	0.094	0.131	0.17	0.21	0.25	0.275	0.30	0.33
9		0.028	0.038	0.047	0.075	0.113	0.14	0.18	0.21	0.235	0.26	0.29
8					0.037	0.056	0.074	0.11	0.15	0.165	0.185	0.21
7					0.037	0.056	0.074	0.093	0.11	0.13	0.15	0.185
6.5							0.053	0.079	0.105	0.105	0.13	0.16
6								0.042	0.083	0.083	0.11	0.125
5.5									0.062	0.062	0.075	0.10
5										0.054	0.072	0.091
4.5											0.057	0.057
4												0.040
3.5												

TABLE 50

VARIATION OF $(R_o - R)/R_o$ WITH FIELD ALLOY (6)

$10^3/T$: H=500 : 700 : 1000 : 1500 : 2000 : 3000 : 4000 : 5000 : 6000 : 8000 (gauss)
13 : 0.057 : 0.095 : 0.148 : 0.20 : 0.26 : 0.31 : 0.335 : 0.355 : 0.395 : 0.43
12 : 0.053 : 0.082 : 0.13 : 0.18 : 0.22 : 0.265 : 0.315 : 0.34 : 0.37 : 0.40
11 : 0.035 : 0.064 : 0.104 : 0.16 : 0.19 : 0.25 : 0.29 : 0.31 : 0.34 : 0.38
10 : 0.032 : 0.055 : 0.098 : 0.14 : 0.175 : 0.22 : 0.26 : 0.28 : 0.31 : 0.35
9 : 0.029 : 0.043 : 0.072 : 0.115 : 0.145 : 0.19 : 0.22 : 0.24 : 0.26 : 0.30
8 : : 0.025 : 0.050 : 0.075 : 0.088 : 0.125 : 0.15 : 0.16 : 0.175 : 0.21
7 : : : : 0.040 : 0.040 : 0.077 : 0.092 : 0.115 : 0.13 : 0.155
6.5 : : : : : 0.0 : 0.06 : 0.10 : 0.10 : 0.10 : 0.12
6 : : : : : : : : 0.0 : 0.08 : 0.08
5.5 : : : : : : : : : : 0.0
5 : : : : : : : : 0.0 : 0.07 : 0.07
4.5 : : : : : : : : : 0.0 : 0.06
4 : : : : : : : : : : 0.0
3.5 : : : : : : : : : : 0.0

TABLE 51

CONDUCTIVITY (Ohm^{-1} cm^{-1}) at zero field

$10^3/T$:	(1)	(2)	(3)	(4)	(5)	(6)	(7)	(8)	(9)	(10)	(11)
13	845	3400	4050	5400	7900	1460	1960	5200	8000	285	620
12	795	3420	4250	5350	7750	1320	1990	5200	7950	290	635
11	750	3400	4300	5290	7600	1190	1940	5200	7900	300	650
10	755	3360	4320	5200	7500	1070	1780	5100	7850	320	680
9	805	3300	4260	5100	7350	1010	1620	5050	7800	380	720
8	1010	3170	4200	4950	7200	1080	1490	4900	7700	515	840
7	1320	3020	4050	4730	7000	1300	1540	4800	7500	790	1140
6.5	1550	2920	3900	4700	6850	1450	1630	4750	7400	990	1380
6	1800	2850	3800	4600	6700	1680	1850	4650	7200	1320	1660
5.5	2130	2850	3750	4500	6450	2000	2120	4500	7050	1700	2020
5	2550	3030	3760	4650	6300	2400	2530	4320	6950	2200	2460
4.5	3030	3340	3850	4880	6300	2950	3120	4300	6850	2850	3000
4	3680	3900	4250	5150	6700	3620	3810	4500	6800	3600	3700
3.5	4410	4680	4800	5300	7100	4450	4650	4850	6850	4400	4500

TABLE 52

HALL CONSTANT (cm^3 / Coulomb) at zero field

$10^3/T$	(1) −	(2) −	(3) −	(4) −	(5) −	(6) +	(7) +	(8) +	(9) +	(10) +	(11) −
13	22.1	2.9	1.75	0.75	0.30	10.5	6.0	0.75	0.23	16.5	9.3
12	21.8	2.9	1.8	0.75	0.30	10.25	6.0	0.75	0.23	16.0	9.2
11	19.7	2.9	1.8	0.75	0.30	10.15	5.9	0.75	0.23	15.0	9.1
10	16.0	2.9	1.8	0.75	0.30	9.2	5.7	0.75	0.23	12.8	8.7
9	10.6	2.9	1.8	0.75	0.30	6.0	5.1	0.75	0.23	8.8	7.6
8	5.4	2.8	1.75	0.75	0.30	4.0	4.0	0.75	0.23	4.6	5.7
7	2.7	2.5	1.65	0.75	0.30	1.3	2.3	0.75	0.23	1.8	3.4
6.5	1.9	2.2	1.6	0.75	0.30	0.50	1.4	0.75	0.23	1.15	2.5
6	1.2	1.8	1.45	0.75	0.30	0.12	0.70	0.72	0.23	0.60	1.7
5.5	0.80	1.4	1.3	0.70	0.30	−0.05	0.30	0.70	0.23	0.32	1.1
5	0.55	0.90	1.00	0.70	0.30	−0.15	0.05	0.60	0.23	0.17	0.70
4.5	0.35	0.60	0.70	0.60	0.27	−0.17	−0.07	0.50	0.22	−0.02	0.50
4	0.25	0.40	0.45	0.50	0.25	−0.15	−0.10	0.30	0.20	−0.10	0.30
3.5	0.15	0.25	0.30	0.35	0.22	−0.12	−0.08	0.15	0.18	−0.12	0.18

TABLE 53

VALUES OF $n_e n_h$ AS A FUNCTION OF 1/T

$10^3/T$:	$n_e n_h$	: $\log (n_e n_h / T^3)$
13	7.22×10^{32}	27.20
12	1.96×10^{33}	27.53
11	5.32	27.85
10	1.515×10^{34}	28.18
9	4.34	28.50
8	1.29×10^{35}	28.82
7	4.03	29.14
6.5	7.27	29.30
6	1.34×10^{36}	29.46
5.5	2.45	29.61
5	4.82	29.78
4.5	9.56	29.94
4.	1.92×10^{37}	30.09
3.5	4.24	30.26

(Calculated from equation (5))

TABLE 54

NUMBER OF ELECTRONS (n_e)

$10^3/T$	(1)	(2)	(3)	(4)	(5)	(6)	(7)	(8)	(9)	(10)	(11)
13	3.28×10^{17}	2.5×10^{18}	4.2×10^{18}	8.5×10^{18}	2.1×10^{19}	-	-	-	-	2×10^{15}	8.0×10^{17}
12	3.30	2.5	4.1	8.5	2.1	2×10^{15}	-	-	-	5	8.05
11	3.40	2.5	4.1	8.5	2.1	7	1×10^{16}	-	-	1.2×10^{16}	8.1
10	3.65	2.5	4.1	8.5	2.1	2×10^{16}	2	-	-	3.2	8.2
9	4.25	2.5	4.1	8.5	2.1	6	4	-	-	8	8.5
8	5.7	2.6	4.2	8.5	2.1	1.5×10^{17}	1.0×10^{17}	-	-	2.0×10^{17}	9.4
7	8.2	2.7	4.25	8.5	2.1	3.8	3	-	-	4.6	1.18×10^{19}
6.5	1.00×10^{18}	2.8	4.3	8.5	2.1	5.5	5	-	-	6.1	1.32
6	1.3	3.0	4.4	8.5	2.1	9	8	1×10^{17}	-	9.6	1.6
5.5	1.7	3.2	4.6	9.0	2.1	1.2×10^{18}	1.1×10^{18}	2	-	1.4×10^{18}	2.0
5	2.4	3.8	5.0	9.0	2.1	1.9	1.6	5	-	2.0	2.6
4.5	3.1	4.4	5.6	9.4	2.2	2.6	2.4	9	2×10^{17}	2.7	3.3
4	4.6	5.8	6.9	1.0×10^{19}	2.25	4.1	3.9	1.8×10^{18}	7×10^{17}	4.2	4.8
3.5	6.7	7.8	8.8	1.2	2.4	6.1	6.6	3.8	1.5×10^{18}	6.3	6.9

TABLE 55

NUMBER OF HOLES (n_h)

10^3/T:	(1)	(2)	(3)	(4)	(5)	(6)	(7)	(8)	(9)	(10)	(11)
13	3×10^{15}	-	-	-	-	7.0×10^{17}	1.23×10^{18}	8.2×10^{16}	2.7×10^{19}	4.42×10^{17}	-
12	5	-	-	-	-	7.02	1.23	8.2	2.7	4.45	5×10^{15}
11	1.6×10^{16}	-	-	-	-	7.07	1.24	8.2	2.7	4.52	1×10^{16}
10	4.0	-	-	-	-	7.2	1.25	8.2	2.7	4.72	2
9	1.0×10^{17}	-	-	-	-	7.6	1.27	8.2	2.7	6.2	5
8	2.4	1×10^{17}	1×10^{17}	-	-	8.5	1.33	8.2	2.7	6.4	1.4×10^{17}
7	5.0	2	1.5	-	-	1.08×10^{18}	1.5	8.2	2.7	9.0	3.8
6.5	6.8	3	2	-	-	1.25	1.7	8.2	2.7	1.05×10^{18}	5.2
6	1.0×10^{18}	5	3	-	-	1.6	2.0	8.2	2.7	1.4	8
5.5	1.4	7	5	5×10^{17}	-	1.9	2.3	8.4	2.7	1.8	1.2×10^{18}
5	2.1	1.3×10^{19}	9	5	-	2.6	2.8	8.7	2.7	2.4	1.8
4.5	2.8	1.9	1.5×10^{18}	9	1×10^{18}	3.3	3.6	9.1	2.72	3.1	3.5
4	4.3	3.3	2.8	1.5×10^{18}	1.5	4.8	5.1	1.0×10^{19}	2.77	4.6	4.0
3.5	6.4	5.3	4.7	3.5	2	6.8	7.7	1.2	2.85	6.7	6.1

TABLE 56

NUMBER OF CHARGE CARRIERS $(n_e + n_h)$

$10^3/T$:	(1)	(2)	(3)	(4)	(5)	(6)	(7)	(8)	(9)	(10)	(11)
13	3.3×10^{17}	2.5×10^{18}	4.2×10^{18}	8.5×10^{18}	2.1×10^{19}	7.0×10^{17}	1.23×10^{18}	8.2×10^{18}	2.7×10^{19}	4.44×10^{17}	8.0×10^{17}
12	3.35	2.5	4.1	8.5	2.1	7.04	1.23	8.2	2.7	4.50	8.1
11	3.55	2.5	4.1	8.5	2.1	7.14	1.25	8.2	2.7	4.64	8.2
10	4.05	2.5	4.1	8.5	2.1	7.4	1.27	8.2	2.7	5.04	8.4
9	5.25	2.5	4.1	8.5	2.1	8.2	1.31	8.2	2.7	6.0	9.0
8	8.1	2.7	4.3	8.5	2.1	1.00×10^{18}	1.43	8.2	2.7	8.4	1.08×10^{18}
7	1.32×10^{18}	2.9	4.4	8.5	2.1	1.46	1.8	8.2	2.7	1.36×10^{18}	1.56
6.5	1.68	3.1	4.5	8.5	2.1	1.80	2.2	8.2	2.7	1.66	1.84
6	2.3	3.5	4.7	8.5	2.1	2.5	2.8	8.4	2.7	2.4	2.4
5.5	3.1	3.9	5.1	9.5	2.1	3.1	3.4	8.6	2.7	3.2	3.2
5	4.5	5.1	4.9	9.5	2.1	4.5	4.4	9.1	2.7	4.4	4.4
4.5	5.9	6.3	7.1	1.03×10^{19}	2.3	5.9	6.0	1.00×10^{19}	2.74	5.8	5.8
4	8.9	9.1	9.7	1.15	2.4	8.9	9.0	1.18	2.84	8.8	8.8
3.5	1.31×10^{19}	1.31×10^{19}	1.35×10^{19}	1.55	2.6	1.29×10^{19}	1.43×10^{19}	1.58	3.0	1.30×10^{19}	1.30×10^{19}

TABLE 57

MOBILITIES ($cm.volt^{-1}\ sec^{-1}$)

$10^3/T$	(1) μ_e	(2) μ_e	(3) μ_e	(4) μ_e	(5) μ_e	(6) μ_h	(7) μ_h	(8) μ_h	(9) μ_h	(10) μ_h	(11) μ_e
13	16000	8500	6050	3970	2350	13000	10000	3950	1850	4000	4850
12	14800	8550	6450	3930	2300	11700	10100	3950	1840	4000	4900
11	13300	8500	6550	3890	2250	10400	9700	3950	1830	4000	4950
10	11900	8400	6600	3820	2230	9000	8750	3900	1820	3950	5050
9	10000	8250	6500	3750	2180	7500	7650	3850	1800	3950	5000
8	8400	7400	6150	3650	2140	6400	6400	3750	1780	3800	4900
7	6800	6600	5800	3500	2080	5200	5100	3650	1740	3600	4700
6.5	6300	6000	5500	3450	2040	4600	4350	3600	1710	3700	4800
6	5400	5250	5150	3400	2000	3800	3850	3450	1660	3450	4500
5.5	4750	4750	4700	3250	1920	3600	3600	3250	1630	3250	4200
5	4000	3950	4100	3050	1870	2950	3200	2950	1600	3000	3800
4.5	3600	3550	3550	2950	1750	2750	2900	2700	1560	2800	3600
4	2900	2900	2900	2800	1750	2250	2300	2400	1500	2250	2900
3.5	2400	2450	2400	2200	1700	1900	1800	1900	1430	1850	2400

TABLE 58

MOBILITIES CALCULATED FROM:-

1. $(R_o - R) / R_o H^2 = 1.38 \mu_R^2 \times 10^{-16}$
2. $(\sigma_o - \sigma) / \sigma_o H^2 = 0.38 \mu_\sigma^2 \times 10^{-16}$
3. μ_e (from Section 5(e))
4. μ_h (from Section 5(e))
5. μ_m (mean mobility = $(n_e \mu_e + n_h \mu_h) / (n_e + n_h)$)

	ALLOY (1)				ALLOY (6)			
$10^3/T$	μ_R	μ_σ	μ_e	μ_m	μ_R	μ_σ	μ_h	μ_m
13	35000	35700	16000	16000	37000	41800	13000	13000
12	33400	33800	14800	14800	35000	39600	11700	11700
11	30600	32300	13300	13200	31000	36200	10400	10400
10	28100	28400	11900	11600	27500	32000	9000	9100
9	25400	25000	10000	9550	24000	27600	7500	7650
8	18000	20400	8400	7800	18500	21700	6400	6700
7	16300	16200	6800	6200	12000	15900	5200	5600
6.5	10400	15100	6300	5600		12600	4600	5100
6	6300	11200	5400	4700		10600	3800	4400
5.5	5000	7200	4750	4200		7200	3600	4000
5	4100	5600	4000	3500		5600	2950	3400
4.5	3200	4800	3600	3000	2600	4800	2750	3000
4	2100	3600	2900	2600		3400	2250	2550
3.5		2800	2400	2150		2800	1900	2100

REFERENCES

(1) Bijl, A.J. & Kolkmeijer, N.H., Proc.Acad.Sci. Amsterdam, 21, 405, 494 (1919)

(2) Brownlee, L.D., Nature 166, 482 (1950)

(3) de Haas, W.J., Sizoo, G.J. & Voogd, J., Proc.Acad.Sci. Amsterdam, 31, 350 (1928)

(4) Sharvin, G., J Phys., U.S.S.R., 9, 350 (1945)

(5) Moesveld, A.L., Z Phys.Chem., A178, 455 (1937)

(6) Busch,G., Wieland, J. & Zoller, H., Helv.Phys.Acta., 24 49 (1951), and Semi-Conducting Materials, Butterworth, p.188 (1951)

(7) Blum, A.I. & Goryunova, N.A., Doklady Akad.Nauk. (S.S.S.R.) 75, 367 (1950)

(8) Kendall, J.T., Proc.Phys.Soc., 63B, 821 (1950)

(9) Pearson, G.L & Bardeen,J., Phys.Rev., 75, 865 (1949)

(10) Cohen, E., Rev.Gen.Sci.Pur.Appl., 21, 523 (1910)

(11) Cohen, E. Chem.Weekblad., 24, 402 (1927)

(12) Cohen.E & Dekker, K.D., Z.Phys.Chem., 127, 178. 183 (1927)

(13) Cohen.E & Lieshout,A.K.,Z.Phys.Chem., A173, 1, 32 (1935)

(14) Tammann, G. & Dreyer,K.L.,Z.anorg.Chem., 199, 97 (1936)

(15) Cohen,E. & Lieshout,A.K., Z.Phys.Chem., A177, 331 (1936)

(16) Cohen,E. & Lieshout,A.K., Proc.Acad.Sci.Amsterdam, 39 352, 1174 (1936)

(17) Mason, C.W. & Forgeng,W.D., Metals and Alloys, 6, 87 (1935

(18) Cohen,E. & de Meester, W.A., Z.Phys.Chem., A183, 190 (1938 and Proc.Acad.Sci.Amsterdam,41, 462 (1938)

(19) Cohen,E., de Meester,W.A & Landsmann,J., Z.Phys.Chem., A181, 124 (1937)

(20) Homer & Watkins, Metal Industry (London), 60, 364 (1942)

REFERENCES (CONT'D)

(21) Heyn,E. & Wetzel,E., Z.Metallkunde, 14, 335 (1922)

(22) Kiplinger,C., J.Chem.Educ., 5, 964 (1928)

(23) Van Heteren, W.J., Z.anorg.Chem., 42, 129 (1904)

(24) Komar,A., J.Exp.Theor.Phys., U.S.S.R., 6, 256 (1936)

(25) Moss, T.S., Photo-conductivity in the Elements, Butterwath, (1952)

(26) Pearson, G.L. & Suhl,H., Phys.Rev., 83, 768 (1951)

(27) Estermann,I. & Foner,A., Phys.Rev., 79, 365 (1950)

(28) Isenberg I., Russell R.B. & Greene R.F., Rev.Sci.Instr. 19, 685 (1948)

PART III - ELECTRONIC CONDUCTION IN SILICON CARBIDE

CONTENTS PAGE

1. Introduction 106
2. Preparation of Pure Silicon Carbide 107
3. Preparation of Impure Silicon Carbide 113
4. Investigation of Electrical Properties 113
5. Preparation of Evaporated Films 115
6. Spectrographic Analyses 116
7. Theoretical Speculation 116
8. Tables I - II 125
9. References. 127

1. INTRODUCTION

Silicon carbide is a solid in which the bonding is intermediate between homopolar and heteropolar. It is similar in its properties to the typically homopolar substance diamond and has a similar crystal structure, but with half the carbon atoms replaced by silicon. Due to the different electron affinities of carbon and silicon, this gives rise to a certain degree of heteropolarity in the crystalline bonds. According to Pauling (1) the SiC bond in silicon carbide is approximately 12% ionic in character. It will be shown in the "Theoretical Speculation" below how this may help to explain semi-conductivity in silicon carbide.

It is noteworthy that electronic conduction in silicon carbide may be of n- or p-type. In the commercial material crystals which are coloured green are n-type conductors, and blue or black crystals are p-type. The commercial material is made in the same way as the original synthesis of Acheson in 1886 by heating together sand and coke in an electric furnace. Many impurities are introduced in this way - chiefly aluminium and iron - and an investigation by Lundquist (2) has indicated that aluminium as impurity may give rise to black p-type crystals, and that iron may give rise to green n-type crystals. The interpretation of Lundquist is not, however, clear-cut since all commercial

crystals contain considerable quantities of both iron and aluminium as well as other elements. Moreover, the preparation of pure silicon carbide by Kendall and Yeo (3) showed that the presence of impurities is not essential for semi-conductivity in silicon carbide.

The present research was, therefore, directed to the following points - (i) preparation of pure and impure specimens of silicon carbide (ii) determination of the type of semi-conductivity produced by changes in the conditions of formation of the crystals and by the introduction of specific impurities, (iii) spectrographic analysis of various specimens of commercial silicon carbide, with a view to determining the relevant impurities.

2. PREPARATION OF PURE SILICON CARBIDE

A method of preparing pure crystalline material has been described by Moers (4) and by Kendall and Yeo (3). Briefly, a carbon filament 0.025 cm. in diameter and about 1.5 cm. long is heated in a stream of hydrogen containing the vapours of silicon tetrachloride and a hydrocarbon such as toluene. The proportions of the reaction constituents and the temperature of the filament can both be varied, and specific impurities can be introduced by means of volatile chlorides. A detailed description of the method has not been published, and since considerable improvements have been made since the publication

of the papers cited above, a detailed description of the method as at present practised will now be given.

The apparatus is illustrated in diagram form in Fig.20 A stream of hydrogen (free from oxygen) is dried by passing over calcium chloride and then passes through three bubbling bottles arranged in parallel. In the first is put toluene, in the second silicon tetrachloride and in the third concentrated sulphuric acid. The bottles are immersed in liquid baths maintained at constant temperature. The amounts of toluene and silicon chloride vapour picked up by the hydrogen stream can thus be separately varied by regulating the rate of bubbling through each bottle and the temperature of its contents. By the addition of volatile chlorides to a fourth bubbling-bottle specific impurities may be introduced. The hydrogen and vapours then pass through the reaction vessel where a carbon filament is maintained at a temperature in the range 1500 to 2400°C. Decomposition of the vapours occurs on the filament with the deposition of crystalline silicon carbide and the formation of hydrogen chloride. The waste gas finally passes through a second calcium chloride column and then aqueous caustic soda to absorb the hydrogen chloride and excess silicon tetrachloride.

The current to the filament is supplied from the A.C mains through a step-down transformer, with a 0-50 amp. ammeter

in series with the secondary winding, controlled by a variable transformer. The temperature of the centre of the filament is measured by a disappearing filament pyrometer. During the build up of a deposit on the filament the resistance of the filament decreases, and the variable transformer must be continually turned up (by hand) to maintain the filament at the desired temperature. After some experience it is not difficult to maintain the filament temperature constant to at least plus or minus 50°C.

Two tungsten rods are sealed into the stopper of the reaction vessel, and the carbon filament (supplied by Edison-Swan Electric Co.Ltd) is secured at each end by means of aquadag. It has been found best to build up a considerable thickness of aquadag at the junctions with a series of thin layers, drying off each layer by passing a small current through the filament before applying the next. After some experience was obtained in making these junctions, it was found that an overheated filament invariably burnt out in the centre and never at the junctions. It was found necessary to cool the outside of the reaction vessel with running cold water.

A typical preparation was carried out as follows: Bubbling bottle number 1 was half filled with toluene, number 2 with silicon tetrachloride, number 3 with concentrated

sulphuric acid. Bubbling bottles numbers 1 and 2 were immersed in water baths at 18°C. A carbon filament was secured to the tungsten leads and the whole apparatus flushed out with hydrogen. Taps 2 and 3 were then closed so that only hydrogen and toluene vapour passed through the reaction vessel at the rate of approximately 3 bubbles per second. The filament was then maintained at 1800°C until it had increased in diameter approximately three times (i.e to a thickness of about 0.075 cm.). This usually took about 3 minutes and required a final filament current of about 25 amps. This preliminary building up of the filament by deposition of carbon was found to be necessary to produce a robustness and decreased tendency to burn out at higher temperatures. Tap 3 was then opened and tap 1 closed so that only pure hydrogen passed through the reaction vessel. The filament temperature was then raised to (say) 2000°C and all the taps opened to (say) the following extents:- through the toluene bottle - 1 bubble per sec., through the silicon tetrachloride bottle - 2 bubbles per sec., through the sulphuric acid bottle - 2 bubbles per second. The filament temperature was maintained constant for about 15 minutes (although it frequently burnt out at a weak spot before that time). By the end of the experiment the filament current was usually about 40 amps.

Crystalline silicon carbide was deposited on the

filament, and a photograph of a typical deposit is shown in Fig.21. The size of the crystals increases towards the centre, since that part is considerably hotter than the ends. A number of variations in the experimental conditions were tried out, and the results of a large number of experimental runs are shown in summarised form below

(a) Variation of Filament Temperature. (Bubbling rates 1 : 2. C_7H_8 : $SiCl_4$)

1500 - 1700°C	Black amorphous deposit, mostly C, but X-ray investigation indicated small amounts of SiC near the centre of the filament.
1700 - 1900°C	Black crystalline deposit of SiC at centre, plus amorphous deposit of C + SiC (very small crystals)
1900 - 2100°C	Yellow crystalline SiC at centre of filament (larger crystals), black crystalline SiC away from centre (small crystals), amorphous C + SiC at ends.
2100 - 2200°C	Best temperature for formation of largest crystals of yellow SiC.
2200 - 2400°C	Filament usually burnt out quickly, otherwise large yellow crystals obtained.

(b) Variation of Bubbling Rates through Toluene and Silicon Tetrachloride

> 5:1, C_7H_8 : $SiCl_4$	C deposited at all temperatures
4:1 - 2:1, C_7H_8 : $SiCl_4$	C deposited below 2200°C; a little SiC (black) detected by X-ray investigation in deposits formed above 2200°C.

1.5:1 - 1:1, C_7H_8 : $SiCl_4$	C deposited below 1900°C; a little black SiC detected by X-ray investigation in deposits formed from 1900-2100; black crystals formed at centre of filaments above 2100°C.
1:1.5 - 1:3, C_7H_8 : $SiCl_4$	As described above under (a)
1:4 - 1:10, C_7H_8 : $SiCl_4$	Black amorphous deposit of SiC deposited at 1500-1700°C; small yellow crystals deposited at 1800-2200°C; no deposition above 2200°C.
< 1 : 10. C_7H_8 : $SiCl_4$	Small yellow microcrystalline deposit at 1500-1800°C. No deposit above 1800°C.

(c) Variation of Bubbling Rate through Sulphuric Acid

This only affected the rate of deposition not the nature of the deposit. A maximum rate of decomposition was found if about 2 bubbles per sec. were passed through the sulphuric acid, although there was little variation up to 5 bubbles per sec. after which the deposition rate fell off significantly.

It should be noted that the vapour pressures of toluene and silicon tetrachloride at 18°C are as follows:

C_7H_8 19.5 mm ; $SiCl_4$ 175 mm.

The latter vapour is therefore in considerable excess in the reaction vessel for the best conditions of formation of silicon carbide.

In all cases β-SiC (the cubic modification) was obtained. This is in agreement with the results of Taylor and Laidler (5) who found that the hexagonal type was only produced at very high temperatures.

3. PREPARATION OF IMPURE SILICON CARBIDE

Volatile chlorides of the following elements were introduced during the preparation:- Ge, Sn, B, Al, P, As. Sb, Bi, Cu, Fe. They were each placed separately in a fourth bubbling bottle in parallel with the other three, and the bottle immersed in a liquid bath at a temperature which would give a reasonable vapour pressure.

In all cases the introduction of an impurity did not appear to affect the appearance of the final product, black and yellow crystals being formed as previously.

4. INVESTIGATION OF ELECTRICAL PROPERTIES OF SILICON CARBIDE PREPARATIONS.

The crystals produced were all too small for any satisfactory measurements to be made of conductivity and Hall constant. It was, however, possible to make a qualitative determination of the sign of the thermo-electric coefficient at room temperature. This information determines whether the crystals are n- or p-type. A crystal was held between two phosphor-bronze electrodes, one of which was heated.

The electrodes were connected externally through a sensitive D.C. galvanometer, and the direction of movement of the needle gave the sign of the thermo-electric coefficient.

It was found that all yellow crystals (whether pure or contaminated with n- or p-type impurities) were n-type semiconductors. Most black crystals were also n-type (although commercial black silicon carbide is p-type), but a few black crystals were found to be p-type. These were obtained only in those deposits formed when the ratio of the bubbling rates through toluene and silicon tetrachloride was equal to or greater than 1 : 1, and when the deposits were pure or contaminated with boron or aluminium. Crystals prepared in the same way, but contaminated by germanium, tin, phosphorus, arsenic, antimony, bismuth, copper or iron were found to be n-type, although identical in appearance. These p-type black crystals were formed at temperatures above 2100°C. The black crystals formed at lower temperatures, and hence with a lower ratio of toluene : silicon tetrachloride, were all found to be n-type even when contaminated by boron or aluminium.

The conclusions from this would seem to be as follows:-

(1) In the preparation of silicon carbide by reaction of silicon tetrachloride and toluene vapours on a hot carbon filament silicon is normally present in great excess over carbon, and the resultant silicon carbide is n-type, even when

pure, due to a stoichiometric excess of silicon. It does not appear possible to introduce sufficient boron or aluminium to neutralise this excess silicon.

(2) If the toluene : silicon tetrachloride ratio is increased pure silicon carbide crystals can be deposited which are p-type, presumably because there is now a stoichiometric excess of carbon. In this case, however, the introduction of n-type impurities appears to reverse the effect of the excess carbon. (3) It thus appears that n- and p-type conductivity in silicon carbide can be caused by non-stoichiometric proportions of silicon and carbon and also by the introduction of impurities (4) The temperature of formation of the silicon carbide appears to have no influence on the type of conductivity.

5. PREPARATION OF EVAPORATED SILICON CARBIDE FILMS

It is of interest that films of silicon carbide can be prepared by evaporating at a high temperature in a vacuum. The carbon filament on which silicon carbide had been deposited was heated to 2500°C in a vacuum approximately 1 cm. away from a silica plate. In most cases the filament burnt out quickly, but in a few cases it remained complete for a sufficient length of time for a thin evaporated layer of silicon carbide to be deposited on the silica plate. In all cases this layer was contaminated with carbon evaporated

simultaneously. The films produced were yellow or black in colour, depending on the degree of carbon contamination and on the colour of the original silicon carbide. It was hoped to prepare evaporated films for measurement of conductivity and Hall constant, but it was not found possible to prepare films of sufficient thickness for this purpose. Since thick films could not be built up the method was not further developed.

6. SPECTROGRAPHIC ANALYSIS OF COMMERCIAL SILICON CARBIDE CRYSTALS.

Various specimens of commercial silicon carbide were analysed spectrographically, using the sensitive "cathode layer" technique. A powdered specimen was placed in a small graphite cathode. The intensities of the lines observed on a photographic film were measured by a phot-electric densitometer and compared with each other. The experimental results are summarised in Table 1, (p.125)

It will be seen that all the crystals contain iron and aluminium in approximately constant ratios, and there does not appear to be any clear-cut corelation between colour, or conductivity type, and nature of impurities.

7. THEORETICAL SPECULATION

(a) General Theoretical Model

We may describe the ionic-homopolar structure (1)

of silicon carbide as some resonant combination of:- Si = C and $[Si]^{4+} + [C]^{4-}$ The relevant atomic and ionic radii are:- C = 0.77 A.U., C^{4-} = 2.60 A.U. ; Si = 1.18 A.U., Si^{4+} = 0.39 A.U. We may therefore have, in the ionic form, missing Si^{4+} ions (cf.CuO) or interstitial Si^{4+} ions (cf.ZnO). The ionisation energy of these "impurity" centres may be calculated from the usual relation:- $E_I = 2\pi me^4/\kappa^2 h^2$ where m = mass of free electrons or hole, e = magnitude of electronic charge, κ = dielectric constant, h = Planck's constant. For silicon carbide κ may be taken as 7. Therefore E_I = 0.275 eV.

This value for the ionisation energy of an "impurity" centre will be the same whether the "impurity" arises from the presence of foreign atoms (electron donators or acceptors), or from non-stoichiometric proportions of carbon and silicon, or from both causes.

At temperatures above absolute zero some of the "impurity" centres will be in excited states. At low concentrations of impurity the electronic levels of these excited states will be localised, and since the number of electrons in them will be small they may generally be neglected in considering the process of activation of free electrons. However, at high concentrations of impurity the excited-state levels will broaden out into bands, as shown by Erginsoy (6). This situation is illustrated in

figure 22. If this occurs we have the possibility of an electron conduction band, since the excited-state impurity electrons will no longer be localised. This can be shown actually to occur in silicon carbide as follows:- The radii of the normal and excited orbits of the impurity electron can be calculated. In a medium of dielectric constant $\varkappa$ the normal radius of the carbon atom, 0.77×10^{-8} cm will expand to $r = \varkappa \times q^2 \times$ Bohr Radius (where q = principal quantum number of the orbit, i.e. 1 for the ground state and 2 for the first excited level). For successive values of q, and $\varkappa = 7.0$ we thus have $r = 5.4 \times 10^{-8}$, 22×10^{-8}, 49×10^{-8} cm. and these will have activation energies of E_I/q^2, i.e. 0.275, 0.07, 0.03 eV. These expanded orbits will allow electronic conduction to take place if the mean distance between disturbing centres is less than twice the orbital radius of the "impurity" electron, for the orbits around neighbouring centres will then overlap as shown in Fig.23.

Now from the experimental results of Busch (7) all crystals of black silicon carbide have approximately the same number of holes, bound and free, approximately 10^{20} per cc. and the number of missing silicon atoms (or electron-acceptor impurities) must therefore be the same. Knowing the lattice parameters of silicon carbide, the mean distance between acceptor centres can therefore be

calculated as about 24×10^{-8} cm. This situation is depicted in Fig.23 and it can be seen that electrons excited to the level corresponding to $q = 2$ will have overlapping orbits and therefore sufficient mobility to form a conduction band, while electrons corresponding to $q = 1$ will be held in localised energy levels. A similar situation arises for p-type semiconduction in silicon and germanium, but in their cases the activation energies are much lower, and for $q > 1$ become so small as to be indistinguishable at ordinary temperatures from the top of the full conduction band. In the case of silicon carbide there is an appreciable activation energy corresponding to $q = 2$ (and even higher) so that at lower temperatures one may expect to find narrow conduction bands corresponding to $q = 2, 3, \ldots$ We are therefore led to propose an energy level diagram for black silicon carbide as in Fig.24a in which disturbing centres of one kind (missing silicon atoms or electron acceptors) give rise to more than one energy level, and the mobility of electrons in the E_1^* level will be dependent on the mean distance between disturbing centres.

For green silicon carbide (an n-type semiconductor) analogous calculations, assuming interstitial silicon atoms or electron-donator impurities, lead to an energy-level diagram as shown in Fig 24b. There is a significant

difference in the two diagrams for black and green silicon carbide. In the former case electrons may be thermally excited from the normally full band, firstly to the excited level, E_i^*, with an activation energy of 0.07, and secondly to the localised level, E_i, with an activation energy of 0.275 eV. (We may neglect the transition from E_i^* to E_i as the number of electrons at the level Eo is always very much greater than at E_i^*) Measurement of conductivity as a function of temperature should therefore give these two activation energies, ε_1 and ε_2, and moreover the ratio of $\varepsilon_1/\varepsilon_2$ should be 0.25. However, in the case of green silicon carbide, electrons must be excited initially from E_i to E_i^*, and subsequently from E_i to E_o. The activation energies observed should therefore be $\varepsilon_1 = 0.20$ eV. and $\varepsilon_2 = 0.275$ eV., and the ratio of $\varepsilon_1/\varepsilon_2$ should be 0.75.

We are thus assuming that for p-type SiC the current carriers are holes in the normally full band and electrons in the impurity conduction band; while for n-type SiC they are electrons in both the normally empty band and in the impurity conduction band.

(b) Comparison with Experiment

The experimental results of Busch (7) for a number of different crystals of silicon carbide are given in Table 2 and there is seen to be a qualitative correlation

with the model given above. To examine the properties of the proposed model in more detail, we may consider the experimental results of Busch and Labhart (8) on black silicon carbide, as shown in Fig.25. According to these results the conductivity is given by

$$\sigma = A_1 \exp. (-\varepsilon_1/2KT) + A2 \exp (-\varepsilon_2/2KT)$$

over ranges I and II of Fig 25 and a maximum conductivity over range III was explained by them as being the result of degeneration in the conduction band. The presence of two different activation energies was explained by them on the assumption of two kinds of disturbance centres having different energy levels and it was found necessary, in order to explain the anomalous Hall constant at low temperatures, to assume that conduction could take place at one of these levels, although there seemed no particular reason why this should occur. The necessity of postulating two kinds of disturbing centre has been avoided in the present model, which turns out to have properties similar to Busch and Labhart's and moreover provides a satisfactory explanation for the magnitude of the activation energies observed, for their different ratios in n- and p-type crystals, and for the occurrence of conduction at one of the disturbance energy levels. Furthermore, the anomalous low Hall constant at low temperature found in black but not in green silicon carbide

may also be accounted for, as will be shown below.

In the temperature range I of Fig 25 conduction will be due to holes in the normally full band and to an equal number of electrons in the disturbance conduction band at E_1^*. The conductivity may be expressed as

$$\sigma = e n_h \mu_h + e n_e \mu_e$$

where e is the magnitude of the electronic charge, nh and ne are the number of holes and electrons, and μ_h and μ_e are their respective mobilities.

i.e. $\sigma = en(\mu_e + \mu_h)/2$

since in this temperature range nh = ne ($=n/2$). The situation will thus be very similar to that obtaining for intrinsic semiconductors, except that electrons in the disturbance conduction band would not be expected to have such a high mobility as would normal conduction electrons owing to the comparatively large mean distance between disturbance centres. For intrinsic semiconductors μ_e is always greater than μ_h, while in the present case the sign and magnitude of the Hall constant show that μ_h is greater than μ_e. The Hall constant will be given by $R = 3\pi/8en\,(\mu_h - \mu_e)/(\mu_h + \mu_e)$. Thus its sign and magnitude will depend on the relative mobilities of holes and electrons, as well as on their number. Since Busch and Labhart obtained abnormally low values of the Hall constant at low temperatures

it seems that μ_h is nearly equal to μ_e and also since there is no change in the sign of the Hall e.m.f. the hole mobility must be slightly higher than the electron mobility. It can also be deduced that μ_h and μ_e must vary with temperature, as otherwise the curve for log R against 1/T would show a small constant positive slope.

In the higher temperature range II, electrons will be excited from the normally full band to localised energy levels at E_i. Hole conduction will therefore become predominant since nh will increase without a corresponding increase in ne. Finally, when $n_h \gg n_e$ the conductivity will be wholly p-type and will be given by the equation $\sigma = enh\mu h$ and the Hall constant by $R = 3\pi/8enh$.

For green silicon carbide Busch and Labhart did not observe the anomalous low Hall constant in the low temperature range (see Figs.4 -7 of their paper, but note that Figs.6 and 7 have been inadvertently transposed), and this is easily understood since in the present model at both high and low temperatures conduction in green silicon carbide is due to <u>electrons</u> exclusively and we do not have the simultaneous hole and electron conduction in the low temperature range. Refinements to the theoretical model may make it possible to determine with more certainty the nature of the disturbance centres causing n- and p-type conduction in silicon carbide.

For other semiconductors the same model may be applicable and its properties will be largely dependent on the dielectric constant of the crystal. For large values of dielectric constant (e.g. germanium and silicon) the activation energies will be low and the disturbance conduction bands will lie very close to the normally full (or empty) band of the crystal. For small values the activation energies will be high and there will be additional localised energy levels, due to the excited states, which do not develop into disturbance conduction bands. For intermediate values (e.g. silicon carbide) an additional energy level may occur which, as indicated above, will contain electrons which are localised or free according to the crystal parameters and the concentration of disturbance centres.

TABLE 1

SPECTROGRAPHIC ANALYSIS OF SILICON-CARBIDE SPECIMENS

Specimen		Impurity elements											Totals	
No:	Type	Al	Fe	Mg	Mn	Cu	Ag	Na	Ca	V	Zn	Ni	Al + Fe	All elements
1	Norwegian, Black	3	3	3	2	2	2	1	2	2	-	-	6	20
2	Swiss, Black	4	4	3	2	2	1	1	2	3	-	-	8	22
3	Norwegian, Blue-Black	2	2	3	2	3	4	1	2	-	-	-	5	20
4.	Norwegian, Blue	5	5	4	4	4	2	2	3	1	-	-	10	30
5	Norwegian, Green	2	3	3	1	5	1	2	1	1	-	1	5	20
6	Swiss, Green	3	2	3	2	5	1	1	2	1	1	-	5	21
7	Swiss, Pale Green	2	2	3	3	1	1	1	3	-	-	-	4	16
8	Norwegian, Pale Green	3	3	3	2	3	3	1	2	-	-	-	6	20
9	Kendall, Yellow	2	2	4	2	3	1	1	3	-	-	-	4	19

5 = Very heavy line
4 = Heavy line
3 = Medium line
2 = Faint line
1 = Very faint line
- = No line observed

TABLE 2

EXPERIMENTAL ACTIVATION ENERGIES (BUSCH)

Black Silicon Carbide (8 different crystals)			Green Silicon Carbide (7 different crystals)		
ε_1	ε_2	$\varepsilon_1/\varepsilon_2$	ε_1	ε_2	$\varepsilon_1/\varepsilon_2$
0.044	0.270	0.16	0.120	0.215	0.56
0.038	0.281	0.14	0.185	0.246	0.75
0.044	0.272	0.16	0.133	0.285	0.47
0.042	0.282	0.15	0.191	0.265	0.72
0.051	0.248	0.21	0.147	0.263	0.56
0.050	0.231	0.22	0.057	0.157	0.36
0.050	0.231	0.22	0.097	0.198	0.49
0.052	0.226	0.23			
Theoretical Activation Energies (Kendall)					
0.07	0.275	0.25	0.20	0.275	0.75

9. REFERENCES

(1) Pauling, L, "Nature of the Chemical Bond", pp.58-75 Cornell Univ.Press (1940)

(2) Lundquist, D, Acta Chemica Scandinavica 2, 177 (1948)

(3) Kendall,J.T. & Yeo,D, Proc.Internat.Cong.Pure & Appl. Chem.11, 167 (1947)

(4) Moers,K, Zeit.anorg.Chem.198, 243 (1931)

(5) Taylor, A & Laidler, Brit.J.Appl.Phys. 1, 174 (1950)

(6) Erginsoy, C, Phys.Rev.80, 1104 (1950)

(7) Busch,G, Helv.Phys.Acta. 19, 167, (1946)

(8) Busch, G & Labhart,H,Helv.Phys.Acta.19, 463 (1946)

PART IV - REVIEW

1. ELEMENTS

Some of the fundamental electronic properties of carbon-silicon-germanium-grey tin are given in Table 1, (p. 121).

The variation of the energy gap $\mathcal{E}$ with the crystal lattice constant a can be empirically correlated by means of the relationship

$$\mathcal{E} = 6.2 \exp(-a^{5.5}/6400)$$

This relationship is shown plotted in Fig.26 and it is seen that all the points lie exactly on a straight line. It is interesting that the substance silicon carbide, which is nearly homopolar in its properties, also lies very near the straight line.

T.S.Moss (1) gives a similar empirical relationship, but the one given here is more accurate.

The dielectric constant $\varkappa$ of grey tin has not been measured, but an estimate may be obtained from the empirical relationship (Moss (1)):-

$$\mathcal{E}\varkappa^2 = 173$$

This gives $\varkappa = (173/0.064)^{\frac{1}{2}} = 52$

For the other elements we have:-

C :- $\mathcal{E}\varkappa^2 = 5.2 \times (5.67)^2 = 167$

Si :- $\mathcal{E}\varkappa^2 = 1.12 \times (11.8)^2 = 164$

Ge :- $\mathcal{E}\varkappa^2 = 0.74 \times (16)^2 = 189$

Mean 173

The mobility of holes in grey tin is the same as in germanium in the lattice scattering range. The mobility of electrons is somewhat smaller. In the impurity scattering range the mobilities in grey tin are very much larger than in germanium or silicon.

In Table 2 the intrinsic conductivities of the homopolar elements are compared at various temperatures. There is seen to be an enormous variation from Diamond to Grey Tin.

In Table 3 the numbers of free intrinsic electrons are similarly compared.

2. COMPOUNDS

Table 1 also includes some data for compounds. Those for AlSb, GaSb and InSb are taken from two recent papers by WELKER (2) (3). The values of σ_o are calculated approximately from his curves of intrinsic σ against 1/T.

It is seen that these binary compounds of Group III with Group V elements have properties similar to those of the Group IV elements. The very large mobility which Welker quotes for InSb should be noted. BRECKENRIDGE (4) gives a similar figure. From the values derived for σ_o the mobilities of AlSb and GaSb will not be so high.

That these binary compounds are not so homopolar as silicon is indicated by the fact that their electron

activation energies do not bear any relation to their lattice constants as was found to hold empirically for the truly homopolar semiconductors.

There are a large number of such binary compounds awaiting investigation, and some interesting properties may be expected. Welker has already found transistor action in InP (3).

TABLE 1

PROPERTIES OF HOMOPOLAR SEMICONDUCTORS

	σ_o	ε	$\delta\varepsilon/\delta T$	$\varkappa$	$\mu_e T^{3/2}$	$\mu_h T^{3/2}$	μ_e/μ_h	a
C	1.2×10^{2}	5.2	1.7×10^{-4}	5.67	4.7×10^{6}	1×10^{6}	4.7	3.56
Si	9.1×10^{3}	1.12	3×10^{-4}	11.8	1.5×10^{6}	0.5×10^{6}	3.0	5.43
Ge	3.3×10^{4}	0.74	1×10^{-4}	16	19×10^{6}	8.9×10^{6}	2.1	5.65
Sn	1.6×10^{4}	0.064	~ 0	~ 50	11.6×10^{6}	8.9×10^{6}	1.3	6.49
SiC		3.5						4.35
AlSb	4×10^{4}	1.65						6.13
GaSb	1.2×10^{4}	0.82						6.12
InSb	2×10^{5}	0.53			$\sim 130 \times 10^{6}$			6.46

TABLE 2

INTRINSIC CONDUCTIVITY (CALCULATED FROM $\sigma = \sigma_0 \exp(-\varepsilon/2KT)$)

$ohm^{-1}\ cm^{-1}$

T(°K)	C	Si	Ge	Sn
1000	1.2×10^{-11}	14	480	11000
500	1.3×10^{-24}	2.3×10^{-2}	7	7500
290	2.4×10^{-43}	2.1×10^{-6}	1.4×10^{-2}	4500
200		9.1×10^{-11}	2.0×10^{-5}	2500
100		9.1×10^{-25}	1.3×10^{-14}	400

TABLE 3

NUMBER OF CHARGE CARRIERS (CALCULATED FROM $n = 2(n_e n_h)^{\frac{1}{2}} =$

$$2(2.3 \times 10^{31} \; T^3 \exp(-\varepsilon/KT) \exp(\beta/K))^{\frac{1}{2}}$$

WHERE $\exp(\beta/K) = 7.4$ FOR C, 32.5 FOR Si, 3.5 FOR Ge, 1.0 FOR Sn

T(°K)	C	Si	Ge	Sn
2000	7.6×10^{14}			
1000	3.7×10^{7}	2.8×10^{18}	8.0×10^{18}	2.2×10^{20}
500	3.3×10^{-6}	1.5×10^{15}	4.0×10^{16}	5.1×10^{19}
290	3×10^{-25}	6.0×10^{10}	4.0×10^{13}	1.3×10^{19}
200		1.6×10^{6}	1.4×10^{10}	4.3×10^{18}
100		5.5×10^{-9}	5.6	1.2×10^{17}
20				8.6×10^{9}

REFERENCES

(1) MOSS T.S. - "Photoconductivity in the Elements", Butterworth (1952)

(2) WELKER H - Z. Naturforschung 7a, 744 (1952)

(3) WELKER H - Z. Naturforschung 8a, 248 (1953)

(4) BRECKENRIDGE R. - Phys.Rev. 90, 488 (1953)

APPENDIX 1

LIST OF SYMBOLS

σ	Conductivity ($ohm^{-1} cm^{-1}$)
K	Boltzmann's constant (= 8.70×10^{-5} eV)
T	Absolute temperature (^{o} Abs.)
n_e	Number of free electrons (cm^{-3})
n_h	Number of free holes (cm^{-3})
n_s	Number of substitutional impurity atoms (cm^{-3})
c	ratio of electron to hole mobility ($\mu e/\mu h$)
μe	Mobility of electrons ($cm^{2}.volt^{-1}sec^{-1}$)
μh	Mobility of holes ($cm^{2}.volt^{-1}sec^{-1}$)
R	Hall constant (cm^{3} Coulombs^{-1})
m	Electronic mass
e	Electronic charge
$\varkappa$	Dielectric constant
h	Planck's constant
EI	Activation energy for impurity electrons (eV)
ε	Activation energy for intrinsic electrons (eV)
H	Magnetic field strength (gauss)
β	Variation of ε with temperature (eV.^{o} Abs^{-1})
Tc	Critical temperature for degeneracy (^{o}Abs.)
a	Crystal lattice constant (Angstrom units)

APPENDIX 2

LIST OF FIGURES

(1) Energy levels in grey tin

(2) Transformation rate of tin (Tammann)

(3) Transformation rate of tin (Cohen)

(4) e.m.f. of white/grey tin electrochemical cell

(5) Vacuum evaporation of tin

(6) Specimen holder for electrical measurements

(7) Electrical measuring circuit

(8) Conductivity of alloys

(9) Hall constant of alloys

(10) Variation of Hall constant in a magnetic field (I)

(11) Variation of Hall constant in a magnetic field (II)

(12) Variation of ($n_e n_h$) with temperature

(13) Variation of T_c with number of charge carriers

(14) Number of charge carriers in alloys

(15) Mobilities of electrons and holes

(16) Variation of σ and R with H (Alloy (1))

(17) Variation of σ and R with H (Alloy (6))

(18) Contact Rectification with Grey Tin

(19) Thermo-electric effect with Grey Tin

(20) Apparatus for preparing Silicon Carbide

(21) Photograph of Silicon Carbide Preparation

(22) Electronic Impurity Bands in a Semiconductor

(23) Radii of Holes in Silicon Carbide

(24) Energy Levels in Silicon Carbide

(25) Conductivity and Hall Constant of Silicon Carbide

(26) Relationship of ϵ with Lattice Constant

APPENDIX 3

ACKNOWLEDGMENTS

The work described in this thesis was carried out during 1950-53 in the Electrical Engineering Department of Imperial College, London. The author wishes to thank Professor Willis Jackson for his help and encouragement and for placing experimental facilities at his disposal, the D.S.I.R. for a grant for equipment, the Leverhulme Fellowships Committee for a Fellowship (1949-52), and the Directors of Metropolitan-Vickers Electrical Co.Ltd. for granting him extended leave of absence. Specimens of commercial silicon carbide were kindly supplied by the Gotthardwerke A.G, Bodio, Switzerland and the Arendal Smeltewerk, Eydehavn, Norway.

APPENDIX 4

REPRINTS OF PUBLICATIONS

Reprints of the following publications are attached:-

1. KENDALL J.T. - Proc. Phys. Soc. 56, 123 (1944)
   "The Rectifying Property of Silicon Carbide"

2. KENDALL J.T. and YEO D - Proc. Internat.Cong. Pure and Appl. Chem. 11, 167 (1947)
   "Preparation of Pure Silicon Carbide".

3. KENDALL J.T. - Proc. Phys.Soc. 63B, 821 (1950)
   "Electrical Conductivity of Grey Tin"

4. KENDALL J.T. - J.Chem.Phys. 21, 821 (1953)
   "Electronic Conduction in Silicon Carbide"

Note : A paper based on Part II of this thesis has been accepted for publication in the Philosophical Magazine.

REPRINTED FROM THE
PROCEEDINGS OF THE PHYSICAL SOCIETY, VOL. LVI, p. 123, 1944
All Rights Reserved
PRINTED IN GREAT BRITAIN

THE RECTIFYING PROPERTY OF CARBORUNDUM

BY J. T. KENDALL,
Research Department, Metropolitan-Vickers Electrical Co., Ltd., Manchester

MS. received 26 *November* 1943

ABSTRACT. A technique is described for obtaining a non-rectifying carbon-carborundum contact. Experimental current-voltage curves are given for single rectifying contacts. These curves show that *green* and *black* carborundum are essentially different types of semi-conductor. Experiment also shows that all the rectification takes place at the contact surface, and that any volume rectification (if it exists) is a second-order effect.

§ 1. INTRODUCTION

MUCH of the literature on the rectifying property of carborundum is confusing, owing to a lack of attention to two important factors. First, there are at least two types of carborundum crystals which are completely different in their electrical properties. In *green* carborundum, rectification takes place in such a way that the direction of easy flow of electrons is from semi-conductor to metal; in *black* or *blue* carborundum, rectification is in the opposite direction. This fact is evidently not generally appreciated, for as recently as 1942, Fairweather, in describing experiments on the carborundum rectifier, omits to mention with what type of crystal he is dealing. On the other hand, as early as 1921 Dowsett distinguished between *green* and *black* crystals, which he called positive and negative; and more recently Russian investigators (e.g. Gokhberg (1937) and Losev (1940)) have distinguished the two types as *excess* and *defect* semi-conductors. (See Wilson (1939) for an explanation of these terms.)

Commercial carborundum, as manufactured in the electric furnace, consists mainly of masses of opaque black or deep blue crystals, but in parts of the furnace the product may consist of clear crystals, varying in colour from green to pale yellow or even colourless. The various crystals differ little, if at all, in chemical composition. They may differ in crystal structure, and an investigation on this point is at present in progress.

Secondly, the fact that experimental data may refer to two contacts in series is often not mentioned. For example, El Sherbini and Yousef (1939, 1941), Khastgir and Das Gupta (1935), Chakravarty and Khastgir (1937), and others, clamp a crystal in metal electrodes and measure the *overall* rectification. If there is no volume rectification this simply gives the difference between the rectification at the two contacts, and the results can become very misleading. As shown below, even a soldered contact does not have under all conditions a resistance small compared with that of a cat's-whisker contact. Fairweather (1942) has avoided the difficulty, and has measured the voltage across a single

contact by a potential probe and balancing e.m.f. This method is theoretically sound, but is comparatively insensitive, especially for small voltages, owing to the high resistance of the measuring circuit.

In the present series of experiments full account has been taken of these two important factors. Data are presented for both green and black carborundum, and the rectification is referred to a single contact by making the resistance of the second contact very small.

The crystal fragments used were roughly rectangular, having a volume of about 0·01 c.c. There is an advantage in experimenting on such a small scale, for commercial carborundum is a mass of irregularly fractured crystals, and it is difficult to obtain a single crystal of larger size.

§2. METHOD OF MAKING A "LOW-RESISTANCE" CONTACT

Three types of low-resistance contact have been tried: solder, mercury and carbon. In the first method, a crystal of carborundum is partially immersed in molten solder, which, on solidification, holds the crystal tightly, and presumably gives a large area of contact. In the second method the crystal is held by means of three screws in a metal cup filled with mercury. In the third method (figure 1) the crystal is clamped between two pipe-clay tubes, through which

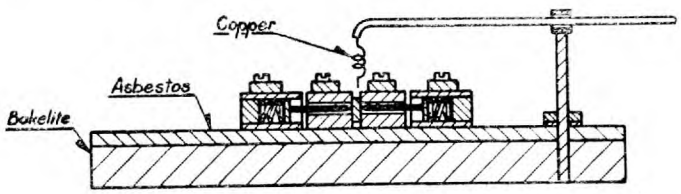


Figure 1.

pass carbon rods (sharpened H.B. pencil leads) which are pressed on to the crystal by springs. The initial resistance of the arrangement is non-linear, of the order of 100,000 ohms at 4 volts. The carbon-carborundum contacts are broken down by passing a heavy current for a short time (e.g. 7 amperes for 10 seconds). The current was obtained from 110 v. A.C. mains with a series limiting resistance. With 7 amperes passing, the crystal reached about 1200° c., judging from its colour. The specific resistance while at bright yellow heat was measured as 0·07 ohm/cm³ (black carborundum). This rose on cooling to about 5 ohms/cm³ In this experiment it was impossible to tell how much of the resistance was localized at the contacts and how much represented *volume* resistivity.

In figure 2, curve I represents voltage plotted against current for two fused carbon-SiC contacts in series, prepared as above. The resistance is linear, of the order of 100 ohms, up to about 7 volts. In curve II, two solder-SiC contacts are in series. The resistance is linear, of the order of 1 megohm, only up to about 0·5 volt. A similar curve is obtained for mercury-SiC. In curve III, a solder-SiC contact is in series with a cat's-whisker contact of copper wire. The two separate branches of these curves represent the two different directions of applied voltage. Curve II coincides with one branch of curve III,

since the direction of easy flow of electrons for the high-resistance (cat's-whisker) contact necessarily corresponds to the direction of difficult flow for the low-resistance (solder) contact. The dotted branch of curve III is obtained when a fused carbon contact is substituted for the solder contact. For this low-resistance branch of curve III, the solder contact is evidently only satisfactory

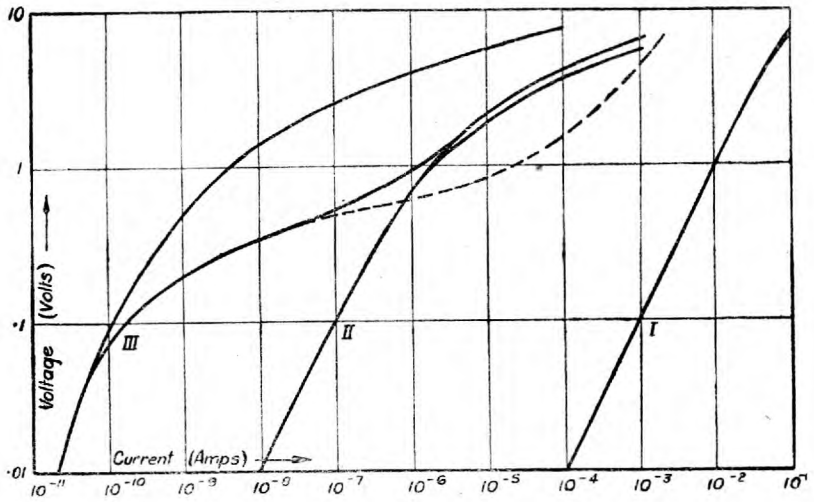


Figure 2. Typical current-voltage relationships.

I. Two fused carbon contacts.

II. Two solder contacts.

III. Cat's whisker and solder contacts.

at low voltages, and this condition is most definitely *not* obtained in much of the published experimental work on crystal rectification. The fused carbon contact used in the present work has such an exceedingly low resistance that distortion of the low-resistance branch does not occur.

§ 3. EXPERIMENTAL RESULTS

The electrical circuit is shown in figure 3. *Voltage* is measured by the multi-range voltmeter connected directly across the carborundum crystal and series resistance. The voltage drop across this resistance is allowed for when

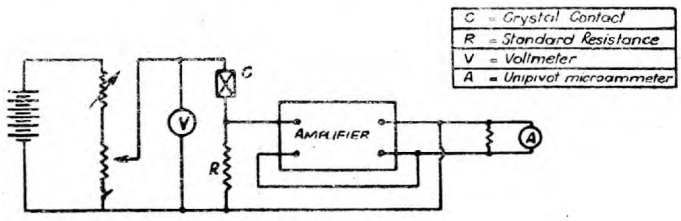


Figure 3. Circuit diagram.

it is significant. Unfortunately this method of measurement, although simple and direct, gives the voltage across *two* metal-SiC contacts. In practice one makes the resistance of one contact small compared with the resistance of the

other, as described above. *Current* is measured by measuring the potential drop across the series resistance, which is variable in steps from 10^2 to 10^7 ohms. For this purpose a D.C. amplifier similar to that described by Vance (1936) is used. This has an input impedance large compared with 10^7 ohms, and is connected so as to give 100 % negative feed-back. The voltmeter in the output stage measures 0·1 or 1 volt full-scale, and the current range is therefore 10^{-8} to 10^{-2} amperes for full-scale deflection.

Experimental curves relating current and voltage for single carborundum contacts are shown in figures 4 and 5. It should be clearly understood that while these curves are *exact* for the given contact and conditions, they are only *typical* of the given contact materials. This limitation will be readily appreciated

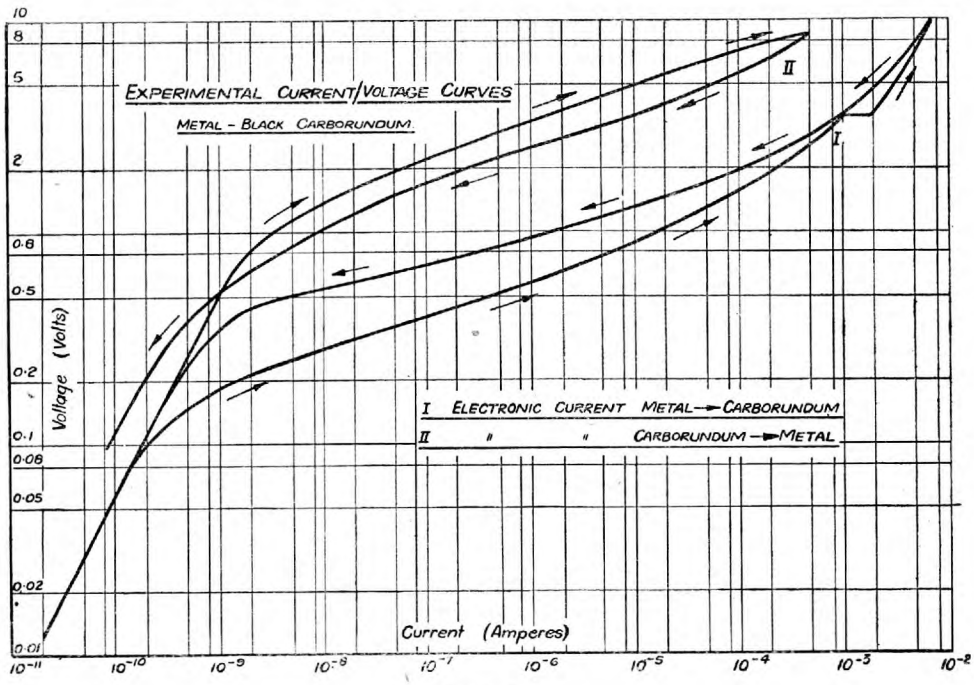


Figure 4.

by anyone who has done any experimental work on crystal rectification. For those who have not, it is as well to emphasize that the effect of such factors as contact pressure, actual (not superficial) contact area, exact composition of contact materials, thickness of any surface layer, previous history of contact, etc., which are factors controllable only with great difficulty, can cause great variation of experimental results. These difficulties are often glossed over in accounts of experimental work, and it is as well to read such accounts with a highly critical eye.

The contact combinations studied are shown in the table, which gives in each case the number of *different* crystals studied, the number of observations using different parts of the *same* crystal and the overall experimental variation observed. The last is expressed arbitrarily by the range of current for a voltage of 1 volt applied across the contacts. This variation is generally enormous

(showing the effect of uncontrolled factors), but this does not invalidate the conclusions given below, for the *direction* of rectification is constant, and for a particular contact the current-voltage curves are approximately repeatable.

In figure 4, a current-voltage curve is given for a cat's-whisker contact of copper-black carborundum. The direction of easy flow of electrons is from metal to semi-conductor. In obtaining this curve, the voltage was raised in small steps to the maximum value and the corresponding currents measured; the voltage was then decreased similarly. This procedure results in two curves for ascending and descending voltage, showing that the current at a given voltage depends on the time of application. A point to notice is that in the direction of easy flow of electrons the current *decreases* with time of application of voltage, while in the direction of difficult flow the current *increases* with time.

Table. Contact combinations studied

Contact	No. of different crystals	No. of different points on same crystal	Total range of current (amp.) at $V=1$ volt	
			Metal+	Metal−
Copper-black SiC	25	10, 10, 6, 2 (remainder 1)	$3\times10^{-9}-6\times10^{-7}$	$4\times10^{-8}-3\times10^{-5}$
Solder-black SiC	4	(all 1)	—	—
Mercury-black SiC	2	1, 1	—	—
Fused C-black SiC	6	(all 1)	—	—
Copper-green SiC	6	3, 2 (remainder 1)	$8\times10^{-6}-1\times10^{-5}$	$6\times10^{-7}-1\times10^{-6}$
Solder-green SiC	1	1	—	—
Mercury-green SiC	1	1	—	—
Fused C-green SiC	1	1	—	—
Green-black SiC	2 pairs	4, 1	$6\times10^{-5}-3\times10^{-4}$	$5\times10^{-8}-8\times10^{-6}$

In figure 5, curve I refers to a cat's-whisker contact of copper-green carborundum. It has been found that the resistance of contacts with green carborundum is always less than similar contacts with black carborundum. Rectification is in the opposite direction, the easy flow of electrons being from semi-conductor to metal. The effect, described in the last paragraph, of the current varying with time was not noticed. Curve II refers to a contact between crystals of green and black carborundum. Rectification is in the direction to be expected by analogy with the results for metal-carborundum contacts, the easy flow of electrons being from green to black carborundum. Contacts of green-green and black-black carborundum also rectify, but less efficiently.

Other experimental points of interest are: similar results were obtained with dull, shiny, striated and fractured surfaces. The crystallographic orientation of the surface was immaterial. Similar results were obtained on a surface which had been exposed to the air for a long time and on newly fractured surfaces.

Heating the crystal in an atmosphere of nitrogen or prolonged washing with hydrofluoric acid had no effect on the contact resistance.

The curves were repeatable except when more than about 12 volts were applied, when the contact resistance began to break down, and was only partially recovered on lowering the applied voltage. At about 20 volts a white glow appeared at the contact. Sillars (1942) has reported that this glow gives a

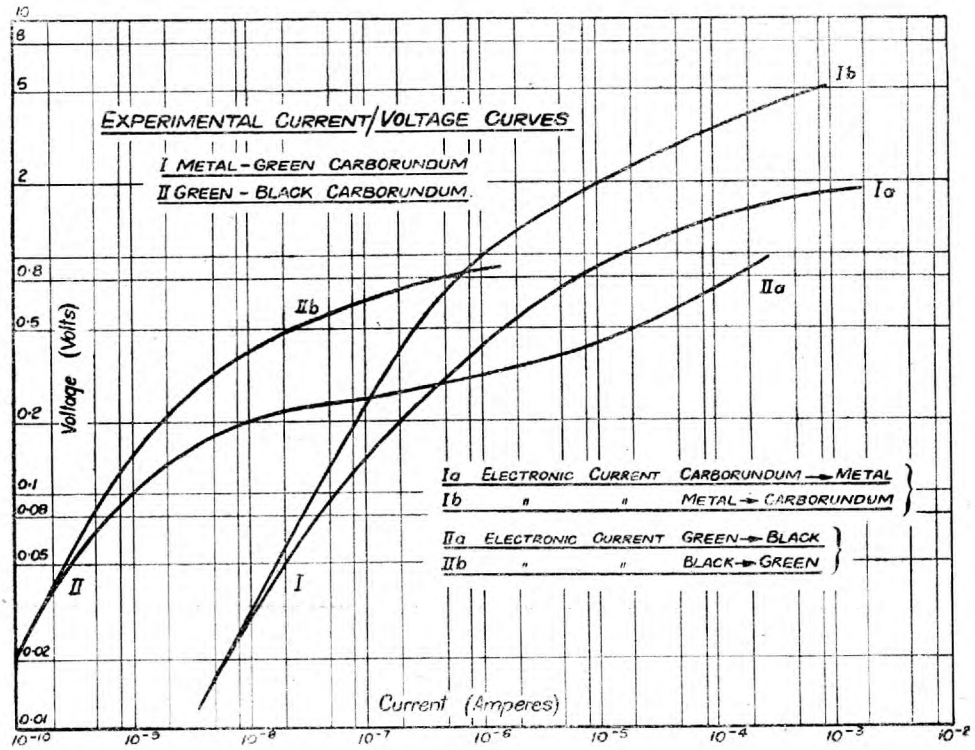


Figure 5.

continuous spectrum. Pressure applied to the contact altered the resistance characteristic. With increasing pressure the resistance decreased and became less dependent on voltage.

At low voltages (or, it may be, at low current-densities) the contact resistance is linear. Over a certain voltage range non-linearity is observed, and at high voltages the resistance apparently tends to become linear again. This latter may, however, be a *contact breakdown* effect.

§ 4. THEORETICAL DISCUSSION

It can be deduced theoretically that for an *excess* semi-conductor the thermo-electric force against a metal is *negative*, while for a *defect* semi-conductor it is *positive*. It has been shown experimentally by Gokhberg (1937), and confirmed by the author, that on this count green and black carborundum should be classed respectively as *excess* and *defect* semi-conductors. The cause of this difference is obscure. Carborundum is certainly an "impurity" semi-conductor, but the identity of the impurities is not known.

It has generally been supposed that there is a surface layer of silica on carborundum crystals, acting as a "barrier-layer", but the evidence is not very convincing. Heine and Scherrer (1940) have, from electron-diffraction experiments, shown that such a layer, if present, must be less than 10 A. thick. Finch and Wilman (1937) have similarly shown that a layer 15 A. thick may sometimes be present, but can be removed by the usual means (e.g. hydrofluoric acid). The fact that a freshly fractured surface is indistinguishable electrically from a natural crystal face shows that any silica film must be formed very rapidly on exposure to the atmosphere. In any case, it is inconceivable that the *thick* barrier-layer (approximately 10^{-3} cm.) required on Mott's theory of contact rectification (1939) can be present. This theory is completely satisfactory only for the copper-oxide rectifier. Wilson's earlier theory (1932) postulates a barrier-layer approximately 10^{-7} cm. thick, and this may possibly be present. Unfortunately, Wilson's theory predicts rectification in the wrong direction. A possible solution to the difficulty may be found in the work of Losev (1940) on the photo-electric effect of carborundum. His experiments indicate that while the bulk of a crystal may have "defect" conductivity, the outer layer (10^{-3} cm. thick) will have "excess" conductivity, the "barrier-layer" occurring at the junction. It does seem necessary to postulate some sort of *physical* barrier-layer, for the formation of an *electrical* barrier seems ruled out by the apparently instantaneous response of the carborundum rectifier to short impulses. One must conclude, then, that the current theories of contact rectification do not apply satisfactorily to carborundum.

§ 5. ACKNOWLEDGMENT

The author wishes to thank Dr. A. P. M. Fleming, C.B.E., Director and Manager, Research and Education Departments, Metropolitan-Vickers Electrical Company, for permission to publish this paper.

REFERENCES

CHAKRAVARTY, M. K. and KHASTGIR, S. R., 1937. *Phil. Mag.* **24,** 127.
DOWSETT, H. M., 1921. *Radio Rev.* **2,** 582, 642.
EL SHERBINI, M. A. and YOUSEF, Y. L., 1939. *Proc. Phys. Soc.* **51,** 449.
EL SHERBINI, M. A. and YOUSEF, Y. L., 1941. *Proc. Phys. Soc.* **53,** 120.
FAIRWEATHER, A., 1942. *J. Instn. Elect. Engrs.* **89,** pt. i, 499.
FINCH, G. I. and WILMAN, H., 1937. *Trans. Faraday Soc.* **33,** 337.
GOKHBERG, B. M., 1937. *J. Theor. Exp. Phys., U.S.S.R.*, **7,** 1090.
HEINE, H. G. and SCHERRER, P., 1940. *Helv. phys. Acta,* **13,** 489.
KHASTGIR, S. R. and DAS GUPTA, A. K., 1935. *Phil. Mag.* **19,** 557.
LOSEV, O. V., 1940. *C.R. Acad. Sci. U.R.S.S.*, **29,** 360.
MOTT, N. F., 1939. *Proc. Roy. Soc.* A, **171,** 27.
SILLARS, R. W., 1942. Private communication.
VANCE, A. W., 1936. *Rev. Sci. Instrum.* **7,** 489.
WILSON, A. H., 1932. *Proc. Roy. Soc.* A, **136,** 487.
WILSON, A. H., 1939. *Semiconductors and Metals* (Cambridge : University Press).

REPRINTED FROM THE
PROCEEDINGS OF THE PHYSICAL SOCIETY, VOL. LVI, p. 270, 1944
All Rights Reserved
PRINTED IN GREAT BRITAIN

DISCUSSION

on paper by J. T. Kendall (*Proc. Phys. Soc.* **56**, 123 (1944)) entitled "The rectifying property of carborundum".

Dr. A. FAIRWEATHER. In referring to some earlier work of mine on the same topic Mr. Kendall asserts (p. 123) that " Fairweather .... omits to mention with what type of crystal he is dealing ". On pp. 514–516 of my paper it was pointed out that there are five known crystalline modifications of carborundum, and that the crystals employed in my work consisted mainly of the second modification. The method of classification adopted by Mr. Kendall, i.e. according to colour, as either green or black or blue, does not seem very definite. The point at issue is, therefore, whether colour or crystal structure is the significant factor, and whether they are alternative descriptions of the same thing. There are several possibilities : thus, different colours might be associated with—

(*a*) different crystalline forms of pure carborundum;

(*b*) different forms containing the same impurity;

(*c*) different impurities in the same form;

(*d*) different impurities in different forms, a specific impurity being, perhaps, always associated with the same crystalline form.

Secondly, Mr. Kendall's fusing technique for the preparation of a low-resistance contact (p. 124) is not free from objection. With the particular material for which it was devised, viz. carborundum, it involved raising the temperature of the crystal to " about 1200° c." Without an experimental check, it cannot be accepted that the properties of the crystal and/or its surface remained unaffected by this treatment. For other materials such a procedure would be impracticable, and the technique would seem, therefore, to be of much more limited application than that described in my paper.

Lastly (p. 128), Mr. Kendall mentions that " At low voltages ..... the contact resistance is linear. Over a certain voltage range non-linearity is observed, and at high voltages the resistance apparently tends to become linear again. The latter may, however, be a *contact breakdown* effect ". A high voltage ohmic region obtained as a result of a contact breakdown (i.e. a non-reversible change in contact structure) cannot be regarded as a fundamental property of a particular contact structure. But there is a high-voltage ohmic region which is not a breakdown effect : the complete current/voltage characteristic, including this high-voltage ohmic region, is reproducible provided that overheating at high voltages is avoided by ensuring that the test current flows for a sufficiently brief period of time. *Prolonged* current flow in this region may, however, result in a non-reversible change in contact structure. The characteristic regions were identified, and their significance discussed, in my paper (p. 500 *et seq.*) : the work described therein related specifically to smooth reversible phenomena (p. 499, p. 509 *et seq.*), and particular care was taken to avoid confusion with non-reproducible effects.

AUTHOR'S reply. The work described in my paper has shown that there are two types of crystal to be found in commercial carborundum, one behaving as an *excess* and the other as a *defect* semi-conductor. This is in confirmation of earlier work, e.g. Dowsett (1921), Gokhberg (1937), which has not, apparently, been generally appreciated. The author has been unable to correlate these electrical properties with crystal structure. As far as present experiments have proceeded, *all* commercial carborundum (including crystals of

both electrical types) is of structure-type II. This evidence is solely from powder photographs and is not quite conclusive, since it is not easy by this method to distinguish between the various structures. It is hoped at a later date to obtain rotation photographs of crystals of different electrical properties.

The various structures are all very similar, and are based on a structure-unit of four carbon atoms arranged tetrahedrally about a central silicon atom. The carbon tetrahedra are joined by sharing corner atoms, and different sizes of unit cell are formed according to the relative rotation of adjacent tetrahedra about their common axis—which becomes an axis of *screw*-symmetry in the crystal. It does not seem likely that such small differences in structure are the cause of such a striking difference as *excess* and *defect* electronic conduction. It remains a possibility that different impurities may cause the production of different structural types as well as different electrical types, but there is no necessity for a correlation between the two.

The author's separation of carborundum crystals according to colour appears to be much more satisfactorily related to electrical properties. The separation between green on the one hand and blue and black crystals on the other is quite definite, and very easily made visually ; it corresponds exactly with the separation according to electrical type. Moreover, it is well known that the formation of colour-centres in crystals is a phenomenon associated with the presence of free electrons, so that one should not be surprised by this correlation of colour and electrical properties.

Commercial carborundum is undoubtedly an *impurity* semi-conductor, and it is to these impurities that its unusual electrical properties must be ascribed. Unfortunately the nature of the impurities is not yet known ; they may be carbon or silicon in excess of stoichiometric proportions, i.e. vacant lattice points, or they may be foreign atoms, e.g. Fe, Al, etc., either substitutional or occupying interstitial positions in the crystal lattice. Since some carborundum crystals behave as *excess* and others as *defect* semi-conductors, it would be convenient to believe that the first possibility is correct, and that excess silicon or carbon results respectively in *excess* or *defect* conductivity, but this view can only be taken as conjectural. Further electrical work starting with pure silicon carbide, and with impurities under exact control, is obviously necessary.

With reference to Dr. Fairweather's second paragraph, the well-known potential-probe method used by him is certainly of more general application than the technique of fusing a contact on to a crystal surface. In the case of carborundum this drastic operation did not, however, affect the electrical properties of the crystal. This was shown by fusing two carbon rods to a crystal in the usual way, and then breaking off the rods at the contact surface, when the electrical properties were quite unaltered. It will be realized that the crystal was at 1200° c. for only a second or two. If it is kept in air at that temperaturre for several minutes a film of silica of high electrical resistance is formed at the surface.

This fusion technique was adopted because of the difficulty of obtaining *single* carborundum crystals of a size sufficiently big to use the potential-probe method. It was considered important to exclude possible electrical effects due to the inter-crystalline contacts which are obviously present in carborundum fragments of appreciable size.

With reference to Dr. Fairweather's third paragraph, the tendency towards ohmic resistance of carborundum contacts at high voltages is explained by him (1942) on the assumption that the resistance of the contact becomes small compared with the bulk resistance of the crystal. This may be true, but the evidence is not yet complete, and the experimental difficulties of obtaining " smooth reversible phenomena " at the higher voltages have not yet been overcome. It is hoped to investigate this range at a later date by applying impulse voltages of very short duration to single carborundum crystals, and observing the current-voltage characteristic directly with a high-speed cathode-ray oscillograph.

Reprinted from: Proceedings of the XI International Congress of Pure & Applied Chemistry, London, (1947).

THE PREPARATION OF PURE SILICON CARBIDE

By J. T. KENDALL, M.A., and D. YEO, B.Sc.

Research Department, Metropolitan-Vickers Electrical Co., Ltd.

Introduction.

SILICON carbide is a solid of the " valence crystal " type, similar in its structure and properties to diamond. It can, in fact, be considered as diamond in which half the carbon atoms have been replaced by silicon. It is obtainable only as a synthetic product, although its formation in nature would not seem to be impossible (for example by the extrusion of quartz at high temperature into a carbonaceous rock), and one natural occurrence has been tentatively reported from Italian Somaliland.(1)

Industrially prepared silicon carbide is an electronic semiconductor, due either to the presence of impurity atoms in the structure or to non-stoichiometric proportions of silicon and carbon. It is made by heating sand and coke—and often certain other substances such as salt and sawdust, which facilitate the manufacture—in an electric furnace at a temperature of 1800–2000° C.

It is evident that in such a process the impurities will be considerable and will vary with different samples of carborundum. Crystals varying in colour from pale yellow to black are often found in different parts of the same furnace, and the electrical properties are often considerably different. For example, commercial green and black carborundum have been shown to be respectively " excess " and " defect " electronic conductors.(2) Unfortunately SiC is extremely difficult to analyse and the impurities have not yet been identified with any certainty or accuracy.

Although it is possible to obtain consistent experimental data on electrical properties from one particular sample of SiC, the agreement between different samples, which are apparently similar, is only qualitatively consistent, due to variations in the proportions and composition of the impurities and the consequent inability to produce identical specimens.

If pure silicon carbide could be prepared, however, it should then be possible to produce specimens containing known impurities of known proportions. With these specimens much valuable quantitative data could be obtained as to the effect of impurities upon the electrical properties ; such data would be of the greatest importance both in the formulation of an adequate theory for the electrical properties of semiconductors, and in the manufacture of an improved " electrical " grade of silicon carbide, which is now being used in large quantities for making non-ohmic electrical resistors.

Previous Preparations.

The preparation of pure silicon carbide has been reported by previous workers—J. M. Pring and W. Fielding(3) in 1909 prepared a crystalline deposit by heating a $\frac{1}{4}$ in. diameter carbon rod in an atmosphere of hydrogen saturated with the vapour of silicon tetrachloride. The crystals formed on the surface of the carbon rod were identified as silicon carbide, but they were heavily contaminated by carbon. E. Friederich and L. Sittig(4) in 1925, and O. Ruff(5) in 1935, prepared amorphous or in some cases very finely crystalline silicon carbide by heating together silica and powdered graphite. Their product was contaminated with traces of iron and aluminium. The purest silicon carbide has previously been prepared by K. Moers(6) in 1931, by heating a fine carbon filament in a stream of hydrogen containing the silicon tetra-

chloride vapour and methane. Moers obtained several types of crystals. At moderately high temperatures (about 1700° C.) black, hexagonal crystals were obtained which were conducting, whereas at filament temperatures above about 2200° C. transparent yellow crystals were obtained ; these crystals had a diamond structure and were non-conducting. (This was shown by the fact that the resistance of the wire did not change with the growth of the layer of carbide.) In addition, green crystals were obtained, but colourless crystals were never found. It was found that the slightest grey colour in the crystals greatly affected the electrical properties, decreasing the resistance, and Moers suggested that this might be due to the presence of excess carbon.

Generally the deposit on the filament was porous, but the individual crystals were firm, stable, and well formed, as was shown by X-ray photographs. At higher temperatures the crystals were larger, and there was a tendency for the crystal structure to be influenced by the crystal structure of the filament. An analysis, which was not too reliable, indicated that there might have been an excess of silicon in the carbide. The crystals formed were small, the largest being about 0.03 cm. cross section.

Experimental.

The method of preparation we have used is similar to that of Moers. A carbon filament 0.025 cm. in diameter, and about 1.5 cm. long was heated in a stream of hydrogen containing the vapour of silicon tetrachloride and a hydrocarbon such as benzene or toluene. The proportions of the reaction constituents were varied as well as the temperature of the filament. The following results may be mentioned.

1. Using silicon tetrachloride and toluene the deposit was found to vary in the following way.

If the proportions of silicon tetrachloride : toluene were varied from about 2 : 1 to 10 : 1 the carbide was first produced at about 1500° C. ; below this temperature carbon was deposited. Between 1500° C. and about 1800° C. a predominantly black crystal deposit was obtained, with quite a large number of yellow crystals present, whereas above about 1850–1900° C. a clear yellow deposit was obtained. Fig. 1 is a photograph of a typical filament produced at these higher temperatures.

When the proportion of silicon tetrachloride was increased above the upper limit of the ratios given above, silicon was deposited at lower temperatures and burnt off at higher temperatures without the formation of any SiC. On the other hand, if the proportion of silicon tetrachloride was decreased to below the lower limit, a black deposit was produced at all temperatures above 1500° C., this deposit being a mixture of silicon carbide and carbon. Finally, if the proportion of silicon tetrachloride was further reduced so that the ratio of silico tetrachloride : toluene was 2 : 3, carbon was deposited at all temperatures. Another feature of the deposition was that within the ratios 1 : 1 to 10 : 1 an increase in the toluene concentration raised the temperature at which a clear yellow deposit was obtained.

2. Methyl silicon trichloride (CH_3SiCl_3) was used by itself. At about 2000° C. a black deposit was obtained, whilst at very high temperatures (2400° C.) yellow crystals were obtained. Di-ethyl silicon dichloride $(C_2H_5)_2SiCl_2$ gave a similar result except that it was not possible to produce a completely yellow deposit.

3. Bubbling coal gas through silicon tetrachloride gave a deposit of carbon ; when the coal gas was diluted with hydrogen (about 20% of coal gas) the deposit was formed under very similar conditions to those pertaining when silicon tetrachloride and toluene were used.

4. Silicon tetrachloride and toluene were used under their own vapour pressures in a partial vacuum. The liquids were mixed in various ratios and either carbon or silicon was deposited, but no deposition of silicon carbide could be obtained at any temperature.

5. Silicon tetrachloride and toluene were used with nitrogen as a carrier instead of hydrogen. No deposit of silicon carbide could be obtained.

6. Using silicon tetrachloride and toluene with hydrogen a number of " impurities " were deliberately introduced by adding the vapour of a volatile chloride such as stannic chloride, ferric chloride or aluminium chloride. The conditions of formation did not appear to be affected,

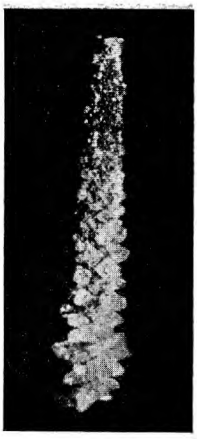


FIG. 1.

The Structure of the Deposit.

The growth of the deposit was most pronounced at the centre of the filament, as is seen in fig. 1. This was probably due to the higher temperature there, because the growth was more rapid at higher temperatures.

A limit was set upon the size of crystals which could be obtained on the filament. When the deposit had increased the filament diameter to about 0.1 cm., carbon was deposited. Presumably this was due to the fact that the temperature of the outer surface dropped as the radius increased. Attempts to increase the temperature by increasing the filament current burnt out the filament.

The yellow crystals were well formed and had well developed faces, but the black crystals were in general small and badly formed. All crystals produced were of the β-type (cubic) structure ; this was an unexpected result. One deposit produced at a low temperature contained free silicon ; this was shown by an X-ray analysis. No free silicon was found in the yellow crystals, but this method of analysis would not be sensitive to very small concentrations.

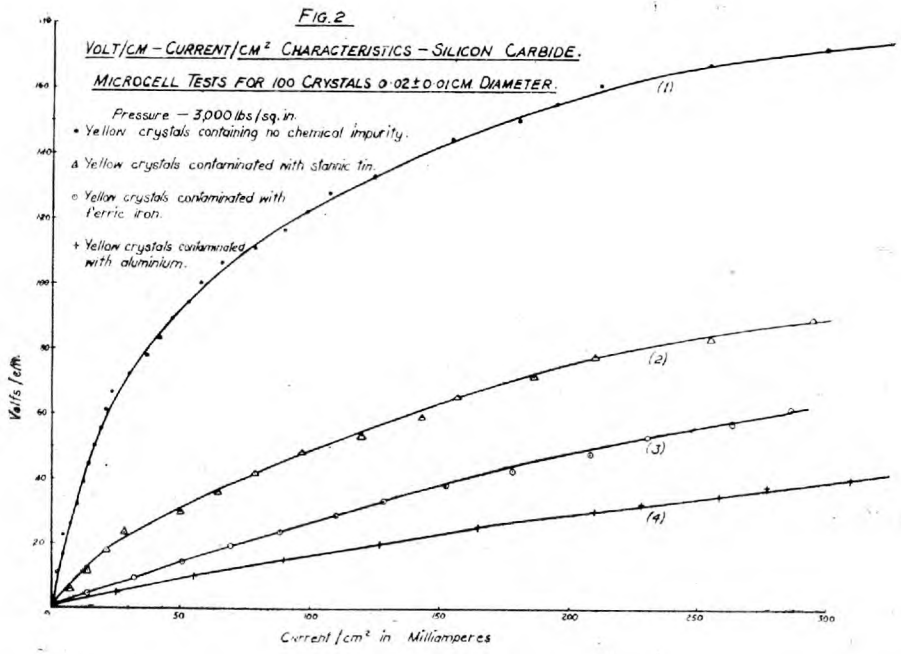
Electrical Properties of the Deposit.

The electrical properties were investigated in two ways : thermoelectric tests and microcell tests. The sign of the thermoelectric e.m.f. gives the type of conduction, and the tests were done by clamping the crystals between two phosphor bronze electrodes and heating one junction. The microcell technique is, briefly, as follows :—

About 100 small crystals are placed in a glass capillary tube between two copper wires acting as electrodes ; the top electrode is loaded to ensure good contacts between crystals and between crystals and the electrodes. The voltage/cm.–amperes/cm.$^{(2)}$ characteristics are obtained for this assembly. This of necessity gives the characteristic over a large number of crystal-crystal contacts in series and in parallel, and so gives no indication of the internal resistance. It was hoped, however, that some information might be obtained from these graphs.

It was found that all completely yellow crystals were *excess* conductors. Some black crystals produced when the ratio of silicon tetrachloride : toluene was about 2 : 3 gave a thermal e.m.f. corresponding to defect conduction, but heating in air so reduced the number of such crystals that this e.m.f. was almost certainly caused by the presence of carbon on the surfaces of the crystals.

Fig. 2 shows typical microcell characteristics for the yellow crystals prepared. Curve (1) is a representative curve for " chemically pure " crystals, and curves (2), (3) and (4) are characteristics for crystals contaminated with stannic tin, ferric iron and aluminium respectively. It is evident that the characteristic is more linear for these



crystals, and the crystal-crystal contact resistance is smaller. These effects are the justification for saying that the impurities entered the crystals. All the crystals were *excess* conductors.

It was noticeable that, whereas for crystals prepared in the laboratory the thermal e.m.f. could be observed simply by clamping the crystals between two electrodes and connecting these electrodes to a galvanometer, it was necessary in general to break down the contact resistance of the commercial carborundum before a measurable current passed through the galvanometer. This was especially so for green carborundum. This suggests that either the thermal e.m.f. is very high for the crystals prepared in this laboratory, or that in the commercial carborundum the e.m.f. is dissipated over a larger contact resistance.

Comparison of microcell characteristics shows that the effect is due to a larger contact resisitance. Fig. 3 shows a typical microcell characteristic for "electrical" carborundum; approximately the same size of crystals was used. Although the pressure was rather different this would not have greatly affected the behaviour. It can be seen that the commercial carborundum has a contact resistance many times larger (some 20–150 times) than the crystals prepared in this laboratory.

Discussion of Results.

From the results given above, it seems certain that SiC can be produced with an appreciable conductivity even in the absence of detectable amounts of impurity. The presence of hydrogen during the formation of silicon carbide by this method seems to be essential. Since the reaction constituents were varied and the crystals obtained were still semiconducting, it seems reasonable to suppose that the conduction is caused by stoichiometric deviations in the silicon and carbon. The presence of excess silicon in some of the crystals seems to indicate that this is associated with *excess* conduction, but this does not preclude the possibility that carbon is also associated with *excess* or *defect* conduction.

No conclusive results were obtained from the introduction of impurities. It is quite likely, however, that only a small proportion of the impurity centres were caused

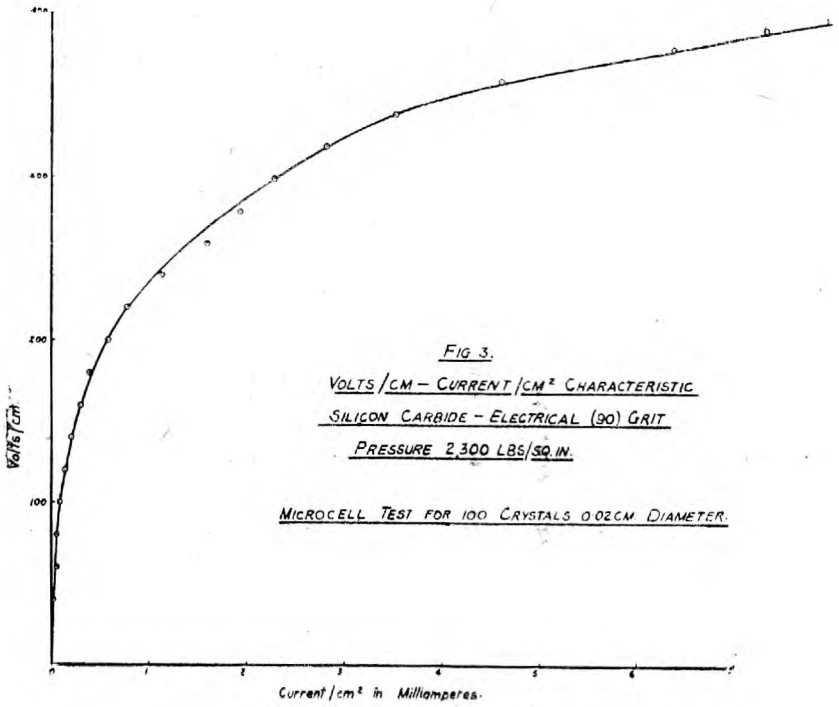


FIG 3.
VOLTS/CM – CURRENT/CM² CHARACTERISTIC
SILICON CARBIDE – ELECTRICAL (90) GRIT
PRESSURE 2,300 LBS/SQ. IN.
MICROCELL TEST FOR 100 CRYSTALS 0·02CM DIAMETER.

by the known impurities being introduced, and that their effect upon the conduction was completely masked by the "impurity centres" arising from stoichiometric deviations.

Black excess conductors were obtained. The empirical classification of commercial black carborundum as a "defect" conductor would seem to be merely fortuitous therefore.

Moers mentioned that the yellow crystals he produced were non-conducting. This was based upon the fact that the filament resistance did not change during the deposition. This is approximately true, but the crystals have, nevertheless, a definite conductivity. One unexpected result was that only cubic crystals were produced, even at quite low temperatures, whereas Moers reported that various hexagonal forms were deposited at these lower temperatures.

Acknowledgment.

The authors wish to thank Sir Arthur P. M. Fleming, C.B.E., D.Eng., Director of Research and Education, and Mr. B. G. Churcher, M.Sc., M.I.E.E., Manager of Research Department, Metropolitan-Vickers Electrical Co., Ltd., for permission to publish this paper.

REFERENCES.

1. P. Aloisi, *Periodico Mineral Roma*, **5,** 191 (1924).
2. Kendall, J. T., *Proc. Phys. Soc.*, **56,** 123 (1944).
3. Pring, J. N. and Fielding, W., *J. Chem. Soc.*, **95,** 1497 (1909).
4. Friederich, E. and Sittig, L., *Z. anorg. allg. Chem.*, **144,** 169 (1925).
5. Ruff, O., *Trans. Electrochem. Soc.*, **68,** 87 (1935).
6. Moers, K., *Z. anorg. allg. Chem.*, **198,** 243 (1931).

Reprinted from THE JOURNAL OF CHEMICAL PHYSICS, Vol. 21, No. 5, 821–827, May, 1953
Printed in U. S. A.

Electronic Conduction in Silicon Carbide

J. T. KENDALL
Department of Electrical Engineering, Imperial College of Science and Technology, London, England
(Received November 4, 1952)

Pure silicon carbide was prepared by decomposition of the vapors of silicon tetrachloride and toluene on a hot carbon filament. Various *n*- and *p*-type impurity atoms were introduced by the addition of volatile metallic chlorides during the preparation. For the pure substance either *n*- or *p*-type crystals could be obtained by varying the ratio of the reaction constituents. The results show that semiconductivity in silicon carbide may be due either to nonstoichiometric proportions of silicon and carbon, or to the presence of impurity atoms, or (as probably occurs in the commercial product) to both circumstances simultaneously.

A theoretical model for electronic conduction in silicon carbide is proposed, which satisfactorily explains the magnitude of the low and high temperature activation energies observed, their different ratios in *n*- and *p*-type crystals, the occurrence of conduction at one of the disturbance energy levels, and the anomalous low Hall constant at low temperatures found in black but not in green silicon carbide. The model may be applicable to other semiconductors in which disturbance centers can give rise to electrons in unlocalized excited states.

1. INTRODUCTION

SILICON carbide is a solid in which the bonding is intermediate between homopolar and heteropolar. It is similar in its properties to the typically homopolar substance diamond and has a similar crystal structure, but with half the carbon atoms replaced by silicon. Because of the different electron affinities of carbon and silicon, this gives rise to a certain degree of heteropolarity in the crystalline bonds. According to Pauling[1] the SiC bond in silicon carbide is approximately 12 percent ionic in character. It will be shown in Sec. 7 how this may help to explain semiconductivity in silicon carbide.

It is noteworthy that electronic conduction in silicon carbide may be of *n*- or *p*-type. In the commercial material crystals which are colored green are *n*-type conductors, and blue or black crystals are *p*-type. The commercial material is made in the same way as the original synthesis of Acheson in 1886 by heating together sand and coke in an electric furnace. Many impurities, chiefly aluminum and iron, are introduced in this way, and an investigation by Lundquist[2] has indicated that aluminum as impurity may give rise to black *p*-type crystals and that iron may give rise to green *n*-type crystals. The interpretation of Lundquist is not, however, clear cut, since all commercial crystals contain considerable quantities of both iron and alumi-

[1] L. Pauling, *Nature of the Chemical Bond* (Cornell University Press, Ithaca, 1940), pp. 58–75.

[2] D. Lundquist, Acta Chemica Scand. **2**, 177 (1948).

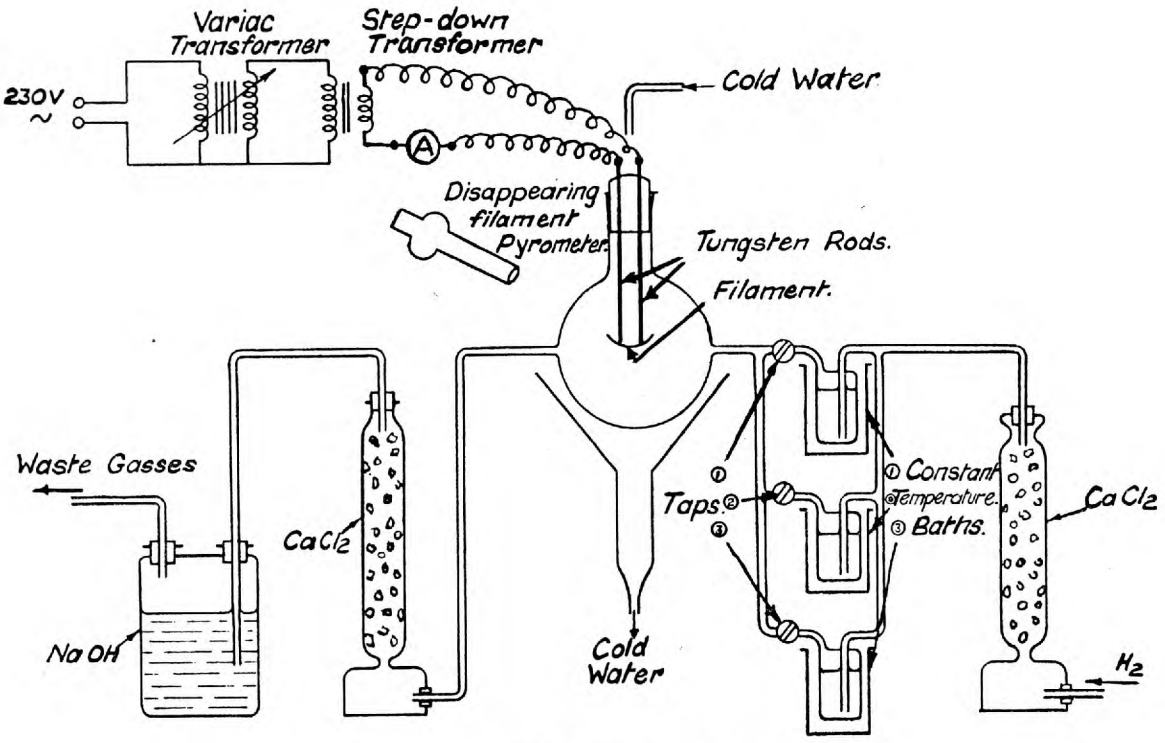


FIG. 1. Apparatus for preparing silicon carbide.

num as well as other elements. Moreover, the preparation of pure silicon carbide by Kendall and Yeo[3] showed that the presence of impurities is not essential for semiconductivity in silicon carbide.

The present research was, therefore, directed to the following points: (1) preparation of pure and impure specimens of silicon carbide, (2) determination of the type of semiconductivity produced by changes in the conditions of formation of the crystals and by the introduction of specific impurities, (3) spectrographic analysis of various specimens of commercial silicon carbide, with a view to determining the relevant impurities.

2. PREPARATION OF PURE SILICON CARBIDE

A method of preparing pure crystalline material has been described by Moers[4] and by Kendall and Yeo.[3] Briefly, a carbon filament 0.025 cm in diameter and about 1.5 cm long is heated in a stream of hydrogen containing the vapors of silicon tetrachloride and a hydrocarbon such as toluene. The proportions of the reaction constituents and the temperature of the filament can both be varied, and specific impurities can be introduced by means of volatile chlorides. A detailed description of the method has not been published, and, since considerable improvements have been made since the publication of the papers previously cited, a detailed description of the method as it is practiced at present will now be given.

The apparatus is illustrated in diagram form in Fig. 1. A stream of hydrogen (free from oxygen) is dried by passing over calcium chloride and then passes through three bubbling bottles arranged in parallel. In the first is put toluene, in the second, silicon tetrachloride, and in the third, concentrated sulfuric acid. The bottles are immersed in liquid baths maintained at constant temperature. The amounts of toluene and silicon chloride vapor picked up by the hydrogen stream can thus be separately varied by regulating the rate of bubbling through each bottle and the temperature of its contents. By the addition of volatile chlorides to a fourth bubbling bottle, specific impurities may be introduced. The hydrogen and vapors then pass through the reaction vessel, where a carbon filament is maintained at a temperature in the range 1500 to 2400°C. Decomposition of the vapors occurs on the filament with the deposition of crystalline silicon carbide and the formation of hydrogen chloride. The waste gas finally passes through a second calcium chloride column and then aqueous caustic soda to absorb the hydrogen chloride and excess silicon tetrachloride.

The current to the filament is supplied from the ac mains through a step-down transformer, with a 0–50 amp-ammeter in series with the secondary winding, controlled by a variable transformer. The temperature of the center of the filament is measured by a disappearing filament pyrometer. During the build-up of a

[3] J. T. Kendall, and D. Yeo, Proc. Intern. Congr. Pure Appl. Chem. **11**, 167 (1947).
[4] K. Moers, Z. anorg. u allgem. Chem. **198**, 243 (1931).

deposit on the filament the resistance of the filament decreases, and the variable transformer must be continually turned up (by hand) to maintain the filament at the desired temperature. After some experience it is not difficult to maintain the filament temperature constant to at least ±50°C.

Two tungsten rods are sealed into the stopper of the reaction vessel, and the carbon filament (supplied by Edison-Swan Electric Company, Ltd.) is secured at each end by means of Aquadag. It has been found best to build up a considerable thickness of Aquadag at the junctions with a series of thin layers, drying off each layer by passing a small current through the filament before applying the next. After some experience was obtained in making these junctions, it was found that an overheated filament invariably burnt out in the center and never at the junctions. It was found necessary to cool the outside of the reaction vessel with running cold water.

A typical preparation was carried out as follows: Bubbling bottle number 1 was half-filled with toluene, number 2 with silicon tetrachloride, number 3 with concentrated sulfuric acid. Bubbling bottles numbers 1 and 2 were immersed in water baths at 18°C. A carbon filament was secured to the tungsten leads and the whole apparatus flushed out with hydrogen. Taps 2 and 3 were then closed so that only hydrogen and toluene vapor passed through the reaction vessel at the rate of approximately 3 bubbles per second. The filament was then maintained at 1800°C until it had increased in diameter approximately three times (i.e., to a thickness of about 0.075 cm). This usually took about 3 minutes and required a final filament current of about 25 amp. This preliminary building up of the filament by deposition of carbon was found to be necessary to produce a robustness and decreased tendency to burn out at higher temperatures. Tap 3 was then opened and tap 1 closed so that only pure hydrogen passed through the reaction vessel. The filament temperature was then raised to (say) 2000°C and all the taps opened to (say) the following extents: through the toluene bottle—1 bubble per sec, through the silicon tetrachloride bottle—2 bubbles per sec, through the sulfuric acid bottle—2 bubbles per sec. The filament temperature was maintained constant for about 15 minutes (although it frequently burnt out at a weak spot before that time). By the end of the experiment the filament current was usually about 40 amp.

Crystalline silicon carbide was deposited on the filament, and a photograph of a typical deposit is shown in Fig. 2. The size of the crystals increases towards the center, since that part is considerably hotter than the ends. A number of variations in the experimental conditions were tried out, and the results of a large number of experimental runs are shown in summarized form below.

(a) Variation of Filament Temperature. (Bubbling Rates 1:2. C_7H_8: $SiCl_4$)

1500–1700°C	Black amorphous deposit, mostly C, but x-ray investigation indicated small amounts of SiC near the center of the filament.
1700–1900°C	Black crystalline deposit of SiC at center plus amorphous deposit of C+SiC (very small crystals).
1900–2100°C	Yellow crystalline SiC at center of filament (larger crystals), black crystalline SiC away from center (small crystals), amorphous C+SiC at ends.
2100–2200°C	Best temperature for formation of largest crystals of yellow SiC.
2200–2400°C	Filament usually burnt out quickly, otherwise large yellow crystals obtained.

(b) Variation of Bubbling Rates through Toluene and Silicon Tetrachloride

>5:1, C_7H_8:$SiCl_4$	C deposited at all temperatures.
4:1–2:1, C_7H_8:$SiCl_4$	C deposited below 2200°C; a little SiC (black) detected by x-ray investigation in deposits formed above 2200°C.
1.5:1–1:1, C_7H_8:$SiCl_4$	C deposited below 1900°C; a little black SiC detected by x-ray investigation in deposits formed from 1900–2100; black crystals formed at center of filaments above 2100°C.

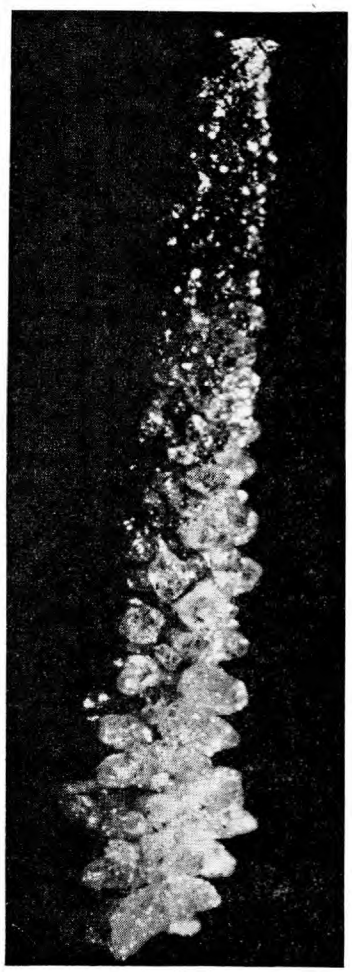


FIG. 2. Photograph of part of a yellow deposit (magnification × 17) showing the variation in crystal size along the length. The size of crystal increases toward the center of the filament.

TABLE I. Spectrographic analysis of silicon carbide specimens.

No.	Specimen Type	Impurity elements[a] Al	Fe	Mg	Mn	Cu	Ag	Na	Ca	V	Zn	Ni	Totals Al+Fe	All elements
1	Norwegian, black	3	3	3	2	2	2	1	2	2	—	—	6	20
2	Swiss, black	4	4	3	2	2	1	1	2	3	—	—	8	22
3	Norwegian, blue-black	2	2	3	2	3	4	1	2	—	—	—	5	20
4	Norwegian, blue	5	5	4	4	4	2	2	3	1	—	—	10	30
5	Norwegian, green	2	3	3	1	5	1	2	1	1	—	1	5	20
6	Swiss, green	3	2	3	2	5	1	1	2	1	1	—	5	21
7	Swiss, pale green	2	2	3	3	1	1	1	3	—	—	—	4	16
8	Norwegian, pale green	3	3	3	2	3	3	1	2	—	—	—	6	20
	Kendall, yellow	2	2	4	2	3	1	1	3	—	—	—	4	19

[a] 5 = Very heavy line. 4 = Heavy line. 3 = Medium line. 2 = Faint line. 1 = Very faint line. — = No line observed.

1:1.5–1:3, C_7H_8:$SiCl_4$	As described above under (a).
1:4–1:10, C_7H_8:$SiCl_4$	Black amorphous deposit of SiC deposited at 1500–1700°C; small yellow crystals deposited at 1800–2200°C; no deposition above 2200°C.
<1:10, C_7H_8:$SiCl_4$	Small yellow microcrystalline deposit at 1500–1800°C. No deposit above 1800°C.

(c) Variation of Bubbling Rate through Sulfuric Acid

This only affected the rate of deposition, not the nature of the deposit. A maximum rate of decomposition was found if about 2 bubbles per sec were passed through the sulfuric acid, although there was little variation up to 5 bubbles per sec after which the deposition rate fell off significantly.

It should be noted that the vapor pressures of toluene and silicon tetrachloride at 18°C are as follows:

C_7H_8 19.5 mm; $SiCl_4$ 175 mm.

The latter vapor is therefore in considerable excess in the reaction vessel for the best conditions of formation of silicon carbide.

In all cases, β-SiC (the cubic modification) was obtained. This is in agreement with the results of Taylor and Laidler,[5] who found that the hexagonal type was only produced at very high temperatures.

3. PREPARATION OF IMPURE SILICON CARBIDE

Volatile chlorides of the following elements were introduced during the preparation: Ge, Sn, B, Al, P, As, Sb, Bi, Cu, Fe. They were each placed separately in a fourth bubbling bottle in parallel with the other three, and the bottle immersed in a liquid bath at a temperature which would give a reasonable vapor pressure.

In all cases, the introduction of an impurity did not appear to affect the appearance of the final product, black and yellow crystals being formed as previously.

4. INVESTIGATION OF ELECTRICAL PROPERTIES OF SILICON CARBIDE PREPARATIONS

The crystals produced were all too small for any satisfactory measurements to be made of conductivity and Hall constant. It was, however, possible to make a qualitative determination of the sign of the thermoelectric coefficient at room temperature. This information determines whether the crystals are *n*- or *p*-type. A crystal was held between two phosphor-bronze electrodes, one of which was heated. The electrodes were connected externally through a sensitive dc galvanometer, and the direction of movement of the needle gave the sign of the thermoelectric coefficient.

It was found that all yellow crystals (whether pure or contaminated with *n*- or *p*-type impurities) were *n*-type semiconductors. Most black crystals were also *n*-type (although commercial black silicon carbide is *p*-type), but a few black crystals were found to be *p*-type. These were obtained only in those deposits formed when the ratio of the bubbling rates through toluene and silicon tetrachloride was equal to or greater than 1:1 and when the deposits were pure or contaminated with boron or aluminum. Crystals prepared in the same way, but contaminated by germanium, tin, phosphorus, arsenic, antimony, bismuth, copper, or iron, were found to be *n*-type, although identical in appearance. These *p*-type black crystals were formed at temperatures above 2100°C. The black crystals formed at lower temperatures and hence with a lower ratio of toluene: silicon tetrachloride, were all found to be *n*-type even when contaminated by boron or aluminium.

The conclusions from this would seem to be as follows:

(1) In the preparation of silicon carbide by reaction of silicon tetrachloride and toluene vapors on a hot carbon filament, silicon is normally present in great excess over carbon, and the resultant silicon carbide is *n*-type, even when pure, as a result of a stoichiometric excess of silicon. It does not appear possible to introduce sufficient boron or aluminum to neutralize this excess silicon.

(2) If the toluene:silicon tetrachloride ratio is increased, pure silicon carbide crystals can be deposited which are *p*-type, presumably because there is now a stoichiometric excess of carbon. In this case, however, the introduction of *n*-type impurities appears to reverse the effect of the excess carbon. (3) It thus appears that *n*- and *p*-type conductivity in silicon carbide can be caused by nonstoichiometric proportions of silicon and carbon and also by the introduction of impurities. (4) The temperature of formation of the silicon carbide

[5] A. Taylor and D. S. Laidler, Brit. J. Appl. Phys. 1, 174 (1950).

appears to have no influence on the type of conductivity.

5. PREPARATION OF EVAPORATED SILICON CARBIDE FILMS

It is of interest that films of silicon carbide can be prepared by evaporating at a high temperature in a vacuum. The carbon filament on which silicon carbide had been deposited was heated to 2500°C in a vacuum approximately 1 cm away from a silica plate. In most cases the filament burnt out quickly, but in a few cases it remained complete for a sufficient length of time for a thin evaporated layer of silicon carbide to be deposited on the silica plate. In all cases this layer was contaminated with carbon evaporated simultaneously. The films produced were yellow or black in color, depending on the degree of carbon contamination and on the color of the original silicon carbide. It was hoped to prepare evaporated films for measurement of conductivity and Hall constant, but it was not found possible to prepare films of sufficient thickness for this purpose. Since thick films could not be built up, the method was not further developed.

6. SPECTROGRAPHIC ANALYSIS OF COMMERCIAL SILICON CARBIDE CRYSTALS

Various specimens of commercial silicon carbide were analyzed spectrographically, using the sensitive "cathode layer" technique. A powdered specimen was placed in a small graphite cathode. The intensities of the lines observed on a photographic film were measured by a photoelectric densitometer and compared with each other. The experimental results are summarized in Table I.

It will be seen that all the crystals contain iron and aluminum in approximately constant ratios, and there does not appear to be any clear-cut correlation between color or conductivity type and nature of impurities.

7. THEORETICAL SPECULATION

(a) General Theoretical Model

We may describe the ionic-homopolar structure[1] of silicon carbide as some resonant combination of Si=C and $[Si]^{4+}\cdot[C]^{4-}$. The relevant atomic and ionic radii are C=0.77A, C^{4-}=2.60A, Si=1.18A, Si^{4+} =0.39A. We may therefore have, in the ionic form, missing Si^{4+} ions (cf. CuO) or interstitial Si^{4+} ions (compare with ZnO). The ionization energy of these "impurity" centers may be calculated from the usual relation $E_I=2\pi^2me^4/\epsilon^2h^2$, where m=mass of free electrons or hole, e=magnitude of electronic charge, ϵ=dielectric constant, h=Planck's constant. For silicon carbide ϵ may be taken as 7. Therefore $E_I=0.275$ ev.

This value for the ionization energy of an "impurity" center will be the same whether the "impurity" arises from the presence of foreign atoms (electron donators or acceptors), or from nonstoichiometric proportions of carbon and silicon, or from both causes.

At temperatures above absolute zero some of the "impurity" centers will be in excited states. At low concentrations of impurity the electronic levels of these excited states will be localized, and, since the number of electrons in them will be small, they may generally be neglected in considering the process of activation of free electrons. However, at high concentrations of impurity the excited-state levels will broaden out into bands, as shown by Erginsoy.[6] If this occurs we have the possibility of an electron conduction band, since the excited-state impurity electrons will no longer be localized. This can be shown actually to occur in silicon carbide as follows: The radii of the normal and excited orbits of the impurity electron can be calculated. In a medium of dielectric constant ϵ the normal radius of the carbon atom, 0.77×10^{-8} cm, will expand to $r=\epsilon\times q^2\times$Bohr radius (where q=principal quantum number of the orbit, i.e., 1 for the ground state and 2 for the first excited level). For successive values of q, and $\epsilon=7.0$, we thus have $r=5.4\times10^{-8}$, 22×10^{-8}, 49×10^{-8} cm, and these will have activation energies of E_I/q^2, i.e., 0.275, 0.07, 0.03 ev. These expanded orbits will allow electronic conduction to take place if the mean distance between disturbing centers is less than twice the orbital radius of the "impurity" electron, for the orbits around neighboring centers will then overlap as shown in Fig. 3.

Now, from the experimental results of Busch[7] all crystals of black silicon carbide have approximately the same number of *holes*, bound and free, approximately 10^{20} per cc, and the number of missing silicon atoms

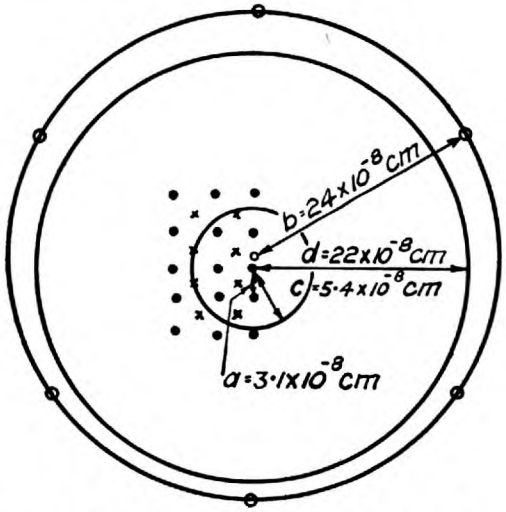


FIG. 3. Black silicon carbide showing radii of holes in ground and excited states. a=carbon-carbon distance=3.1×10^{-8} cm (shown ● and ×); b=missing silicon-missing silicon distance =24×10^{-8} cm (shown ○); c=radius of hole in ground state =5.4×10^{-8} cm; d=radius of hole in excited state =22×10^{-8} cm.

[6] C. Erginsoy, Phys. Rev. **80**, 1104 (1950).
[7] G. Busch, Helv. Phys. Acta **19**, 167 (1946).

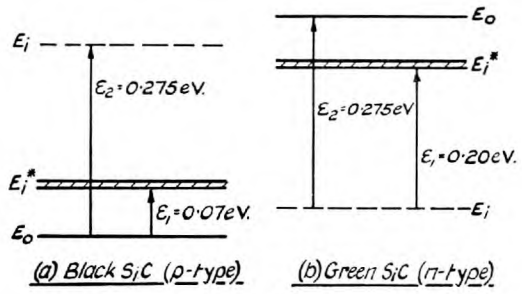


FIG. 4. Energy levels in SiC.

(or electron-acceptor impurities) must therefore be the same. Knowing the lattice parameters of silicon carbide, the mean distance between acceptor centers can therefore be calculated as about 24×10^{-8} cm. This situation is depicted in Fig. 3, and it can be seen that electrons excited to the level corresponding to $q=2$ will have overlapping orbits and therefore sufficient mobility to form a conduction band, while electrons corresponding to $q=1$ will be held in localized energy levels. A similar situation arises for p-type semiconduction in silicon and germanium, but in their cases the activation energies are much lower and, for $q>1$, become so small as to be indistinguishable at ordinary temperatures from the top of the full conduction band. In the case of silicon carbide there is an appreciable activation energy corresponding to $q=2$ (and even higher), so that at lower temperatures one may expect to find narrow conduction bands corresponding to $q=2, 3, \cdots$. We are therefore led to propose an energy level diagram for black silicon carbide as in Fig. 4(a), in which disturbing centers of one kind (missing silicon atoms or electron acceptors) give rise to more than one energy level, and the mobility of electrons in the E_i^* level will be dependent on the mean distance between disturbing centers.

For green silicon carbide (an n-type semiconductor) analogous calculations, assuming interstitial silicon atoms or electron-donator impurities, lead to an energy-level diagram as shown in Fig. 4(b). There is a significant difference in the two diagrams for black and green silicon carbide. In the former case electrons may be thermally excited from the normally full band, first to the excited level E_i^* with an activation energy of 0.07, and second to the localized level E_i with an activation energy of 0 275 ev. (We may neglect the transition from E_i^* to E_i as the number of electrons at the level E_0 is always very much greater than at E_i^*.) Measurement of conductivity as a function of temperature should therefore give these two activation energies ε_1 and ε_2 and, moreover, the ratio of $\varepsilon_1/\varepsilon_2$ should be 0.25. However, in the case of green silicon carbide, electrons must be excited initially from E_i to E_i^*, and subsequently from E_i to E_0. The activation energies observed should therefore be $\varepsilon_1=0.20$ ev and $\varepsilon_2=0.275$ ev, and the ratio of $\varepsilon_1/\varepsilon_2$ should be 0.75.

We are thus assuming that for p-type SiC the current carriers are holes in the normally full band and electrons in the impurity conduction band; while for n-type SiC they are electrons in both the normally empty band and in the impurity conduction band.

(b) Comparison with Experiment

The experimental results of Busch[7] for a number of different crystals of silicon carbide are given in Table II, and there is seen to be a qualitative correlation with the model given above. To examine the properties of the proposed model in more detail, we may consider the experimental results of Busch and Labhart[8] on black silicon carbide, as shown in Fig. 5. According to these results, the conductivity is given by

$$\sigma=A_1\exp[-\varepsilon_1/2KT]+A_2\exp[-\varepsilon_2/2KT]$$

over ranges I and II of Fig. 5, and a maximum conductivity over range III was explained by them as being the result of degeneration in the conduction band. The presence of two different activation energies was explained by them on the assumption of two kinds of disturbance centers having different energy levels, and it was found necessary, in order to explain the anomalous Hall constant at low temperatures, to assume that conduction could take place at one of these levels, although there seemed no particular reason why this should occur. The necessity of postulating two kinds of disturbing center has been avoided in the present model, which turns out to have properties similar to Busch and Labhart's, and moreover, provides a satisfactory explanation for the magnitude of the activation energies observed, for their different ratios in n- and p-type crystals and for the occurrence of conduction at one of the disturbance energy levels. Furthermore, the anomalous low Hall constant at low temperature found in black but not in green silicon carbide may also be accounted for, as will be shown below.

In the temperature range I of Fig. 5, conduction will be due to *holes* in the normally full band and to an equal number of *electrons* in the disturbance conduction band at E_i^*. The conductivity may be expressed as

$$\sigma=en_+b_++en_-b_-,$$

TABLE II. Experimental activation energies (Busch).

Black silicon carbide (8 different crystals)			Green silicon carbide (7 different crystals)		
ε_1	ε_2	$\varepsilon_1/\varepsilon_2$	ε_1	ε_2	$\varepsilon_1/\varepsilon_2$
0.044	0.270	0.16	0.120	0.215	0.56
0.038	0.281	0.14	0.185	0.246	0.75
0.044	0.272	0.16	0.133	0.285	0.47
0.042	0.282	0.15	0.191	0.265	0.72
0.051	0.248	0.21	0.147	0.263	0.56
0.050	0.231	0.22	0.057	0.157	0.36
0.050	0.231	0.22	0.097	0.198	0.49
0.052	0.226	0.23			
Theoretical activation energies (Kendall)					
0.07	0.275	0.25	0.20	0.275	0.75

[8] G. Busch and H. Labhart, Helv. Phys. Acta **19**, 463 (1946).

where e is the magnitude of the electronic charge, n_+ and n_- are the number of holes and electrons, and b_+ and b_- are their respective mobilities, i.e.,

$$\sigma = en(b_+ + b_-)$$

since in this temperature range $n_+ = n_- (= n)$. The situation will thus be very similar to that obtaining for intrinsic semiconductors, except that electrons in the disturbance conduction band would not be expected to have such a high mobility as would normal conduction electrons owing to the comparatively large mean distance between disturbance centers. For intrinsic semiconductors b_- is always greater than b_+, while in the present case the sign and magnitude of the Hall constant show that b_+ is greater than b_-. The Hall constant will be given by $R = 3\pi/8en(b_+ - b_-)/(b_+ + b_-)$. Thus its sign and magnitude will depend on the relative mobilities of holes and electrons, as well as on their number. Since Busch and Labhart obtained abnormally low values of the Hall constant at low temperatures, it seems that b_+ is nearly equal to b_-, and also, since there is no change in the sign of the Hall emf, the hole mobility must be slightly higher than the electron mobility. It can also be deduced that b_+ and b_- must vary with temperature, as otherwise the curve for $\log R$ against $1/T$ would show a small constant positive slope.

In the higher temperature range II, electrons will be excited from the normally full band to localized energy levels at E_i. Hole conduction will therefore become predominant, since n_+ will increase without a corresponding increase in n_-. Finally, when $n_+ \gg n_-$, the conductivity will be wholly p-type and will be given by the equation $\sigma = en_+b_+$, and the Hall constant by $R = 3\pi/8en_+$.

For green silicon carbide Busch and Labhart did not observe the anomalous low Hall constant in the low temperature range (see Figs. 4–7 of their paper, but note that Figs. 6 and 7 have been inadvertently transposed), and this is easily understood, since in the present model at both high and low temperatures, conduction in green silicon carbide is due to *electrons* exclusively, and we do not have the simultaneous hole and electron conduction in the low temperature range. Refinements to the theoretical model may make it possible to determine with more certainty the nature of the disturbance centers causing n- and p-type conduction in silicon carbide.

For other semiconductors the same model may be applicable, and its properties will be largely dependent on the dielectric constant of the crystal. For large values of dielectric constant (for example, germanium and silicon) the activation energies will be low, and the disturbance conduction bands will lie very close to the normally full (or empty) band of the crystal. For small values the activation energies will be high, and there will be additional localized energy levels as a result of the excited states, which do not develop into disturbance conduction bands. For intermediate values (e.g., silicon carbide) an additional energy level may occur which, as indicated above, will contain electrons which are localized or free according to the crystal parameters and the concentration of disturbance centers.

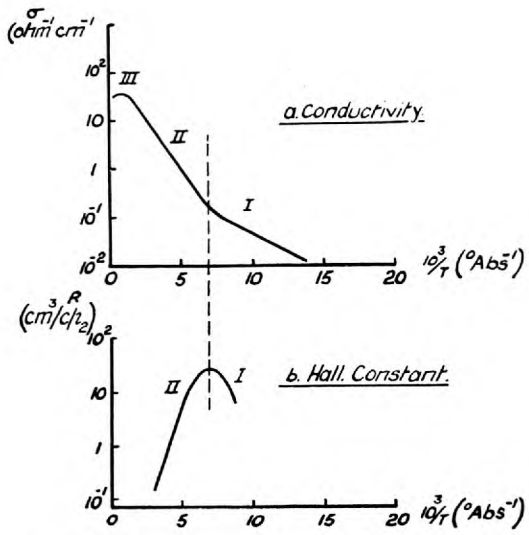


FIG. 5. Conductivity and Hall constant of black SiC. (Experimental results of Busch and Labhart.)

ACKNOWLEDGMENTS

The author wishes to acknowledge the award of a Leverhulme Research Fellowship (1949–1951) and to thank the Directors of Metropolitan-Vickers Electrical Company, Ltd., Manchester for granting him extended leave of absence. He also wishes to thank Professor Willis Jackson in whose department the work has been carried out and the D.S.I.R. for a grant for equipment. The spectrographic analyses were carried out in the Research Department of Metropolitan-Vickers Electrical Company Ltd. by Miss J. M. Rooke. Specimens of commercial silicon carbide were kindly supplied by the Gotthardwerke A. G., Bodio, Switzerland and the Arendal Smeltewerk, Eydehavn, Norway.

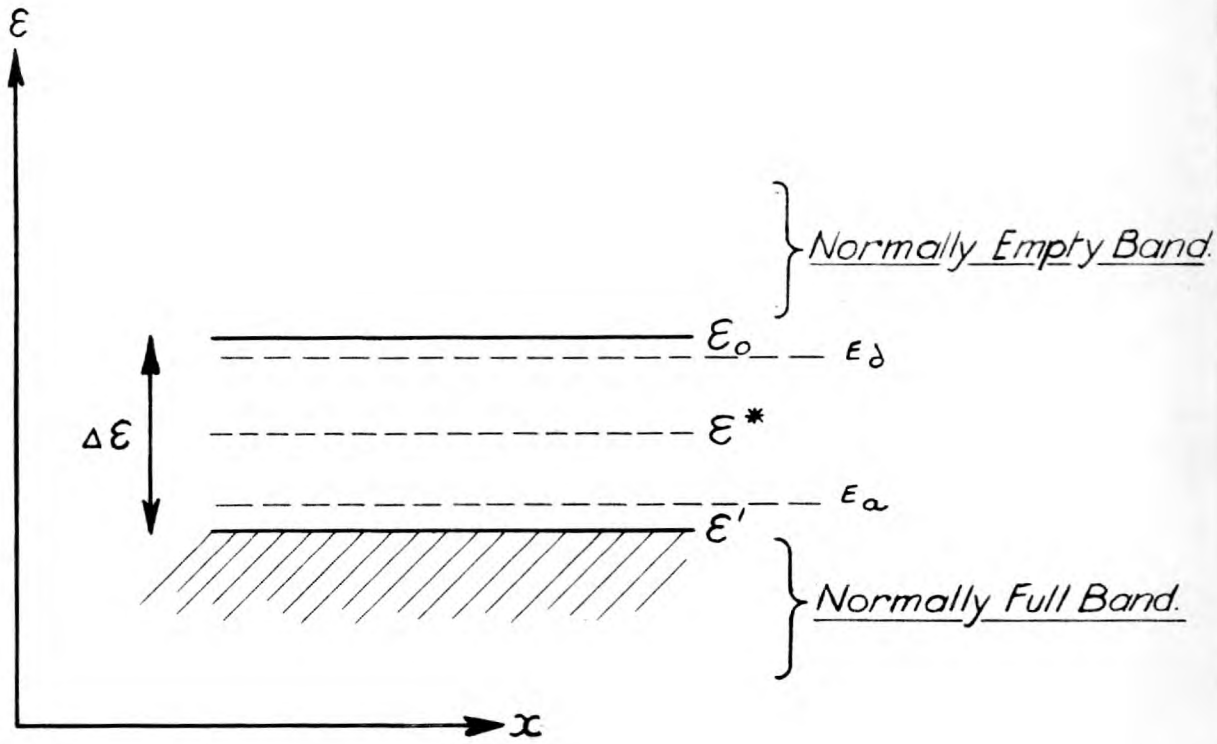


FIG. 1

ELECTRON ENERGY LEVELS

IN GREY TIN.

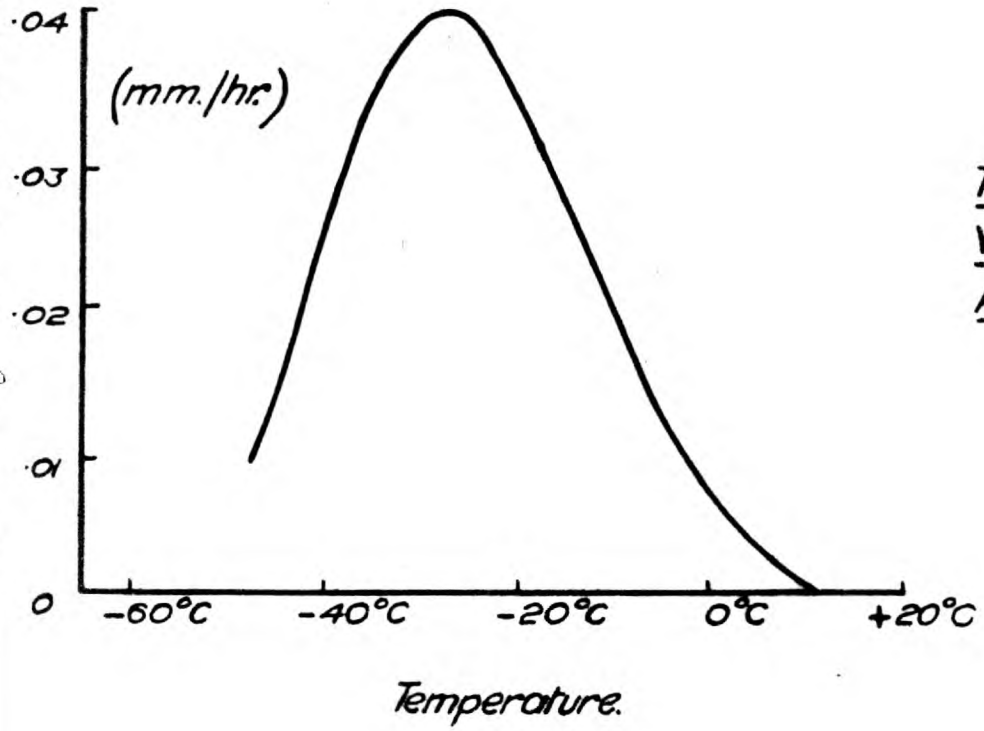


FIG. 2.
TRANSFORMATION VELOCITY
WHITE TIN ⇌ GREY TIN
ACCORDING TO TAMMANN &
DREYER (1931).

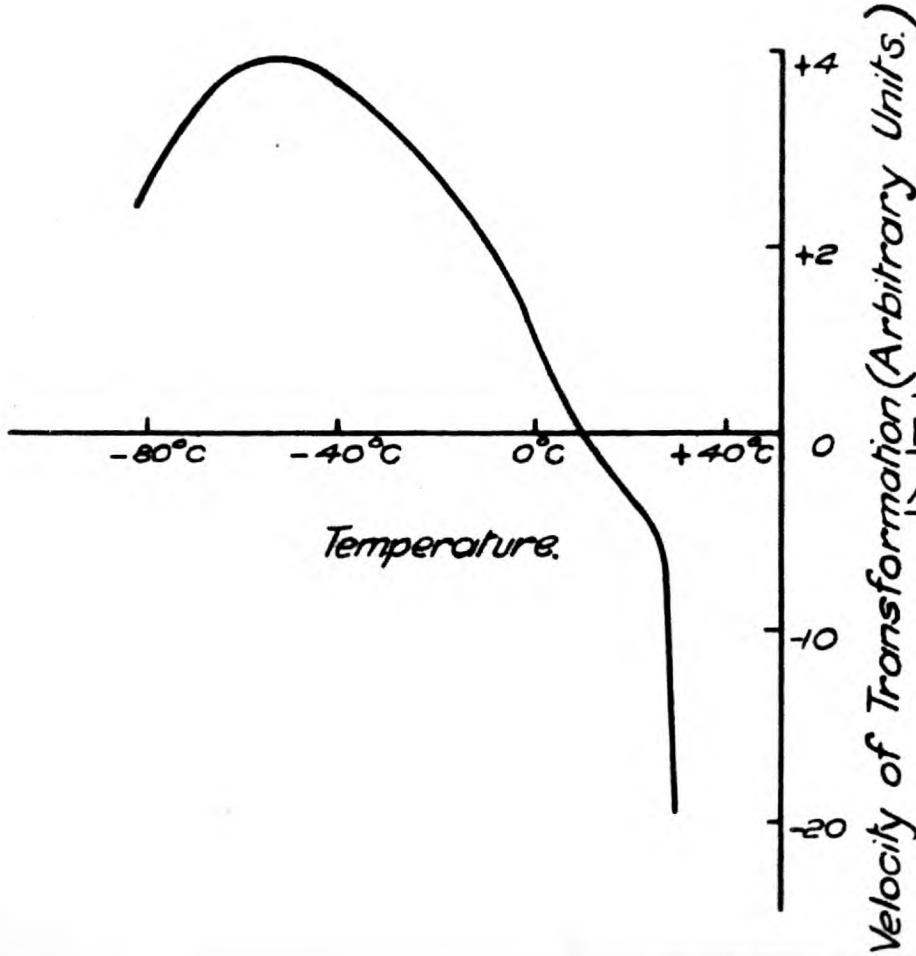


FIG. 3.
TRANSFORMATION VELOCITY
WHITE TIN ⇌ GREY TIN
ACCORDING TO COHEN &
LIESHOUT (1935).

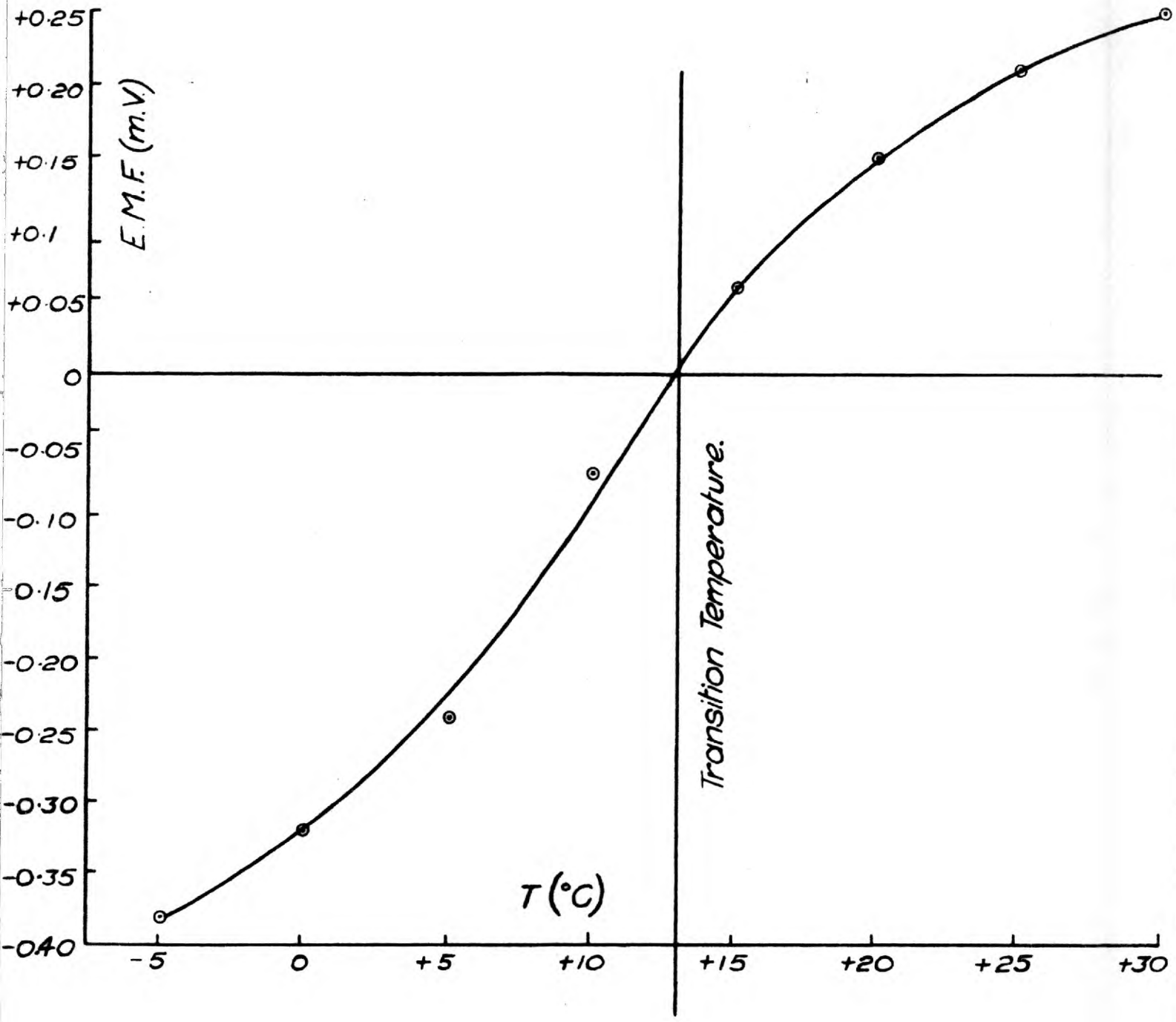


FIG. 4

VARIATION OF E.M.F. OF GREY TIN/ WHITE TIN CELL WITH TEMPERATURE.

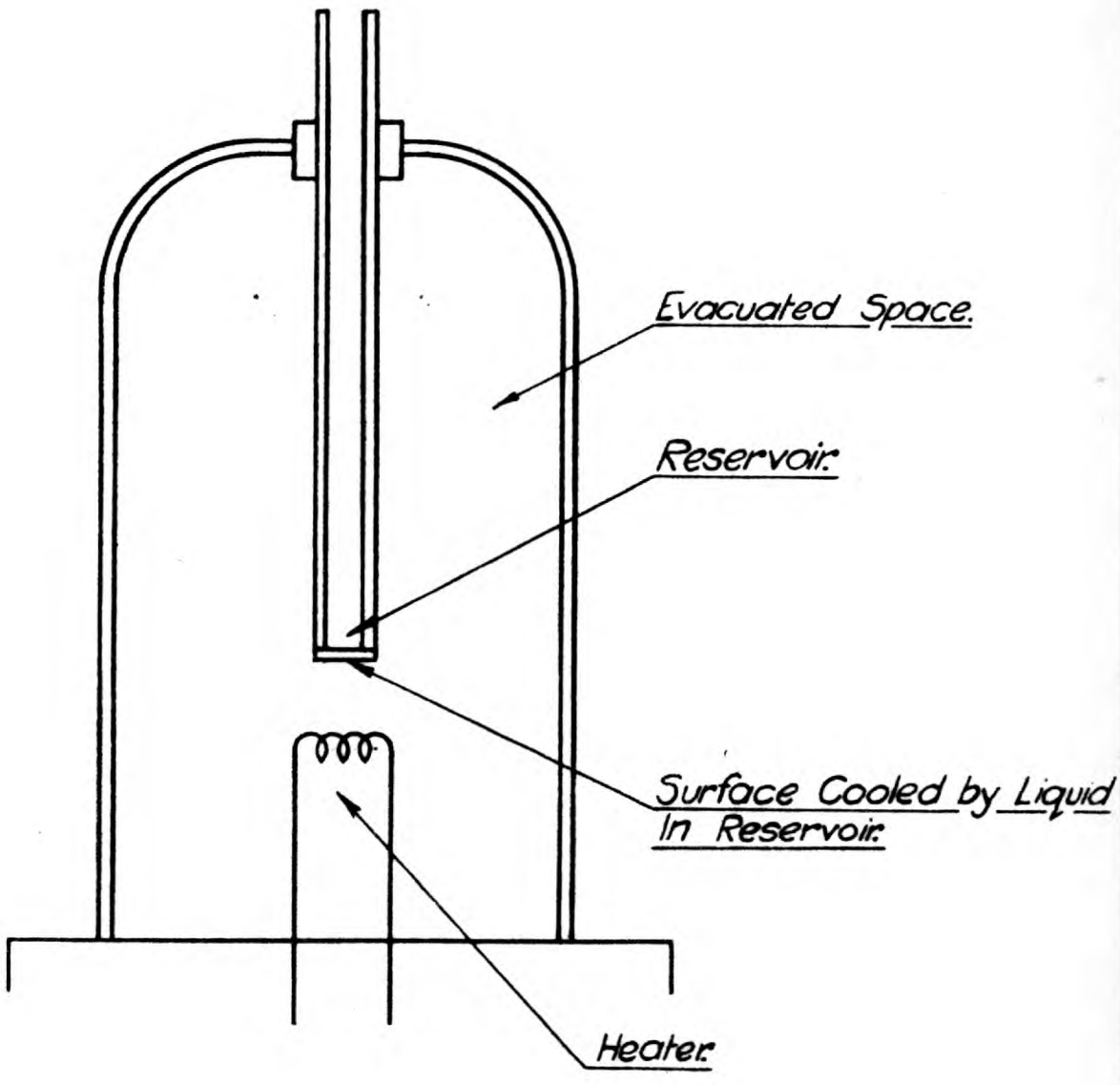
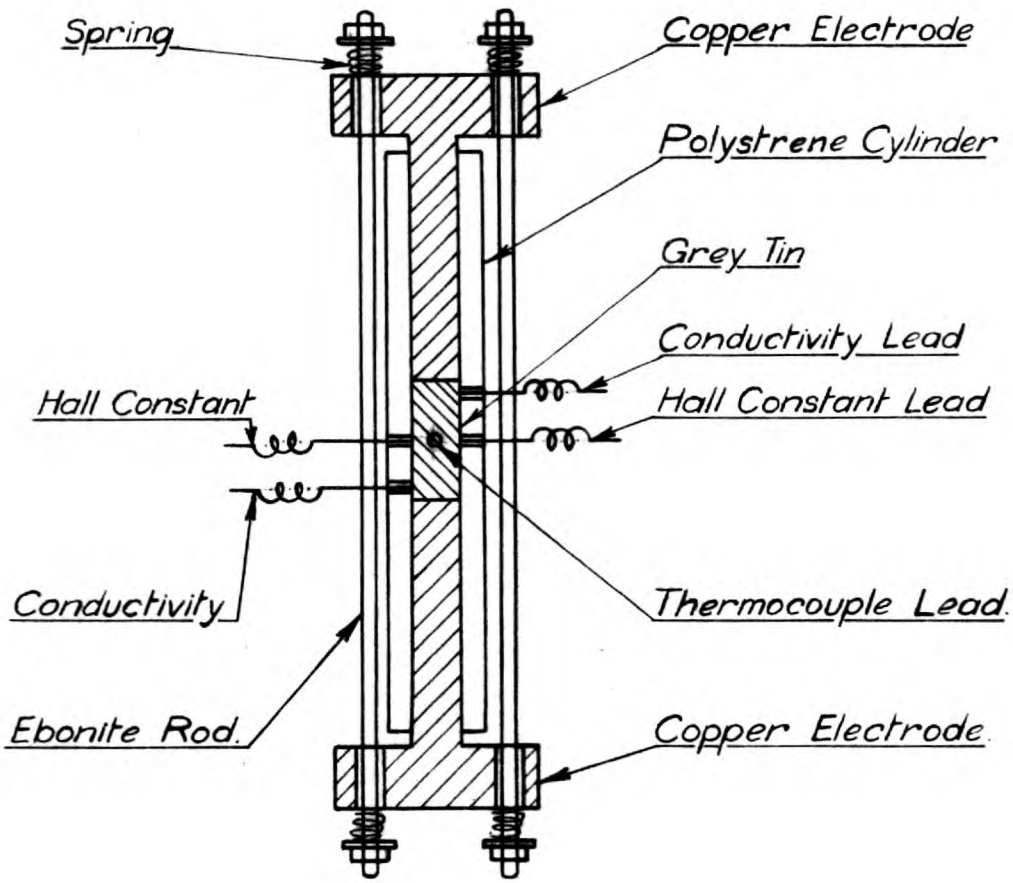


FIG. 5.

VACUUM EVAPORATION OF TIN ON A COOLED SURFACE.



Scale: Full Size

FIG. 6

SPECIMAN HOLDER.

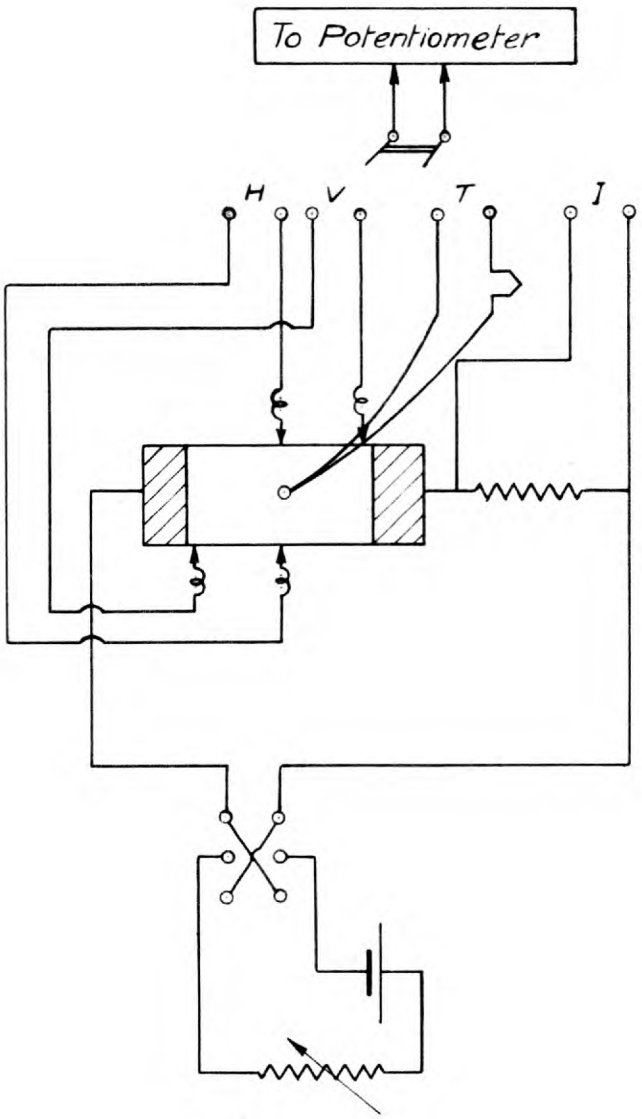
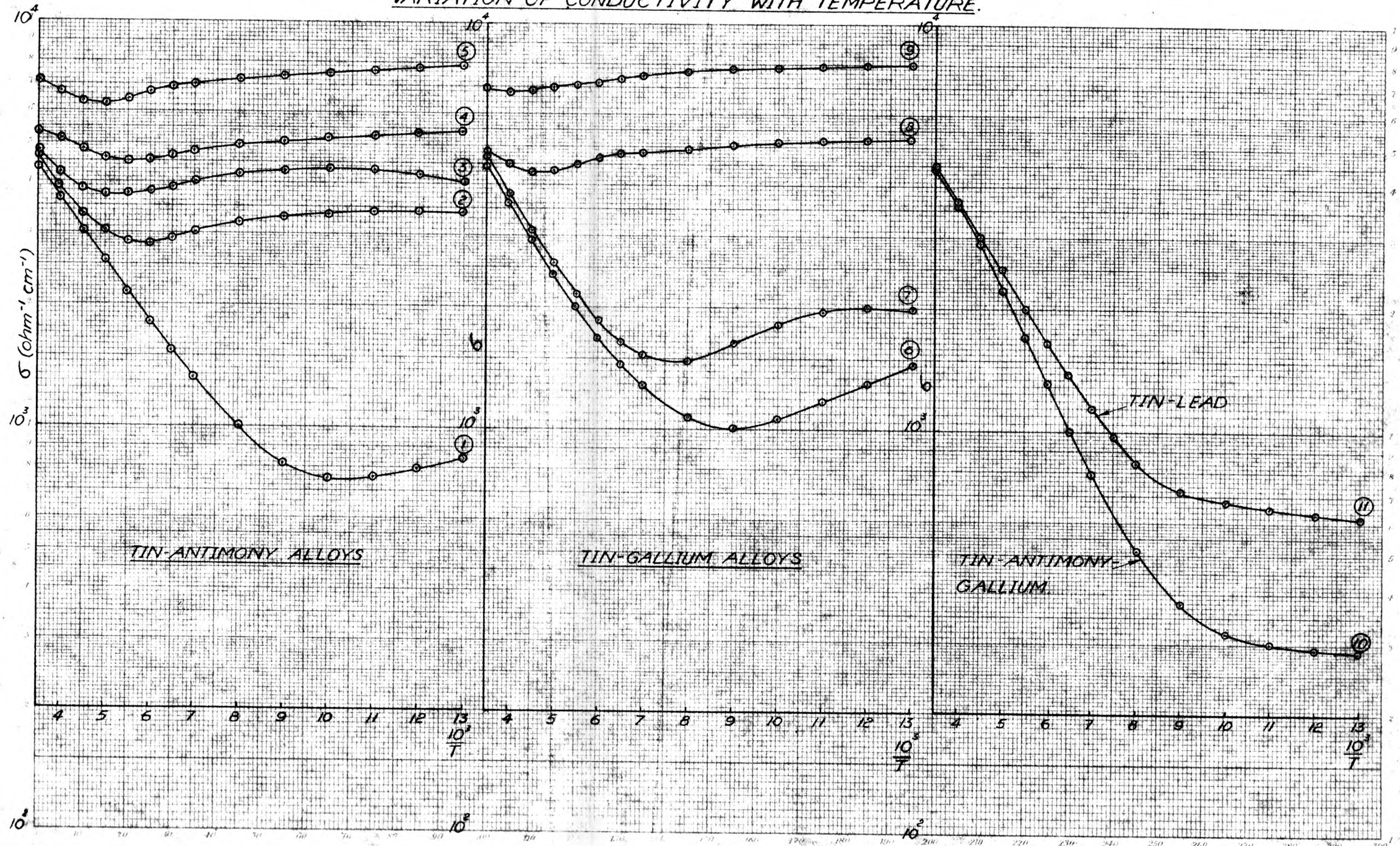


FIG. 7

CIRCUIT DIAGRAM.

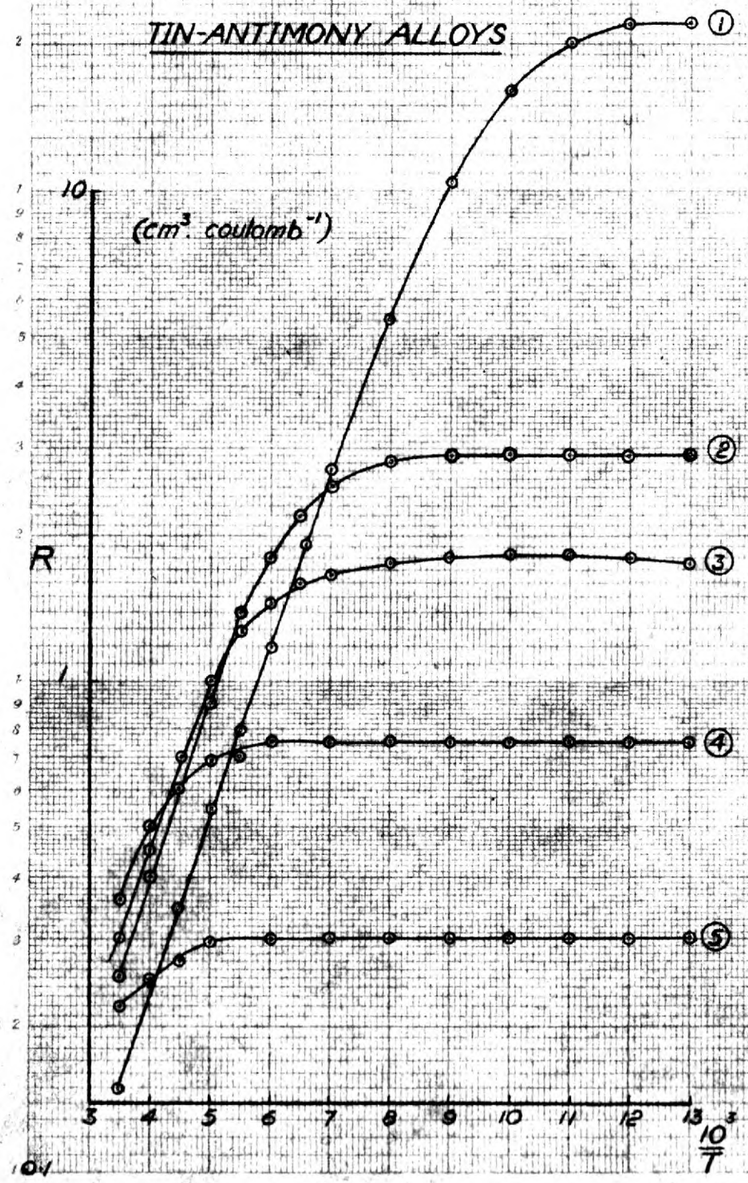
FIG. 8

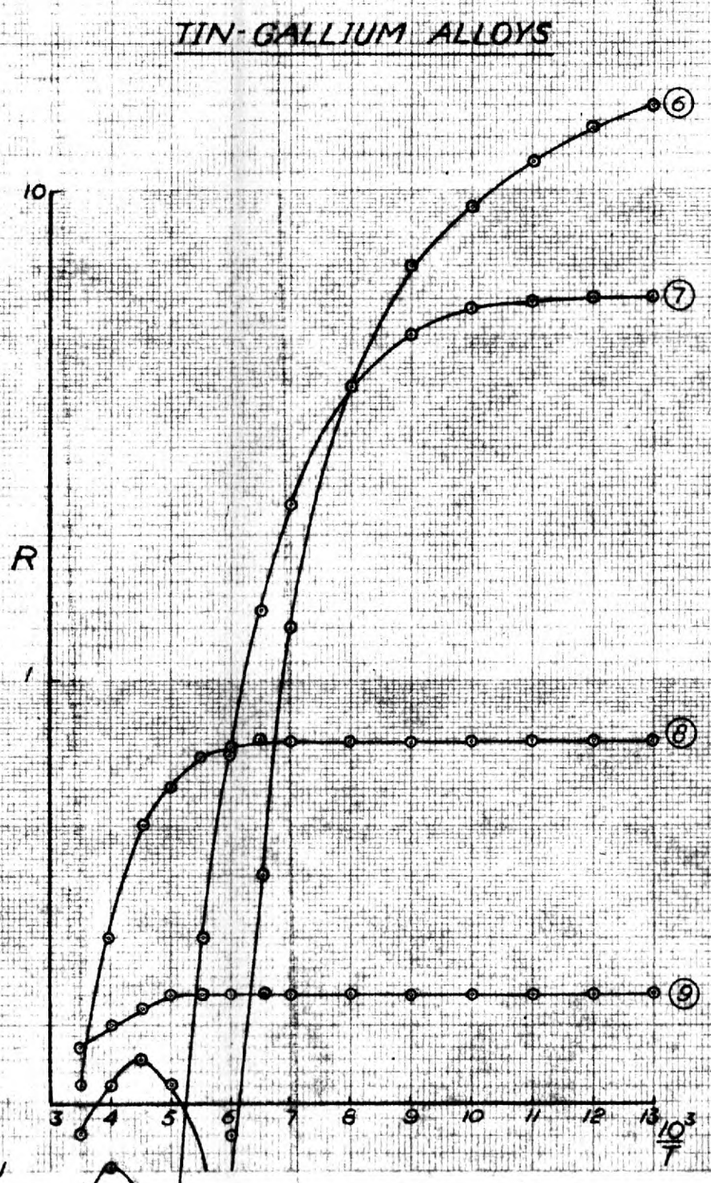
VARIATION OF CONDUCTIVITY WITH TEMPERATURE.

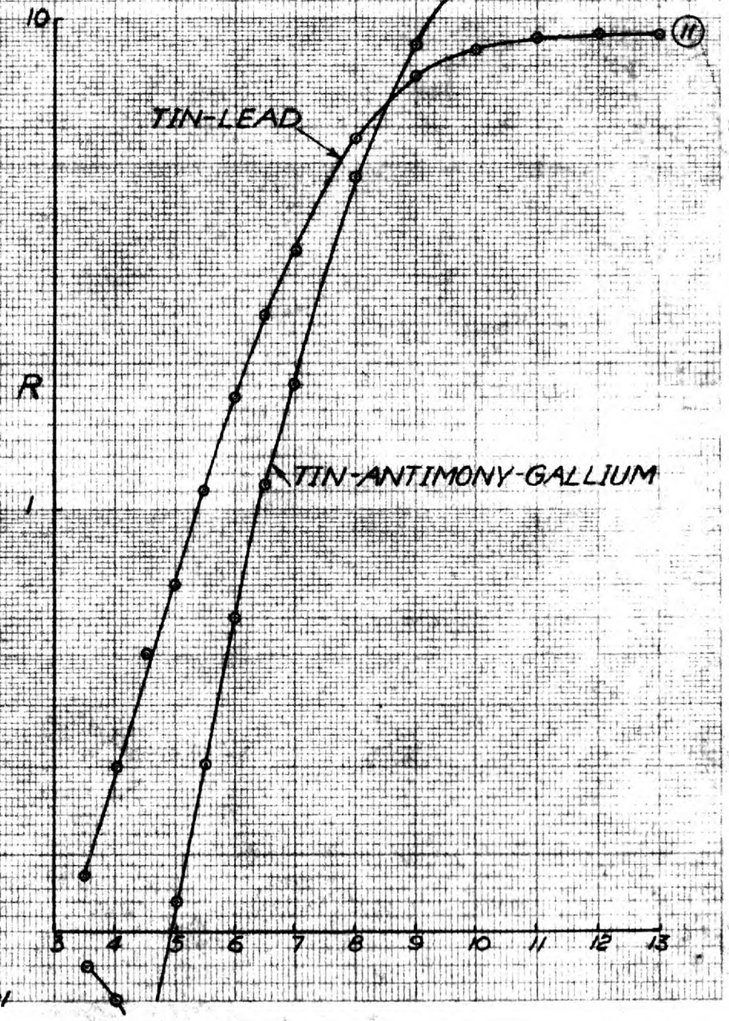


W. GRIFFIN MOUNTAIN LTD.
ARTILLERY HOUSE, ARTILLERY ROW, WESTMINSTER, S.W.1
(A4 SHEET NO 34X LOGARITHMIC X 20 CYCLES)

FIG 9
VARIATION OF HALL CONSTANT WITH TEMPERATURE







DATA SHEET 10 INCH LOGARITHMIC 3 CYCLE

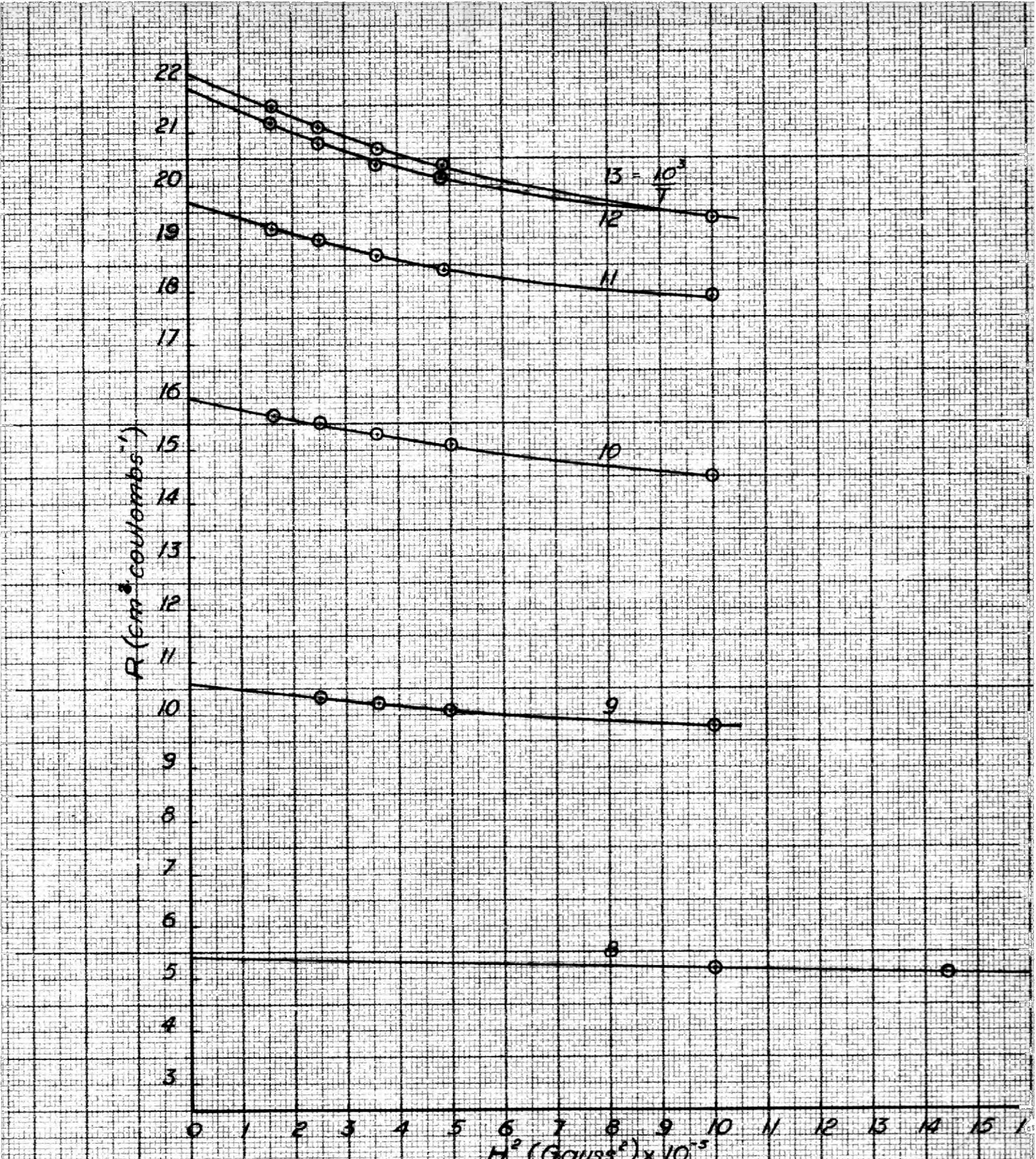


FIG. 10
VARIATION OF HALL CONSTANT
WITH MAGNETIC FIELD
ALLOY (1)

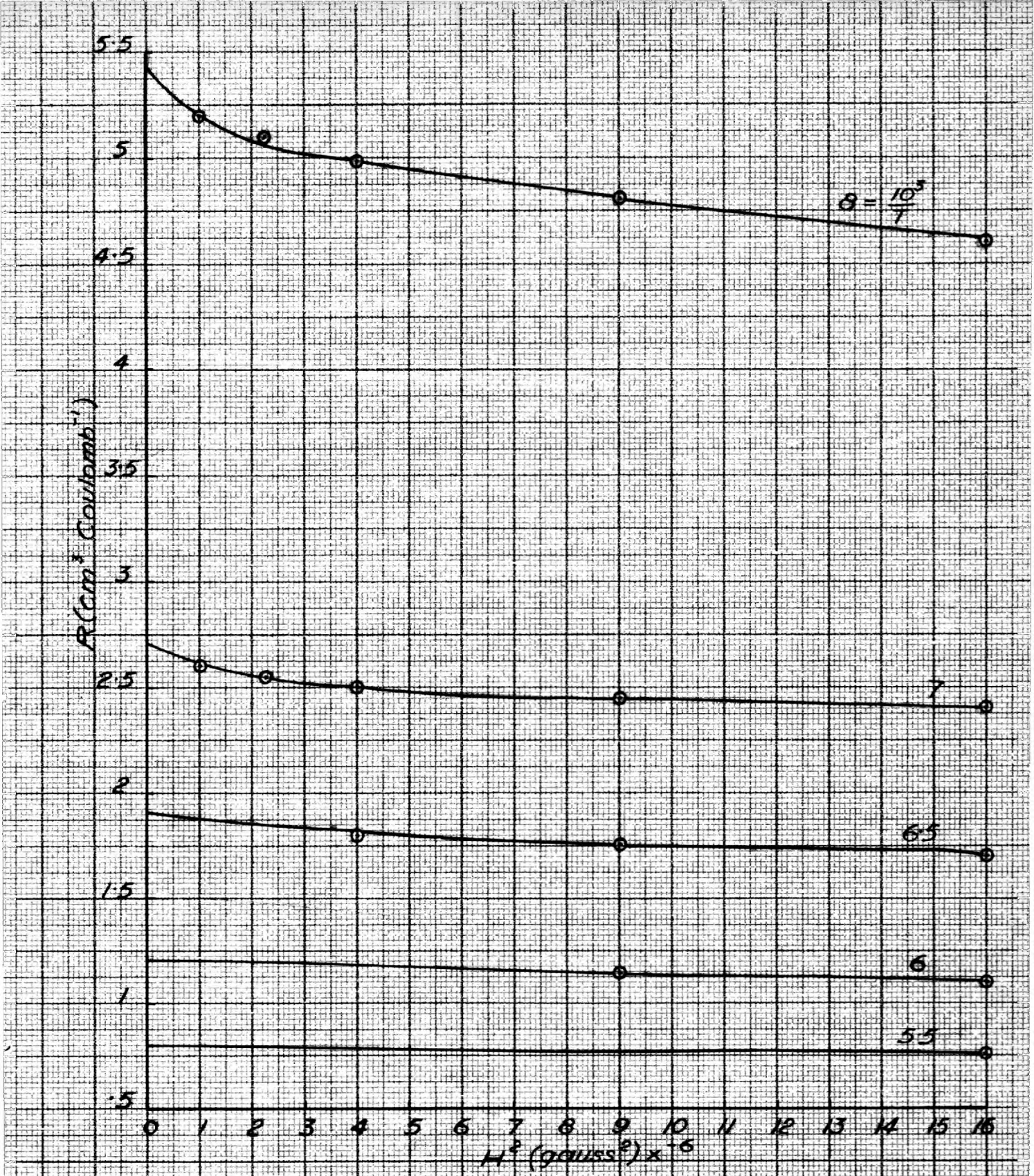


FIG. 11
VARIATION OF HALL CONSTANT WITH MAGNETIC FIELD ALLOY D

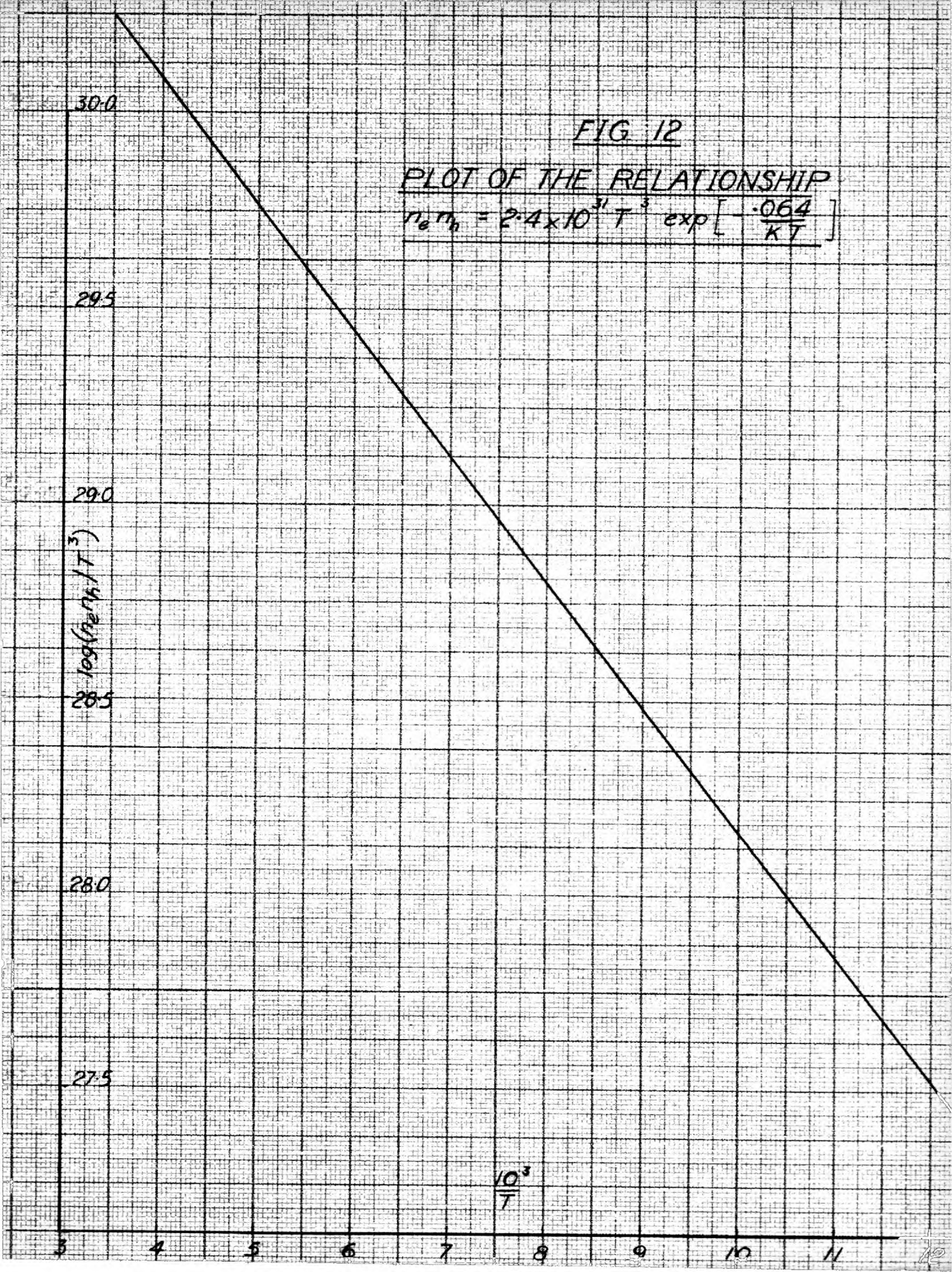

FIG 12
PLOT OF THE RELATIONSHIP
$n_e n_h = 2{\cdot}4 \times 10^{31} T^3 \exp\left[-\frac{{\cdot}064}{KT}\right]$
30·0
29·5
29·0
28·5
28·0
27·5
$\log(n_e n_h / T^3)$
$\frac{10^3}{T}$
3
4
5
6
7
8
9
10
11

FIG. 13

DEGENERACY TEMPERATURE AS A FUNCTION OF CARRIER DENSITY.

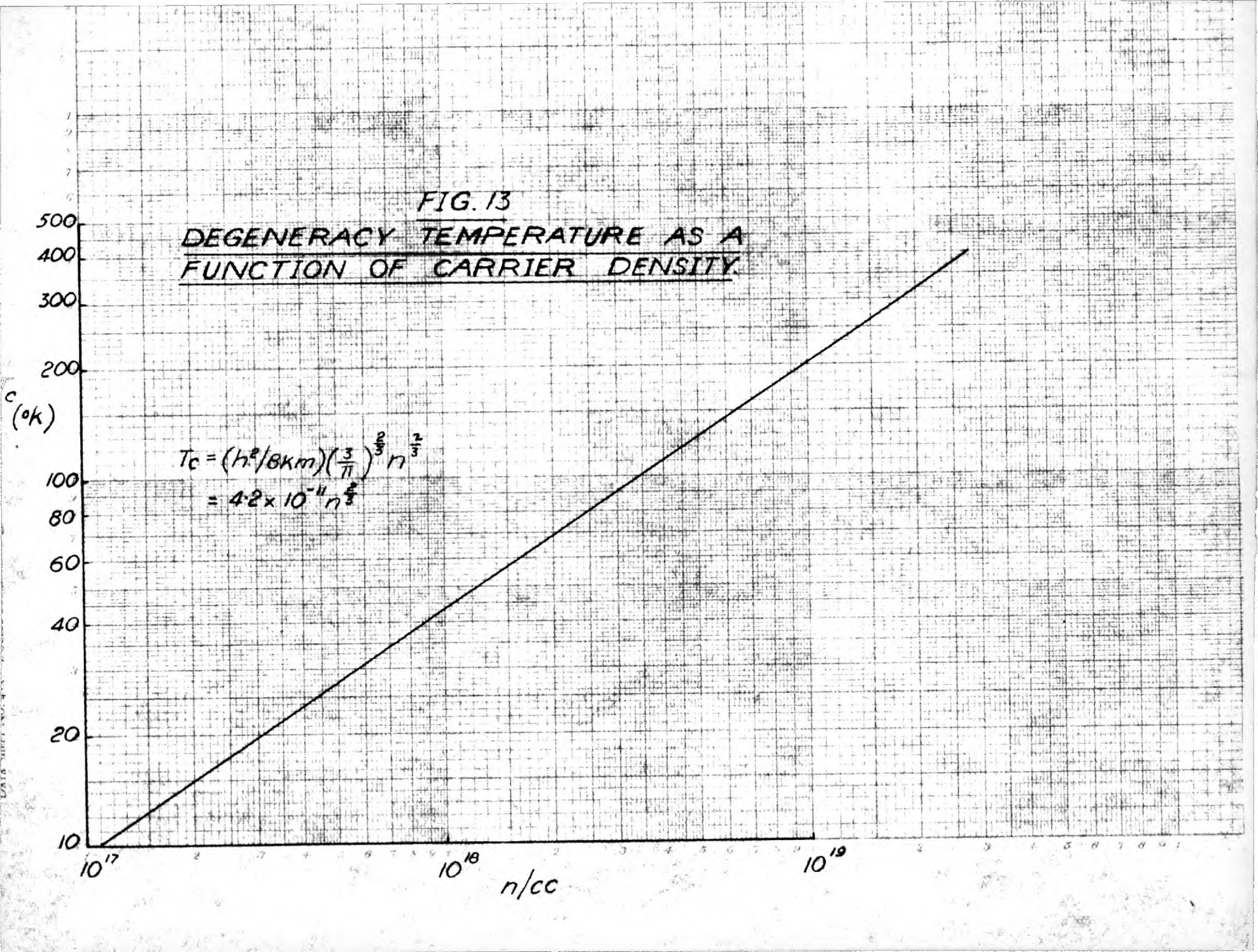
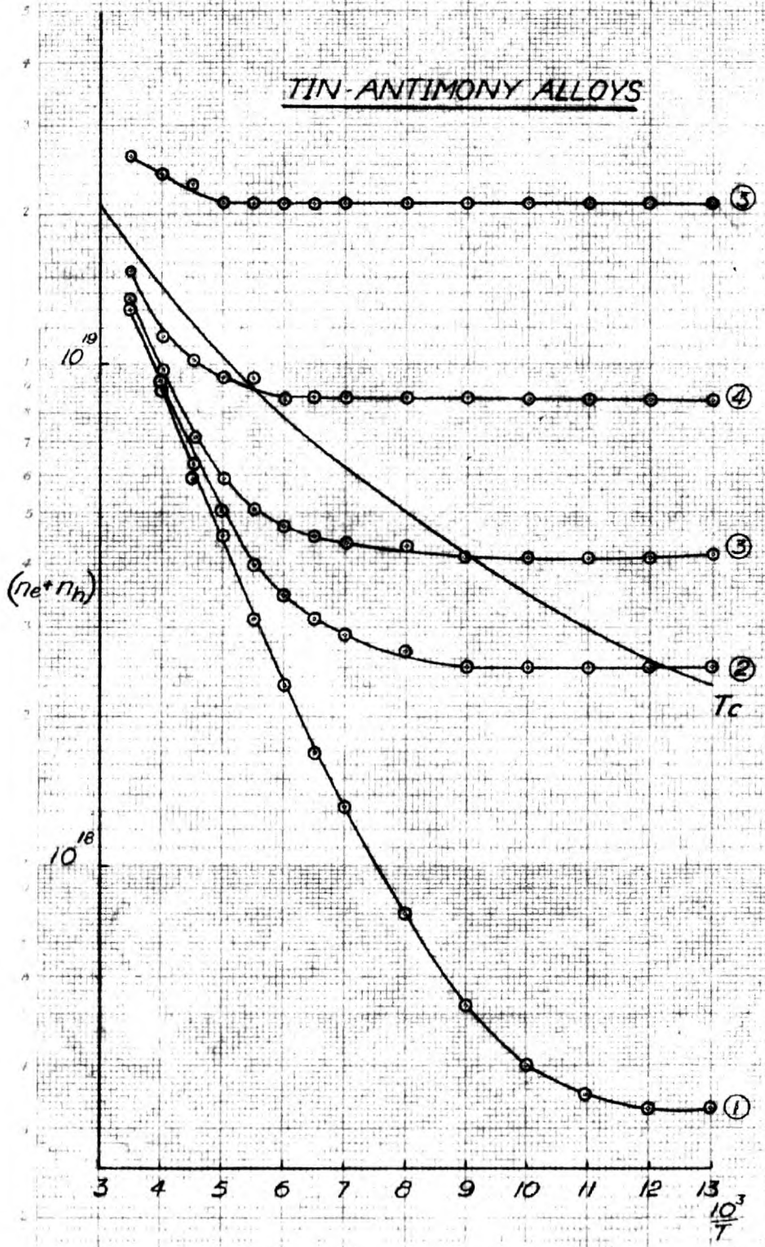
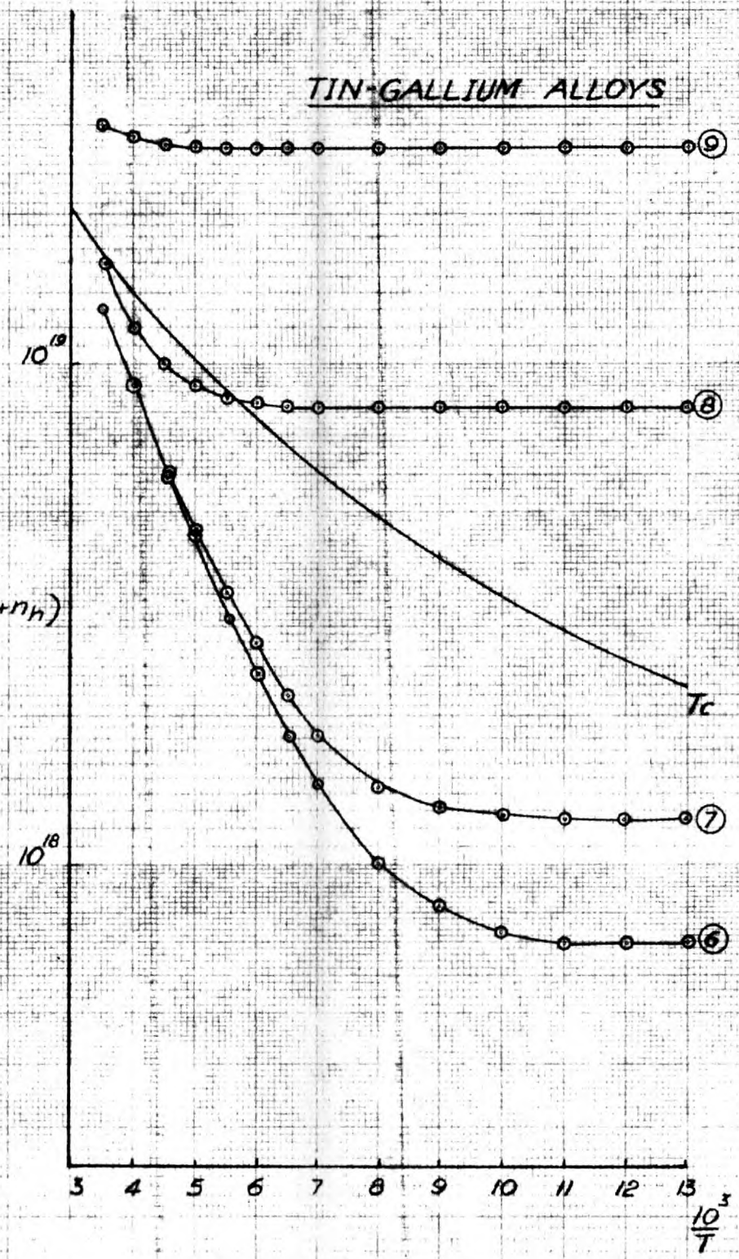
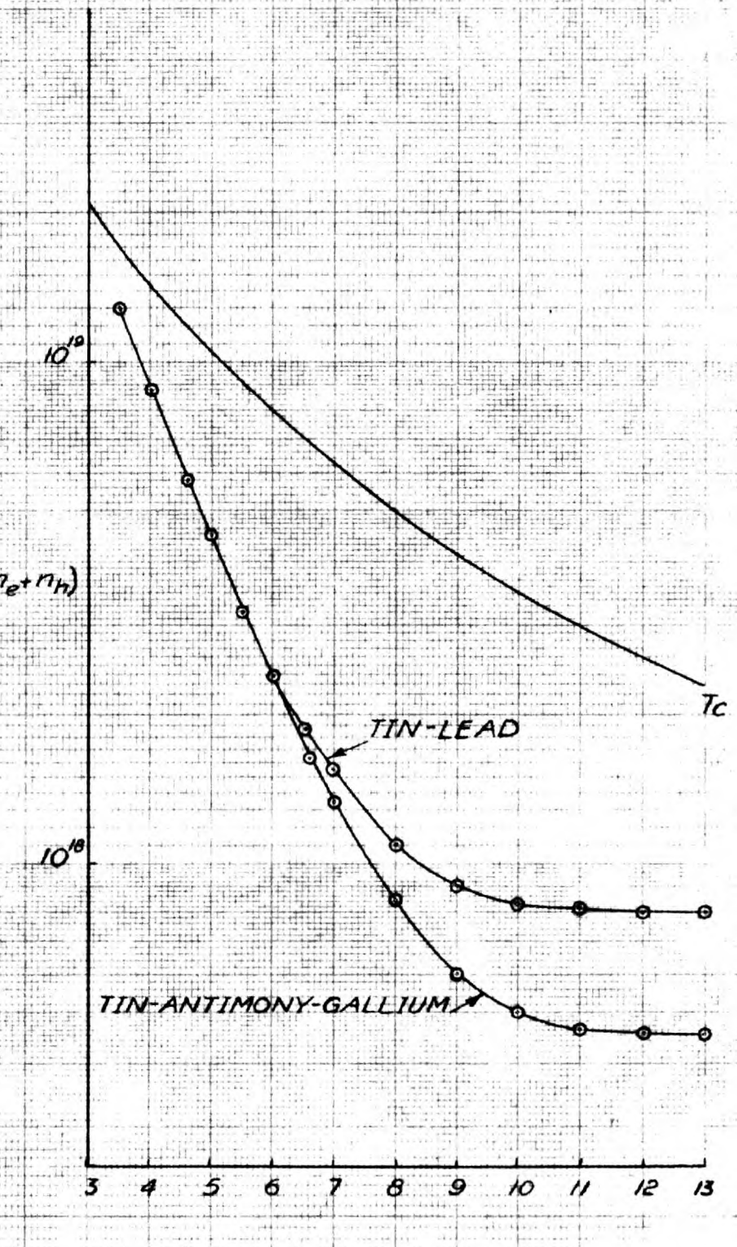


FIG. 14

VARIATION OF NUMBER OF CHARGE-CARRIERS WITH TEMPERATURE







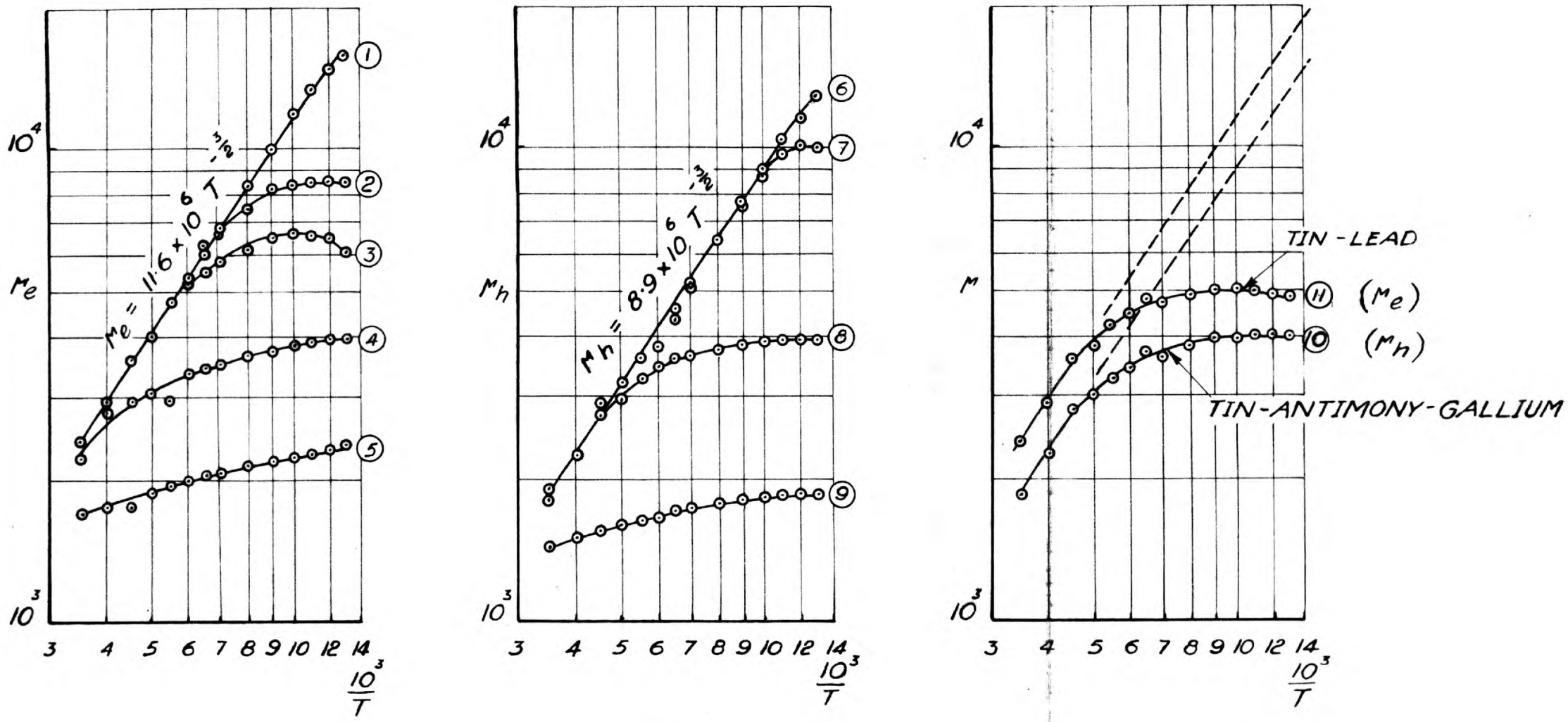
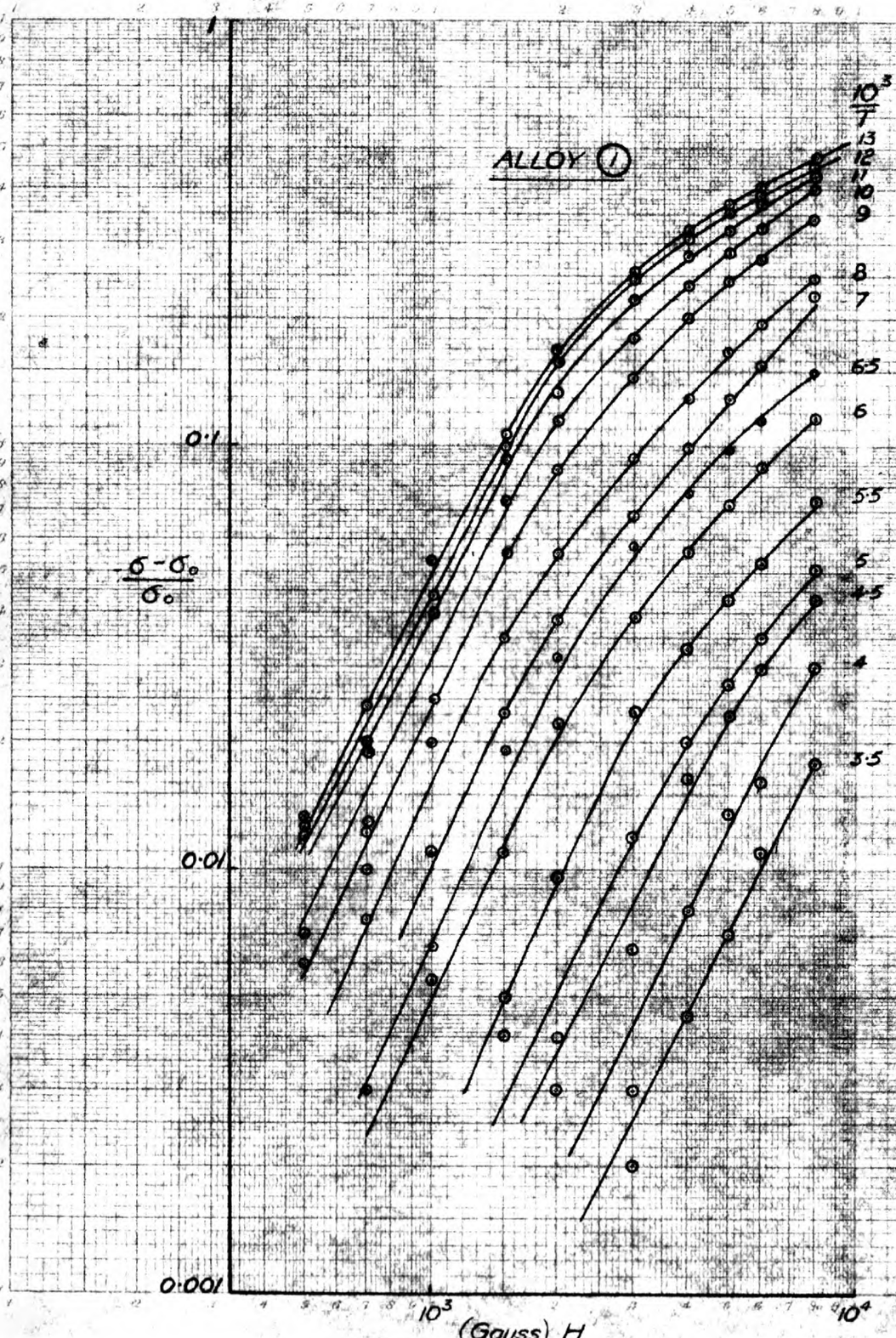


FIG. 15

VARIATION OF CARRIER MOBILITY WITH TEMPERATURE.



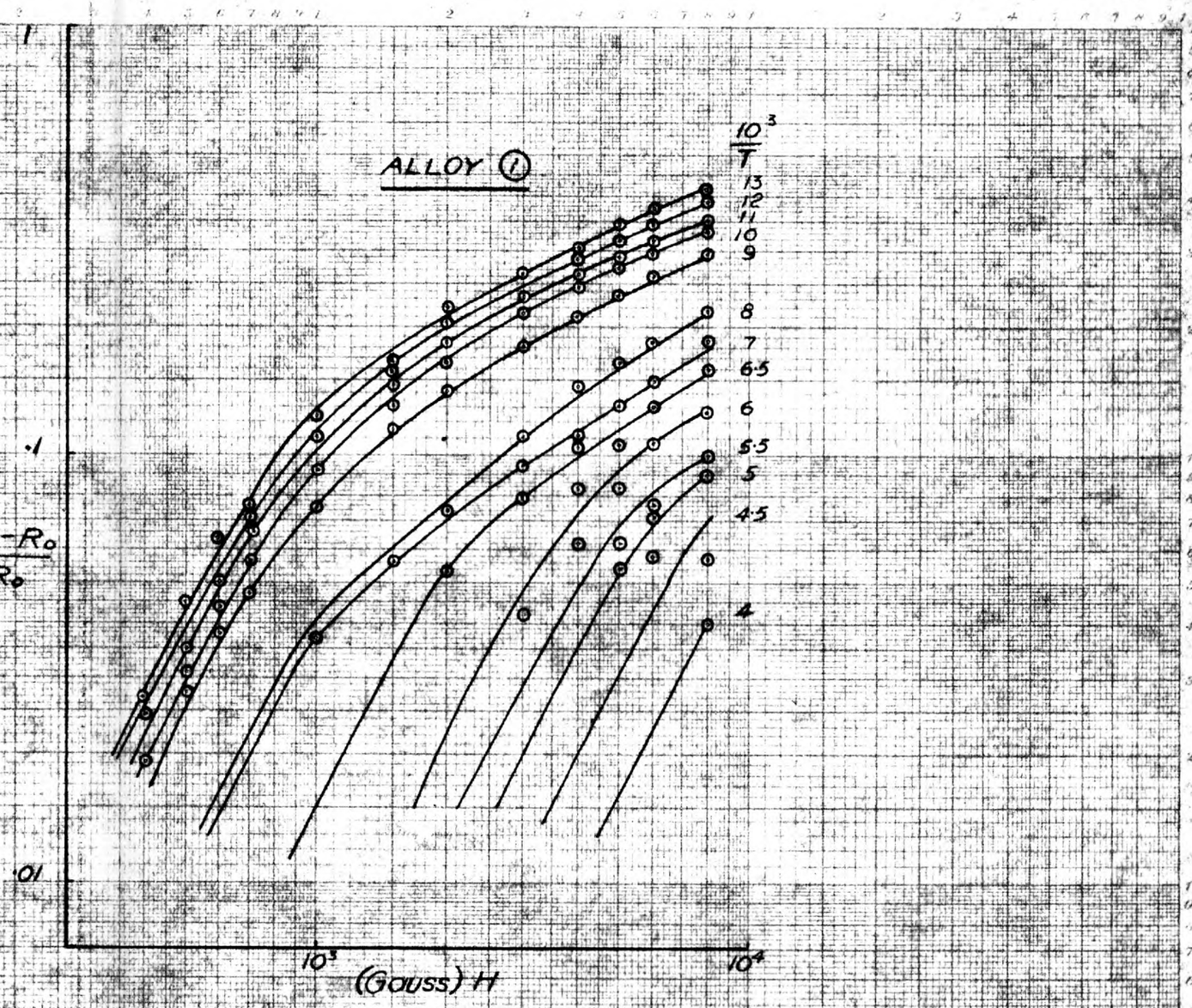
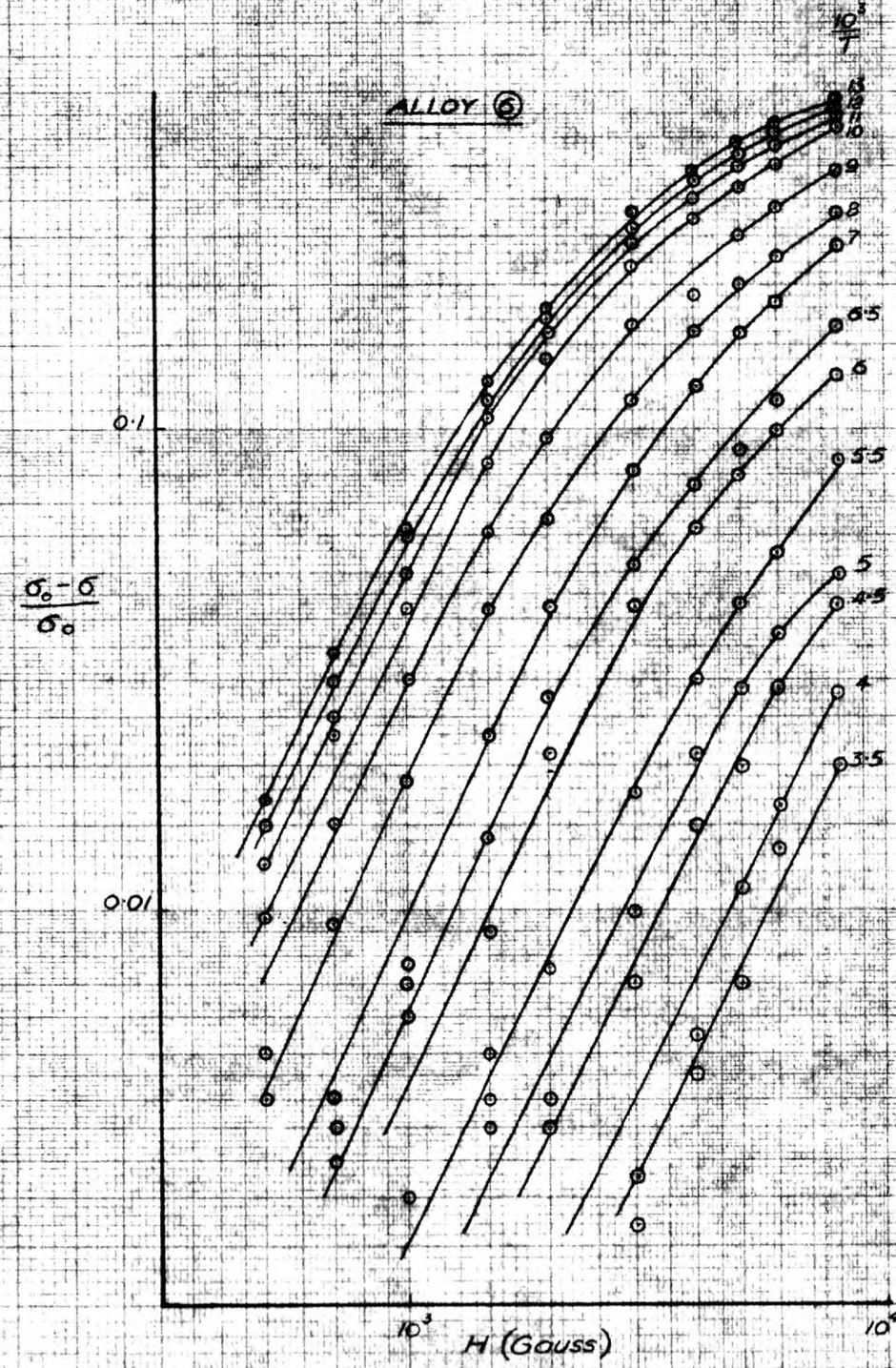


FIG 16

VARIATION OF CONDUCTIVITY AND HALL CONSTANT WITH MAGNETIC FIELD



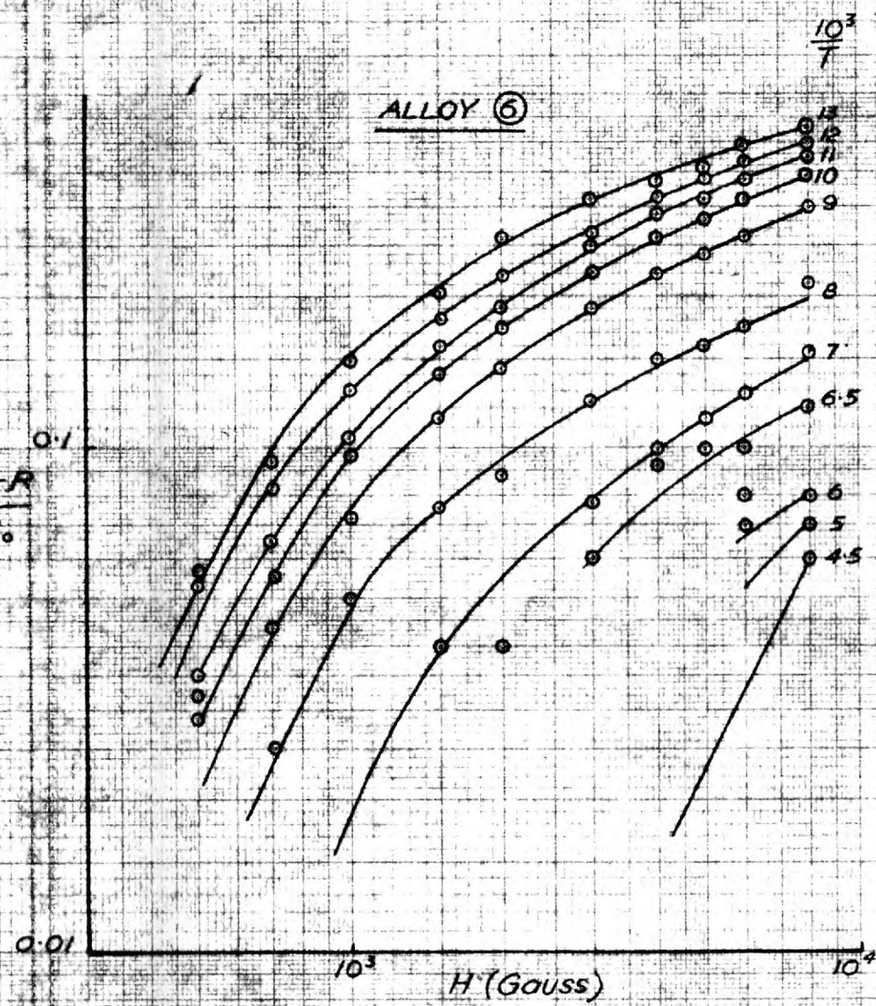


FIG. 17
VARIATION OF CONDUCTIVITY AND HALL CONSTANT WITH MAGNETIC FIELD.

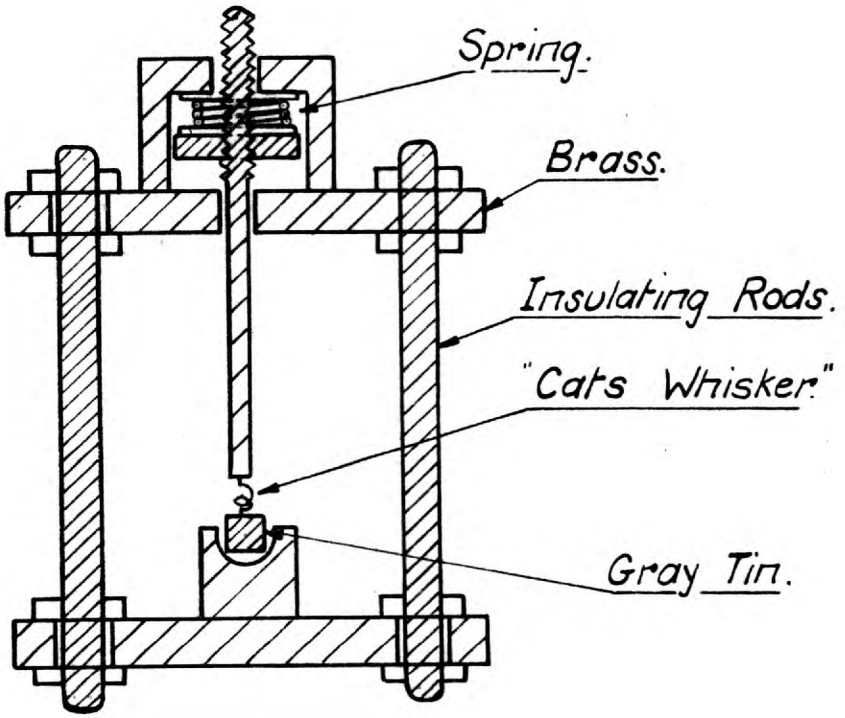


FIG. 18.

CONTACT RECTIFICATION WITH GRAY TIN.

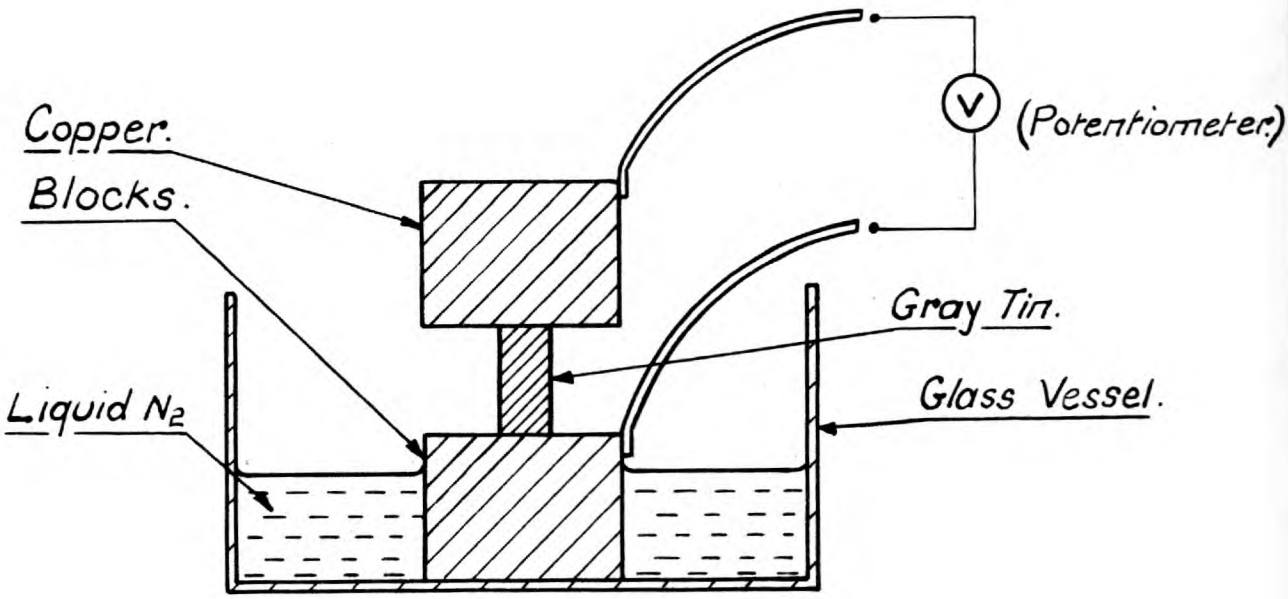


FIG. 19.

DETERMINATION OF SIGN OF THERMO-ELECTRIC CO-EFFICIENT.

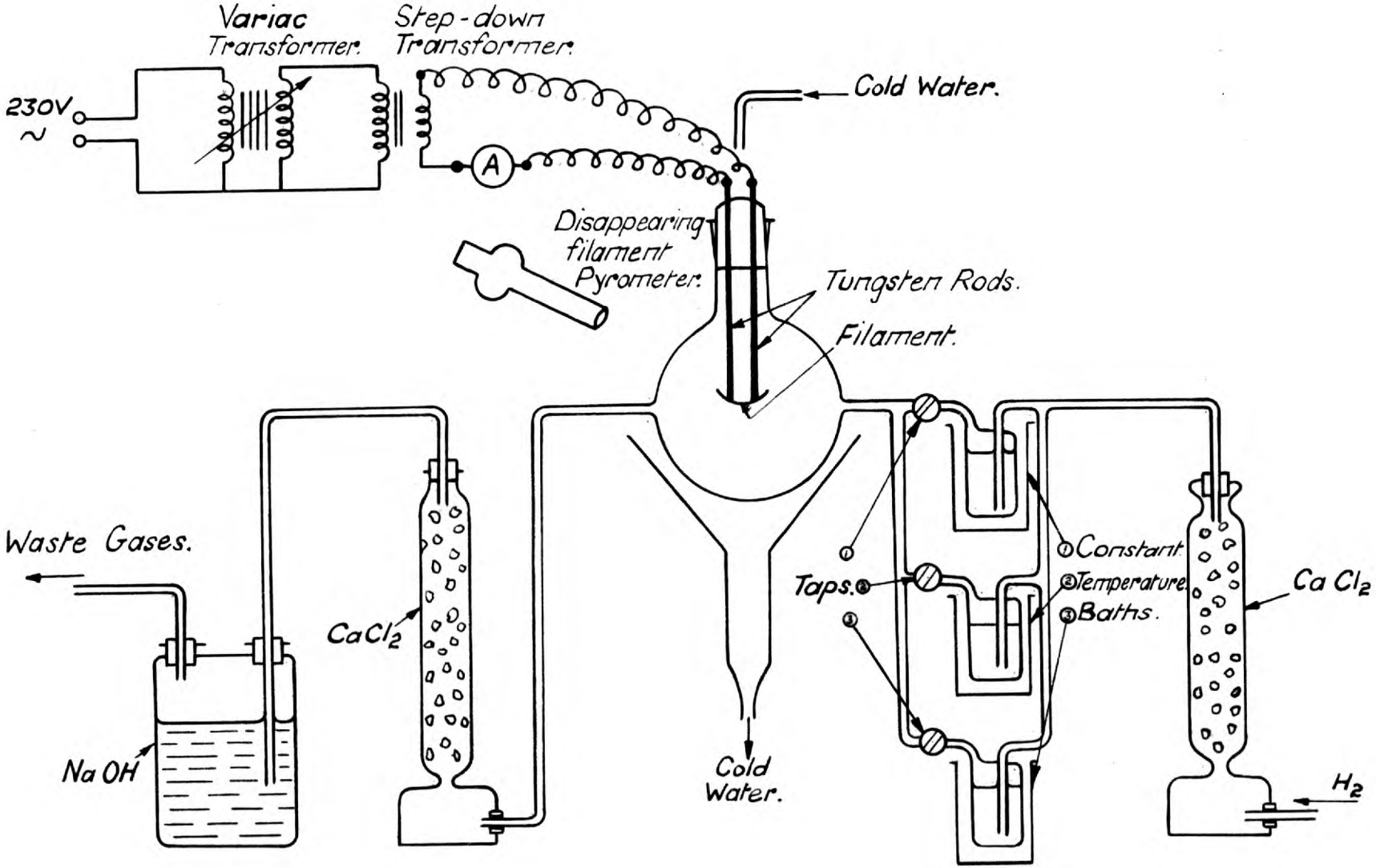


FIG. 20.

APPARATUS FOR PREPARING SILICON CARBIDE.



FIG. 21

Photograph of part of a yellow deposit (magnification x 17) showing the variation in crystal size along the length. The size of crystal increases towards the centre of the filament.

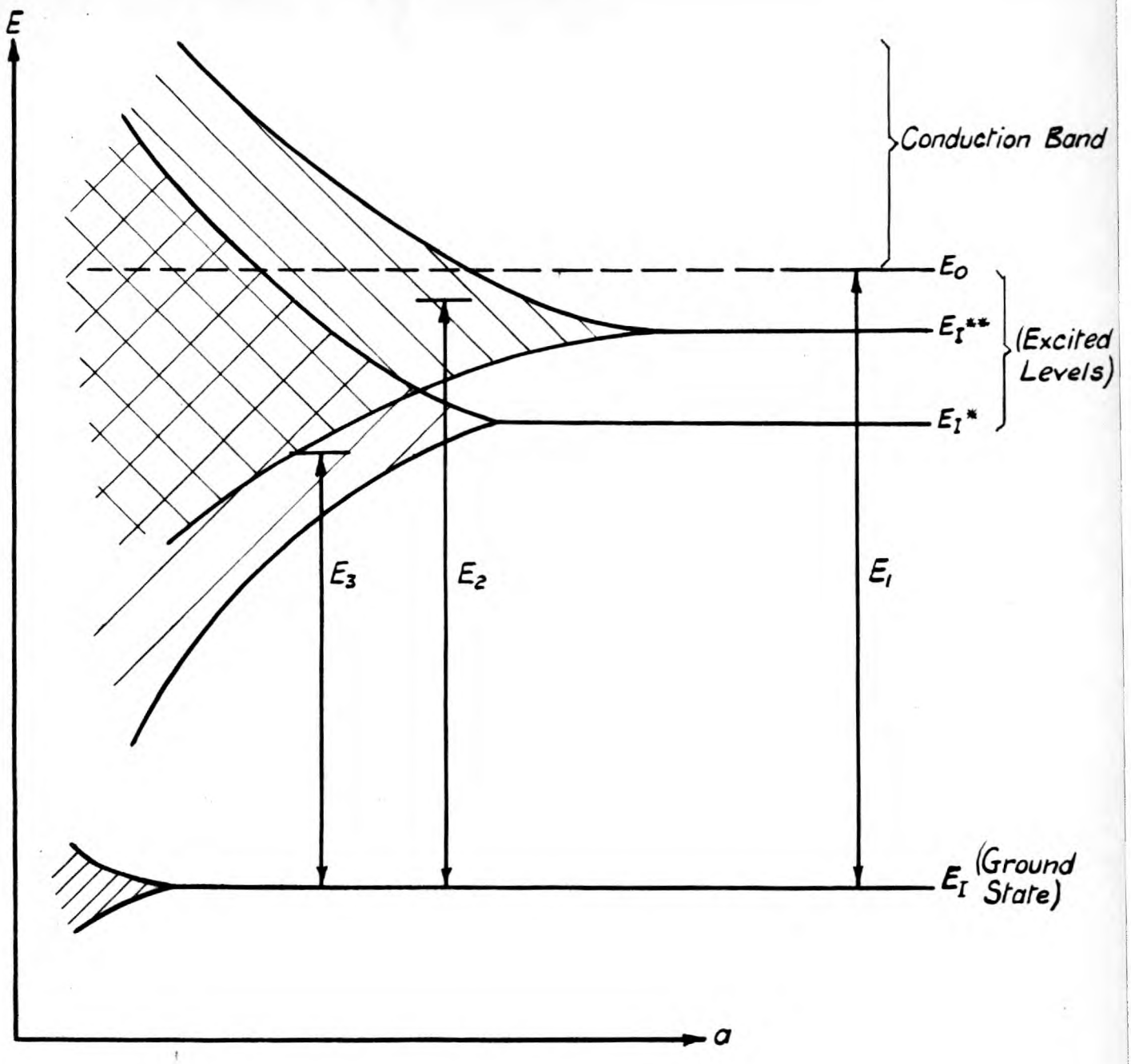
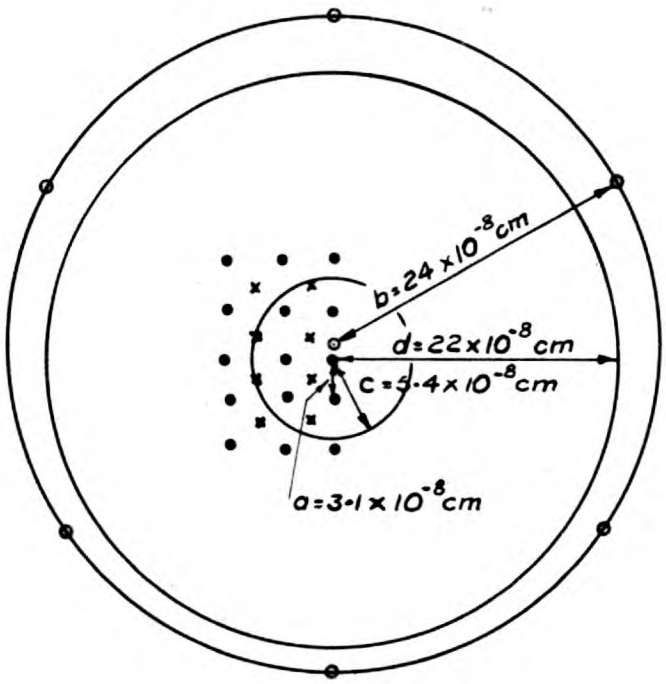


FIG.22.

SCHEMATIC REPRESENTATION OF THE BROADENING OF THE DISCRETE IMPURITY STATES WITH INCREASING CONCENTRATION OF DONATOR-TYPE IMPURITY ATOMS IN AN N-TYPE SEMICONDUCTOR. a = AVERAGE DISTANCE BETWEEN NEIGHBOURING CENTRES E_1 = NORMAL ACTIVATION ENERGY AT LOW CONCENTRATIONS. E_2 = ACTIVATION ENERGY AS REDUCED BY PRESENCE OF EXCITED STATES. E_3 = LOW TEMPERATURE ACTIVATION ENERGY GIVING LOW MOBILITY CONDUCTION IN THE EXCITED IMPURITY BAND.



a = Carbon - carbon distance = $3{\cdot}1 \times 10^{-8}$ cm (Shown • and x)

b = Missing silicon - missing silicon distance = 24×10^{-8} cm (Shown ○)

c = Radius of hole in ground state = $5{\cdot}4 \times 10^{-8}$ cm.

d = Radius of hole in excited state = 22×10^{-8} cm.

FIG.23.

BLACK SILICON CARBIDE SHOWING RADII OF HOLES IN GROUND AND EXCITED STATES.

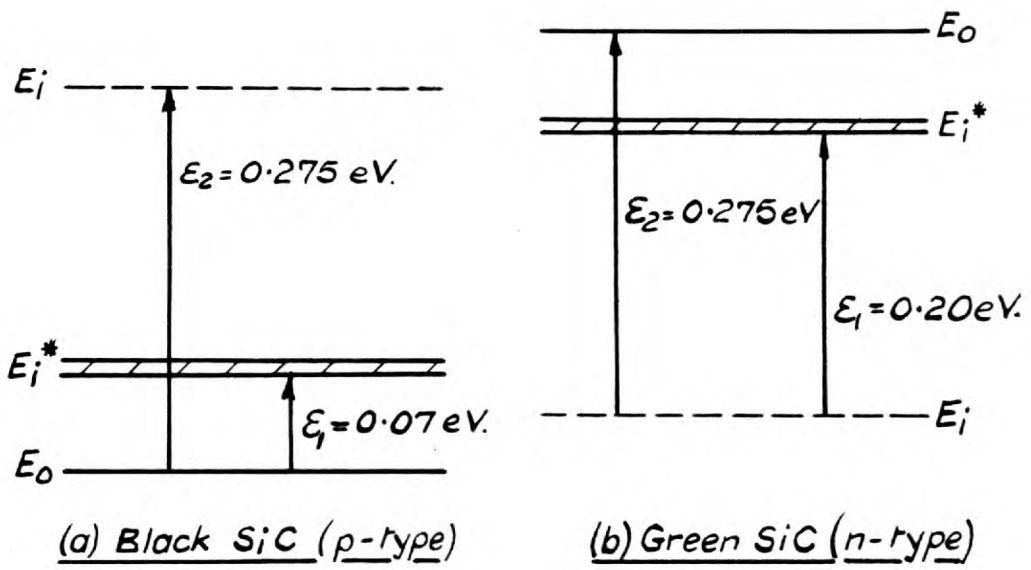


FIG. 24.

ENERGY LEVELS IN SiC.

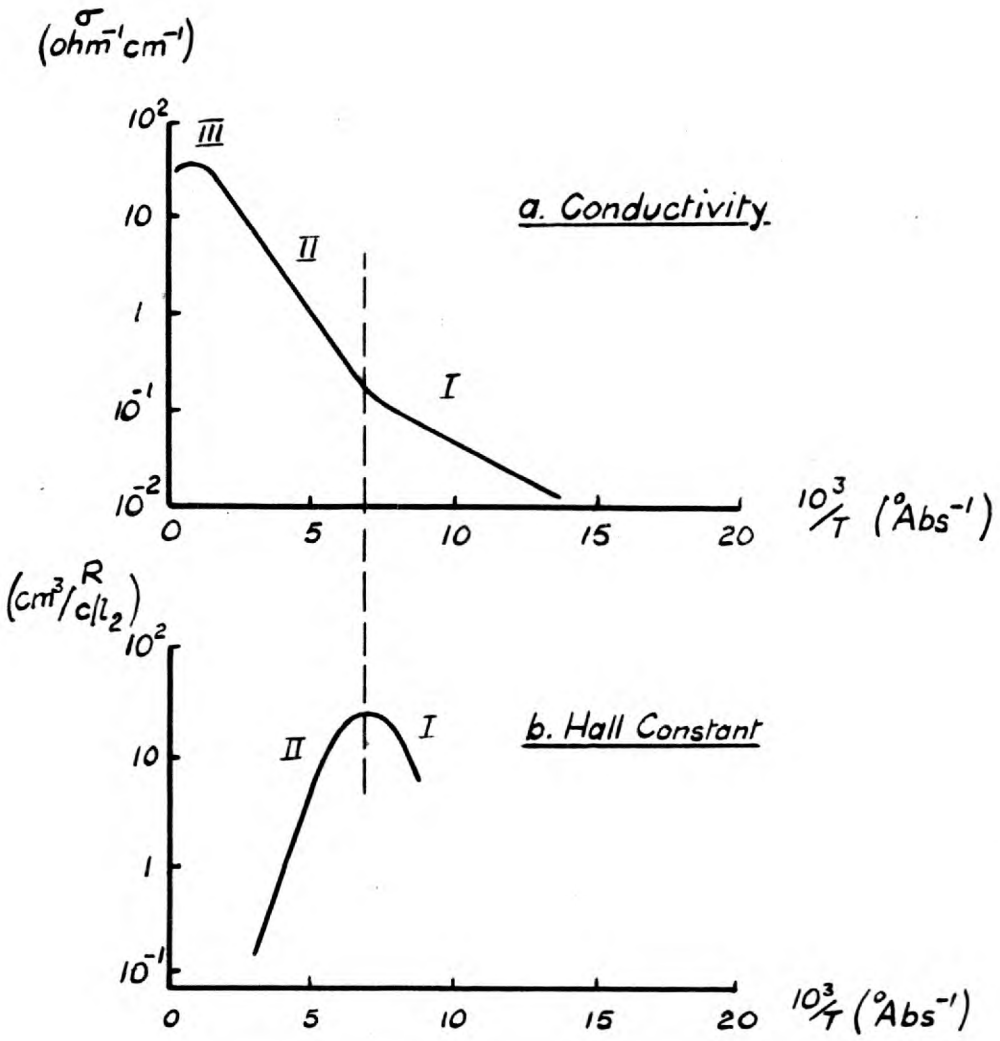


FIG.25.

CONDUCTIVITY AND HALL CONSTANT OF BLACK SiC

(EXPERIMENTAL RESULTS OF BUSCH & LABHART)

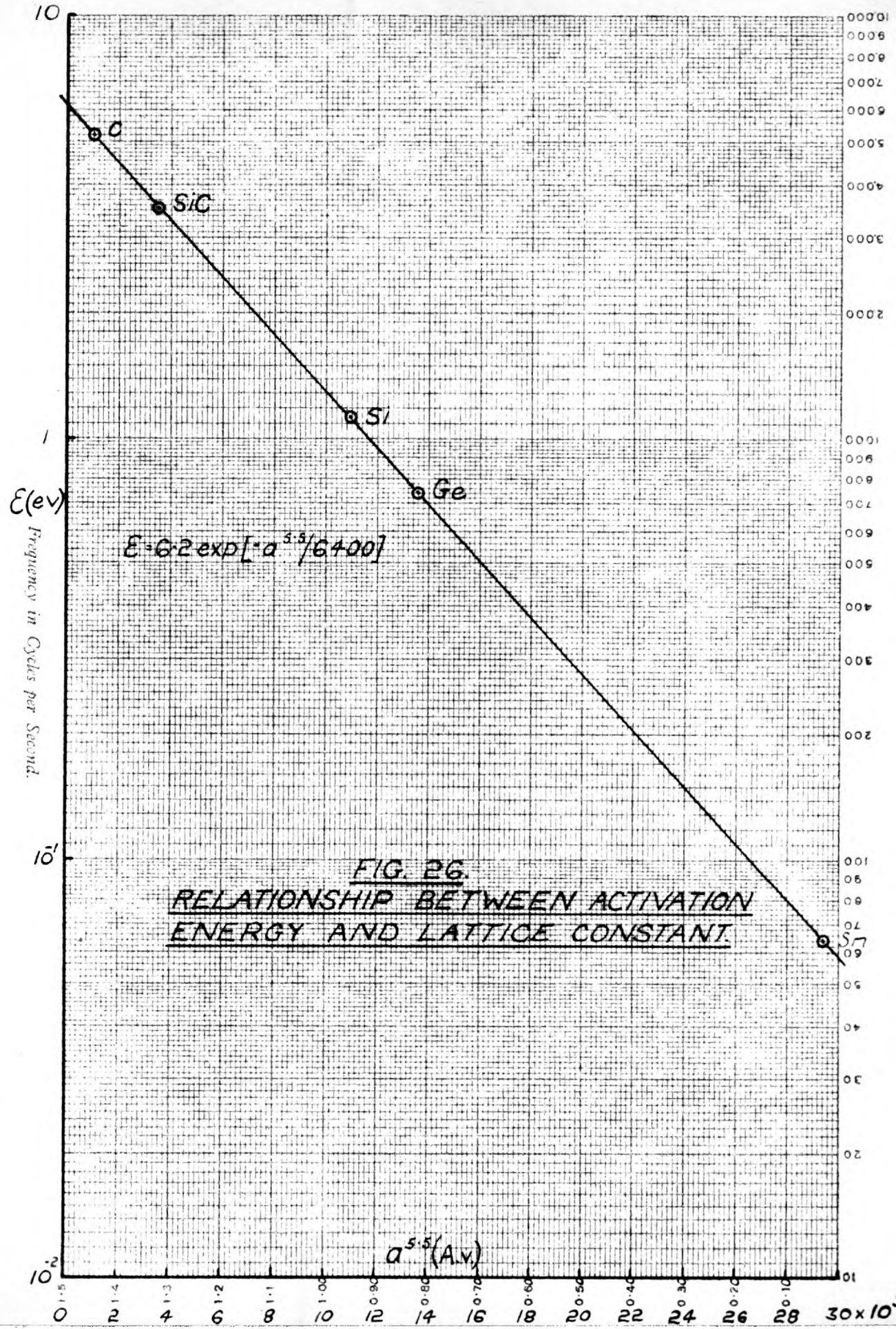


FIG. 26.

RELATIONSHIP BETWEEN ACTIVATION ENERGY AND LATTICE CONSTANT.

DATA SHEET NO. 16. LOGARITHMIC X M/M (3 CYCLE)

WIGHTMAN MOUNTAIN LTD.
ARTILLERY HOUSE, ARTILLERY ROW, WESTMINSTER, S.W.1